

NO-A187 986

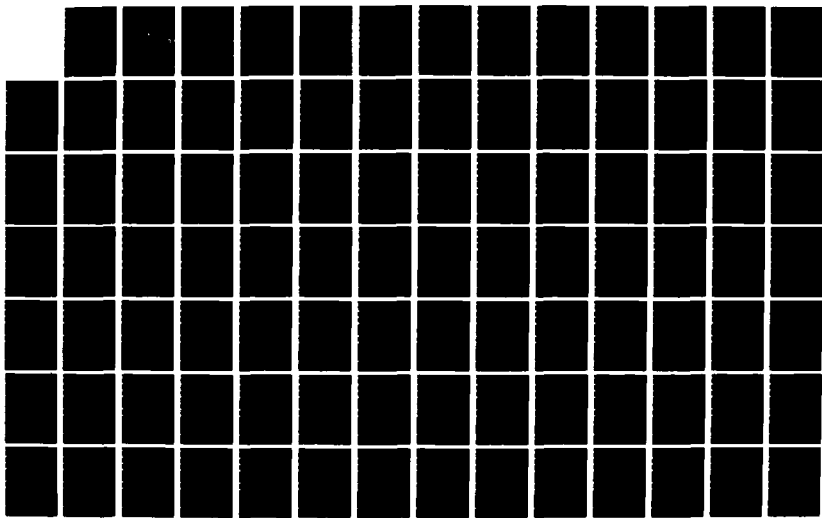
PROJECT SKYLITE: A DESIGN EXPLORATION(U) NAVAL
POSTGRADUATE SCHOOL MONTEREY CA W J WELCH ET AL.
SEP 87

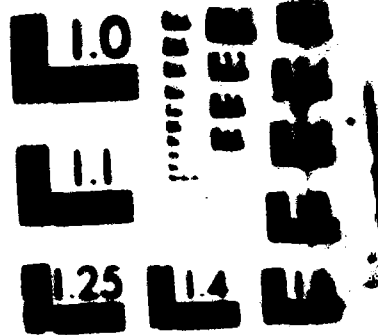
1/2

UNCLASSIFIED

F/G 4/1

NL





2

AD-A187 906

NAVAL POSTGRADUATE SCHOOL

Monterey, California



DTIC
ELECTE
JAN 05 1988
S D E

THESIS

PROJECT SKYLITE
A
DESIGN EXPLORATION

by

William J. Welch
and
Mark F. Landers

September 1987

Thesis Advisor

Richard C. Olsen

Approved for public release; distribution is unlimited.

87 12 29 013

UNCLASSIFIED

SECURITY CLASSIFICATION OF THIS PAGE

REPORT DOCUMENTATION PAGE

1a REPORT SECURITY CLASSIFICATION UNCLASSIFIED		1b RESTRICTIVE MARKINGS NONE	
2a SECURITY CLASSIFICATION AUTHORITY N/A		3 DISTRIBUTION/AVAILABILITY OF REPORT Approved for public release; Distribution is unlimited	
2b DECLASSIFICATION/DOWNGRADING SCHEDULE N/A			
4 PERFORMING ORGANIZATION REPORT NUMBER(S)		5 MONITORING ORGANIZATION REPORT NUMBER(S)	
6a NAME OF PERFORMING ORGANIZATION Naval Postgraduate School	6c OFFICE SYMBOL (if applicable) 72	7a NAME OF MONITORING ORGANIZATION Naval Postgraduate School	
6b ADDRESS (City, State and ZIP Code) Monterey, California 93943-5000		7b ADDRESS (City, State and ZIP Code) Monterey, California 93943-5000	
8a NAME OF FUNDING SPONSORING ORGANIZATION	8b OFFICE SYMBOL (if applicable)	9 PROCUREMENT INSTRUMENT IDENTIFICATION NUMBER	
6d ADDRESS (City, State and ZIP Code)		10 SOURCE OF FUNDING NUMBERS	
		PROGRAM ELEMENT NO	PROJECT NO
		TASK NO	WORK UNIT ACCESSION NO
11 Include Security Classification			
Project SKYLITE: A Design Exploration			
12 AUTHOR(S) Welch, William J. and Landers, Mark F.			
13 TYPE OF REPORT Master's Thesis	14 TIME COVERED FROM TO	15 DATE OF REPORT (Year, Month, Day) 1987 September	16 PAGE COUNT 144
17 SUPPLEMENTARY NOTES			
18a COSAC CODES		18b SUBJECT TERMS (Continue on reverse if necessary and identify by block number)	
FIELD	GROUP	SUB GROUP	
		SKYLITE, Satellite Design, Spacecraft Design Satellite, Spacecraft, Orbit Analysis, Thermal Analysis, Orbital Selection	
19 ABSTRACT (Continue on reverse if necessary and identify by block number)			
<p>This thesis proposes a design for the project SKYLITE satellite. Project SKYLITE is an experiment which will assess compensating techniques designed to reduce laser wave front distortion caused by the atmosphere. The satellite will measure and downlink the propagated beam irradiance of the Mid-IR Advance Chemical Laser (MIRACL), based at the White Sands Missile Range (WSMR), New Mexico. The spacecraft will be designed to measure beam quality and power of both high and low power laser experiments. The irradiance and power values will vary as different compensating methods are employed. The spacecraft, which is gravity gradient stabilized, provides an array of IR sensors in the 3.6 to 4.2 micron window to measure laser irradiance. The use of several retroreflectors appended to the satellite will provide for precision pointing and turbulence correction measurements using a ground based</p>			
20 DISTRIBUTION/AVAILABILITY OF ABSTRACT <input checked="" type="checkbox"/> UNCLASSIFIED/UNLIMITED <input type="checkbox"/> SAME AS RPT <input type="checkbox"/> DTIC USERS		21 ABSTRACT SECURITY CLASSIFICATION UNCLASSIFIED	
22a NAME OF RESPONSIBLE INDIVIDUAL Olsen, Richard C.		22b TELEPHONE (Include Area Code) 408-646-2019	22c OFFICE SYMBOL Code 61

DD FORM 1473, 84 MAR

83 APR edition may be used until exhausted
All other editions are obsoleteSECURITY CLASSIFICATION OF THIS PAGE
UNCLASSIFIED

Alexandrite laser. Due to the high energy involved during the lasing experiment, highly reflective, radiation shielding of both sensitive equipment and the solar array will be required to allow for survivability throughout its three year life without thermal or structural degradation. To minimize cost, Project SKYLITE will utilize the STS (Space Shuttle) standard canister for small self-contained payloads known as the Extended Get Away Special (GAS) Can. The satellite has been designed to use the Orion bus currently being designed by NPS. The use of off-the-shelf technology for both economy and rapid procurement processes has been a prime consideration throughout the design to meet the Initial Operational Capability deadline of first quarter FY-89. The satellite expense, estimated with the AIR Force Unmanned Spacecraft Cost Model, is approximately 3.9M\$ for recurring costs and 14.8M\$ for nonrecurring costs.

Approved for public release; distribution is unlimited.

Project SKYLITE
a
Design Exploration

by

William J. Welch
Lieutenant, United States Navy
B.S., United States Naval Academy 1979

and

Mark F. Landers
Lieutenant, United States Navy
B.S., United States Naval Academy 1981

Submitted in partial fulfillment of the
requirements for the degree of



Accession For	
NTIS GRA&I	<input checked="" type="checkbox"/>
DTIC TAB	<input type="checkbox"/>
Unannounced	<input type="checkbox"/>
Justification	
By	
Distribution/	
Availability Codes	
Dist	Avail and/or Special
A-1	

MASTER OF SCIENCE IN SYSTEM TECHNOLOGY
(SPACE SYSTEMS OPERATIONS)

from the

NAVAL POSTGRADUATE SCHOOL

September 1987

Authors:

William J. Welch
William J. Welch

Mark F. Landers
Mark F. Landers

Approved by:

Richard C. Olsen
Richard C. Olsen, Thesis Advisor

Philip A. Durkee
Philip A. Durkee, Second Reader

Rudolf Panholzer
Rudolf Panholzer, Chairman,
Space Systems Academic Group

Gordon E. Schacher
Gordon E. Schacher,
Dean of Science and Engineering

ABSTRACT

This thesis proposes a design for the project SKYLITE satellite. Project SKYLITE is an experiment which will assess compensating techniques designed to reduce laser wave front distortion caused by the atmosphere. The satellite will measure and downlink the propagated beam irradiance of the Mid-IR Advance Chemical Laser (MIRACL), based at the White Sands Missile Range (WSMR), New Mexico. The spacecraft will be designed to measure beam quality and power of both high and low power laser experiments. The irradiance and power values will vary as different compensating methods are employed. The spacecraft, which is gravity gradient stabilized, provides an array of IR sensors in the 3.6 to 4.2 micron window to measure laser irradiance. The use of several retroreflectors appended to the satellite will provide for precision pointing and turbulence correction measurements using a ground based Alexandrite laser. Due to the high energy involved during the lasing experiment, highly reflective, radiation shielding of both sensitive equipment and the solar array will be required to allow for survivability throughout its three year life without thermal or structural degradation. To minimize cost, Project SKYLITE will utilize the STS (Space Shuttle) standard canister for small self-contained payloads known as the Extended Get Away Special (GAS) can. The satellite has been designed to use the Orion bus currently being designed by NPS. The use of off-the-shelf technology for both economy and rapid procurement processes has been a prime consideration throughout the design to meet the Initial Operational Capability deadline of first quarter FY-89. The satellite expense, estimated with the Air Force Unmanned Spacecraft Cost Model, is approximately 3.9 M\$ for recurring costs and 14.8M\$ for nonrecurring costs.

TABLE OF CONTENTS

I.	INTRODUCTION	14
II.	SKYLITE MISSION OVERVIEW	16
	A. PROJECT SKYLITE MISSION REQUIREMENTS	16
	1. Orbit	16
	2. Attitude Control	16
	3. Retroreflector	16
	4. IR Sensors	17
	5. Gravity Gradient Boom	17
	6. Satellite Survivability	17
	7. Electrical Interfaces	17
	8. Launch Requirement	17
	B. SKYLITE SATELLITE DESCRIPTION	17
	C. SKYLITE LAUNCH PROFILE	20
	D. MISSION OPERATION SUMMARY	20
III.	THE ORION CONCEPT	22
IV.	ORBITAL ANALYSIS	25
	A. INTRODUCTION	25
	B. ORBITAL INCLINATION	27
	C. MINIMUM ORBITAL ALTITUDE	28
	D. MAXIMUM ORBITAL ALTITUDE	28
	E. FREQUENCY AND DURATION OF LASING PERIODS	30
	F. CONCLUSION	34
V.	PROPULSION ANALYSIS	35
	A. INTRODUCTION	35
	B. TOTAL FUEL AVAILABLE	37
	C. FUEL REQUIREMENTS	38

	1. Orbital Decay	38
	2. Spacecraft Spin Up and Spin Down, and Boom Length Determination	41
	3. Spacecraft Insertion	45
	D. CONCLUSION	48
VI.	THERMAL ANALYSIS	49
	A. INTRODUCTION	49
	B. SATELLITE TEMPERATURE FLUCTUATIONS	51
	C. EFFECTS OF DIRECT SUNLIGHT ON THE SATELLITE	51
	D. EFFECTS OF THE EARTH'S ALBEDO ON SATELLITE TEMPERATURE	56
	E. EFFECTS OF THERMAL RADIATION FROM THE EARTH ON THE SATELLITE	57
	F. EFFECTS OF INTERNAL HEAT DISSIPATION	58
	G. EFFECTS OF INCIDENT LASER ENERGY ON THE SATELLITE	59
	H. CALCULATING THE AVERAGE HOT AND COLD TEMPERATURES	60
	I. CALCULATING THE MAXIMUM AND MINIMUM TEMPERATURES	61
	J. PASSIVE THERMAL CONTROL	64
	K. CONCLUSION	64
VII.	SPACECRAFT POWER ANALYSIS	66
	A. INTRODUCTION	66
	B. POWER SOURCES	67
	1. Solar Array	67
	2. Minimum Power Orbit	69
	3. Maximum Power Orbit	73
	4. Battery	76
	C. SOLAR CELL PROTECTION	78
	D. CONCLUSION	80
VIII.	SPACECRAFT STABILIZATION	81
	A. INTRODUCTION	81

	B.	GRAVITY GRADIENT BOOM LENGTH DETERMINATION	82
	1.	Boom Length Calculations	83
	C.	ATTITUDE SENSING	87
	D.	CONCLUSION	88
IX.		STRUCTURAL ANALYSIS	90
	A.	INTRODUCTION	90
	B.	STRUCTURAL LOADING	90
	C.	CENTER OF MASS VARIANCES	91
	D.	MOMENT OF INERTIA DETERMINATION	94
	1.	Baseplate Moment of Inertia	96
	2.	Cylinder Moment of Inertia	97
	E.	MAXIMUM STRESS EVALUATION	98
	F.	MAXIMUM STRUCTURAL DEFLECTION	102
	G.	VIBRATION LIMITATIONS UNDER BASE EXCITATION	103
	H.	MAXIMUM STRESS AND DEFLECTION OF THE DEPLOYED STABILITY BOOMS	106
	I.	CONCLUSION	109
X.		RETROREFLECTOR DESIGN	110
XI.		IR SENSOR SELECTION	113
	A.	INTRODUCTION	113
XII.		COMMUNICATIONS CONSIDERATIONS - DATA & TELEMETRY	117
	A.	INTRODUCTION	117
	B.	RADIO FREQUENCY SUBSYSTEM	117
	C.	TELEMETRY, TRACKING AND CONTROL (TT&C) SUBSYSTEM	118
	D.	PRELIMINARY COMMUNICATIONS ANALYSIS	119
	1.	Satellite Downlink	119
	2.	Data Storage	119
	3.	Transmitter Power On/Off Capability	119
	E.	CONCLUSION	120

XIII.	PROJECT SKYLITE COST ESTIMATION UTILIZING THE SPACE DIVISION UNMANNED SPACECRAFT COST MODEL 121	
A.	INTRODUCTION	121
B.	THE FOUR METHODS OF COSTING	121
C.	UNMANNED SPACECRAFT COST MODEL DESCRIPTION	123
	1. Unmanned Spacecraft Data Base	123
	2. Nonrecurring vs Recurring Cost	123
	3. Areas of Activity	123
	4. The Model Methodology	125
D.	SKYLITE COST ESTIMATES	127
	1. SKYLITE Cost Estimates	127
	2. Cost Variations	130
	3. Normalized Cost Estimates	131
	4. Launch and Payload Costs	132
E.	CONCLUSION	133
XIV.	CONCLUSIONS	135
	LIST OF REFERENCES	138
	BIBLIOGRAPHY	140
	INITIAL DISTRIBUTION LIST	142

LIST OF TABLES

1. POTENTIAL FUEL REQUIREMENTS FOR SKYLITE	38
2. PROPELLANT BUDGET FOR SKYLITE MISSION	48
3. POWER BUDGET FOR SKYLITE (WATTS)	76
4. SKYLITE EQUIPMENT POWERED DURING EXPERIMENT (WATTS)	76
5. SKYLITE LOADING TABLE (LB)	92
6. DISTANCE OF SKYLITE LOADS, REFERENCED TO THE BASE	94
7. TECHNICAL AND PROGRAMMATIC SUMMARY (FROM AFSD)	124
8. TECHNICAL AND PROGRAMMATIC SUMMARY (CONTINUED)	126
9. UNMANNED SPACECRAFT COST MODEL DATABASE HISTORY (FROM AFSD)	128
10. SKYLITE NONRECURRING COSTS, FY 87S (COST IN THOUSANDS \$)	129
11. SKYLITE RECURRING COSTS, FY87S (COST IN THOUSANDS)	130
12. SKYLITE NORMALIZED NONRECURRING COSTS, FY 87S (COST IN THOUSANDS \$)	131
13. SKYLITE NORMALIZED RECURRING COSTS, FY87S (COST IN THOUSANDS \$)	132
14. APPROXIMATE PAYLOAD COSTS FOR SKYLITE	133

LIST OF FIGURES

2.1	SKYLITE Spacecraft Flight Configuration	19
3.1	Extended GAS Canister	23
3.2	Propulsion vs Payload Tradeoffs of Orion	24
4.1	MIRACL Laser Firing Limitations, Side and Top View	26
4.2	Firing Limitation Cone	27
4.3	Velocity Components of Spacecraft Depend on Elevation	29
4.4	MIRACL Slew Rate vs Skylite Alt (elevation = 80 deg)	31
4.5	Number of Daily SKYLITE Passes Through Laser Cone	32
4.6	Number of Daily 60 Second Lasing Periods Available	33
5.1	Orbital Decay Based on Atmospheric Density	39
5.2	Orion with booms deployed, front and top view	42
5.3	STS Orbits Allowing Skylite Injection with 31 kg	46
5.4	Depiction of ΔV at Perigee and Apogee	47
6.1	Eclipse and Sunlight Temperature Fluctuations	52
6.2	Configuration of Fractional Suntime Variables	55
7.1	Solar Array Arrangement on SKYLITE	68
7.2	Orbital Position Causing Minimum Solar Array Power	70
7.3	Projected Area Available-Minimum Power Orbit	72
7.4	Orbital Geometry Creating Maximum Power Output	74
7.5	Projected Area Available-Maximum Power Orbit	75
8.1	Forces Acting On SKYLITE	83
8.2	Free Body Diagram of SKYLITE	84
9.1	Loading and Placement of ORION Components	93
9.2	Cross Sectional Diagram of the ORION Baseplate	96
9.3	Cross Section of the ORION Cylindrical Shell	97
9.4	SKYLITE Position in the STS Cargo Bay	99
9.5	Loading Diagram of Skylite At Launch	100
9.6	Deflection limits for SKYLITE	103

9.7	Representation used for SKYLITE natural response frequency	104
9.8	Forces Acting on SKYLITE During Spin Up	107
10.1	Geometry determining Retroreflector Field of View	111
11.1	Sensor FOV required for Measuring Irradiance	114
11.2	Angle Between Earth's Limbs at Orbital Altitude	115
11.3	Components Required for SKYLITE Sensors	116

ACKNOWLEDGEMENTS

The authors would like to thank all of the Government and Aerospace industry personnel who have assisted in lending advice and guidance during the research and writing of this design feasibility study. Special thanks is extended to Dr. Alexander Naval Postgraduate School for his special guidance and invaluable assistance throughout the project. In addition, we would like to thank the engineers and researchers who provided great insight into the art of spacecraft design and spent a portion of their time to discuss the issues involved in designing the various subsystems of SKYLITE.

Aerospace Corporation

Mr. Rich Claster
Mr. Val Chabotov
Mr. Ernie Frank
Mr. Hans Karrenberg
Mr. Norm Lantz
Mr. Terrence Lenneman
Mr. Nelson Wallace

Ford Aerospace Corp.

Mr. Tim Abbott
Mr. Clair Miller
Mr. Howard Pollard
Mr. Vern Schmidt
Mr. Gerald Zwiern

Santa Barbara Research Center

Mr. Peter Bratt
Mr. Stillman Chase
Mr. Aram Mika
Mr. Paul Norton

ASTRO Aerospace Corp.

Mr. Karl Knapp

Optical Coating Laboratory Inc.

Mr. Isadore Sachs
Mr. W. T. Beauchamp

The following thesis is a conceptual design of a spacecraft which meets the requirements of project SKYLINE. These requirements together with satellite mission objectives are listed in chapter two. Since the SKYLINE spacecraft is a modified design of a common Orion satellite bus, the characteristics of Orion are listed for reference in chapter three. The bulk of the thesis involves the engineering analysis of the various satellite subsystems which satisfy the stated mission objectives. This analysis covering orbital selection, propulsion, thermal balance, stabilization, power requirements, and structural design is detailed in chapters four through nine. The orbital analysis solves the unique problem of satisfying orbital requirements driven by a stated laser dwell rate and geographic firing limitations. Propulsion considerations are evaluated in chapter five addressing the fuel requirements throughout the satellite lifetime. Included are orbital decay periods of spin stabilization, and orbital insertion. The thermal balance discussed in chapter six discusses why spacecraft temperature varies throughout the orbit as well as the effects of the laser generated heat upon satellite temperature. The means of satisfying electrical power demands is detailed in chapter seven. Also explained is the method of evaluating average power produced by the body mounted solar cells. Due to the method of stabilization selected, covered in chapter eight, the apparent solar area is time varying and an approach for predicting the area at any instant is provided. The stress, deflection, and vibrational requirements prescribed by NASA for C-AS can launches are analyzed in chapter nine. The attributes of the experiment payload are presented in chapters ten through twelve. Chapter ten outlines the characteristics of a retroreflector which is necessary for measuring atmospheric distortion. Chapter eleven evaluates potential sensors available for sampling the laser irradiance balancing their attributes against deficiencies when measuring relatively high power levels. The means to convey the sampled laser power to the WSMR site is described in chapter twelve. The communications demands are minimal since no storage capability is required and the data rate is relatively low. The thesis concludes with a cost estimate of the SKYLINE satellite based on the Air Force's Unmanned Spacecraft Cost Model. Several problems which arose after using this particular model for estimating small satellites and are also listed in chapter thirteen. The thesis provides the reader with the calculations, reasoning, and methodology used in the design analysis to fulfill the specified requirements.

II. SKYLITE MISSION OVERVIEW

A. PROJECT SKYLITE MISSION REQUIREMENTS

1. Orbit

The SKYLITE satellite must be designed to operate in Low Earth Orbit. The basis for the altitude and inclination selection were several requirements levied on the satellite's design by the experimenters at PMW-145. The conditions that affected the orbital selection were:

- Peak elevation of 90 Degrees
- Laser slew rate of 10 to 20 mrad/sec
- Satellite lifetime of 36 months
- Northward laser firing azimuth.
- Laser firing periods of at least 60 seconds.
- One day revisit time, allowing at least one 60 second lasing period.

Although not requested by the experimenters, the orbital selection must also depend on spacecraft survivability considerations. An orbital altitude must be selected that minimizes thermal radiation effects on the spacecraft during the high energy lasing experiment.

2. Attitude Control

The attitude of the satellite must be known to ensure that the angle of arrival of the laser beam will be within the calibrated acceptance cone of the IR sensors for significant portions of most passes within sight of the ground site. In addition, the satellite's orientation must not change rapidly or be unpredictable during the laser test. Spacecraft attitude must be known to within three degrees during the laser test.

3. Retroreflector

Retroreflectors are necessary to enhance the apparent cross-sectional area of the satellite. Several retroreflectors of light at a wavelength of 0.755 micrometers, with an effective cross-sectional area of 1.3×10^6 meters², must be attached to the Earth-end of the satellite. The retroreflectors must be able to keep the ground laser site within its acceptance cone at all times when the spacecraft is above 45 degrees elevation as viewed from the ground laser site.

4. IR Sensors

Multiple IR sensors in distributed arrays are required to detect and measure the propagated beam irradiance of the laser beams. The sensors must be capable of measuring energy in the 3.6 to 4.2 micron region at various power levels as low as 0.25 mW cm² and as high as 4.0 W/cm².

5. Gravity Gradient Boom

The SKYLITE satellite uses gravity gradient stabilization. This technique requires a gravity gradient boom for attitude stabilization. It is important that the boom is designed not only to deploy but also to retract, in case of failure to capture the spacecraft into gravity gradient stabilization. It is also important to have the ability to deploy the boom at various rates and to have an indication of boom length deployed. It will be necessary to coat or polish the boom to minimize thermal gradients which cause bending when the boom is in sunlight or in the laser beam.

6. Satellite Survivability

All structures and systems of the SKYLITE satellite are required to survive a 36 month exposure to the natural charged particle radiation environment appropriate to the 700 kilometer orbit and the transient temperature increases which occur during the high power laser test.

7. Electrical Interfaces

While on the launch pad, provisions must be made to monitor the SKYLITE satellite using hardlines to the crew monitoring station in the cabin. Provisions must also be made to maintain battery charge while on the pad.

8. Launch Requirement

While awaiting launch from the GAS can into a parking orbit, it will be required to maintain temperatures in the GAS can to those of the survivable limits of the satellite.

B. SKYLITE SATELLITE DESCRIPTION

The SKYLITE satellite is a gravity gradient stabilized 125 kilogram cylindrical main structure, 35 inches long and 19 inches in diameter with 1) a gravity gradient boom extending 10 meters from the space end of the structure, and 2) four 1.33 meter long sensor arms extending in the $\pm x$ and $\pm y$ directions located at the mid-section of the spacecraft. The end of the gravity gradient boom contains a tip mass of 10 kilograms with solar cells attached to the space end. The spacecraft configuration and

mass is designed to fit into the extended Get-Away-Special (GAS) can onboard the Space Shuttle. The design will also assure that the lifetime of the mission will exceed 36 months when placed into an orbit of 700 kilometers. The SKYLITE spacecraft flight configuration, shown in Figure 2.1, illustrates the features of the SKYLITE satellite.

Because of the spacecraft structure and the nature of gravity gradient stabilization, the sensor plane on the SKYLITE satellite will be oriented approximately normal to the Earth radius, and facing Earth, while the opposite end will be pointed toward space. A five eye sun sensor and a magnetometer will be used to determine the attitude of the satellite.

To satisfy SKYLITE mission requirements, the satellite contains an array of IR sensors for evaluation of radiation from the MIRACL laser. These sensors are located on the Earth-end of the satellite and on the ends of the four booms extending from the mid-section of the spacecraft.

Several retroreflectors are attached to the Earth-end of the satellite. An Alexandrite laser, housed directly on top of the MIRACL laser, will be used with the retroreflectors to measure atmospheric parameters along the path followed by the MIRACL laser beams. This atmospheric probe beam from the Alexandrite laser is reflected from the retroreflector to a ground based receiver at the laser site and is used to characterize the column of air through which the probe beam traveled.

Based on the measured intensity variations across the wave front of the reflected beam measured at the laser site, the MIRACL laser optics are adjusted to compensate for atmospheric effects and an adapted MIRACL laser beam is directed through nearly the same atmospheric column just measured, toward the sensor array on the satellite. The MIRACL laser beam's cross sectional intensity is sampled, at a high data rate, and measured by the IR sensors. This data is transmitted in real time to a ground station, which is located at either White Sands or a designated Spacecraft Ground Link System (SGLS) site, and relayed to the laser facility for processing.

The power subsystem is designed to supply power for one experiment which will last no longer than one minute in duration, during a minimum sun orbit. On the average, six to eight experiments per year will be conducted. SKYLITE power is provided by solar cells mounted on the body of the satellite and on the space-end of the gravity gradient tip mass. The 0.602 square meters of solar collectors produce between 53 and 64 watts of energy. One 130 watt-hour NiCad battery stores the energy until it is required.

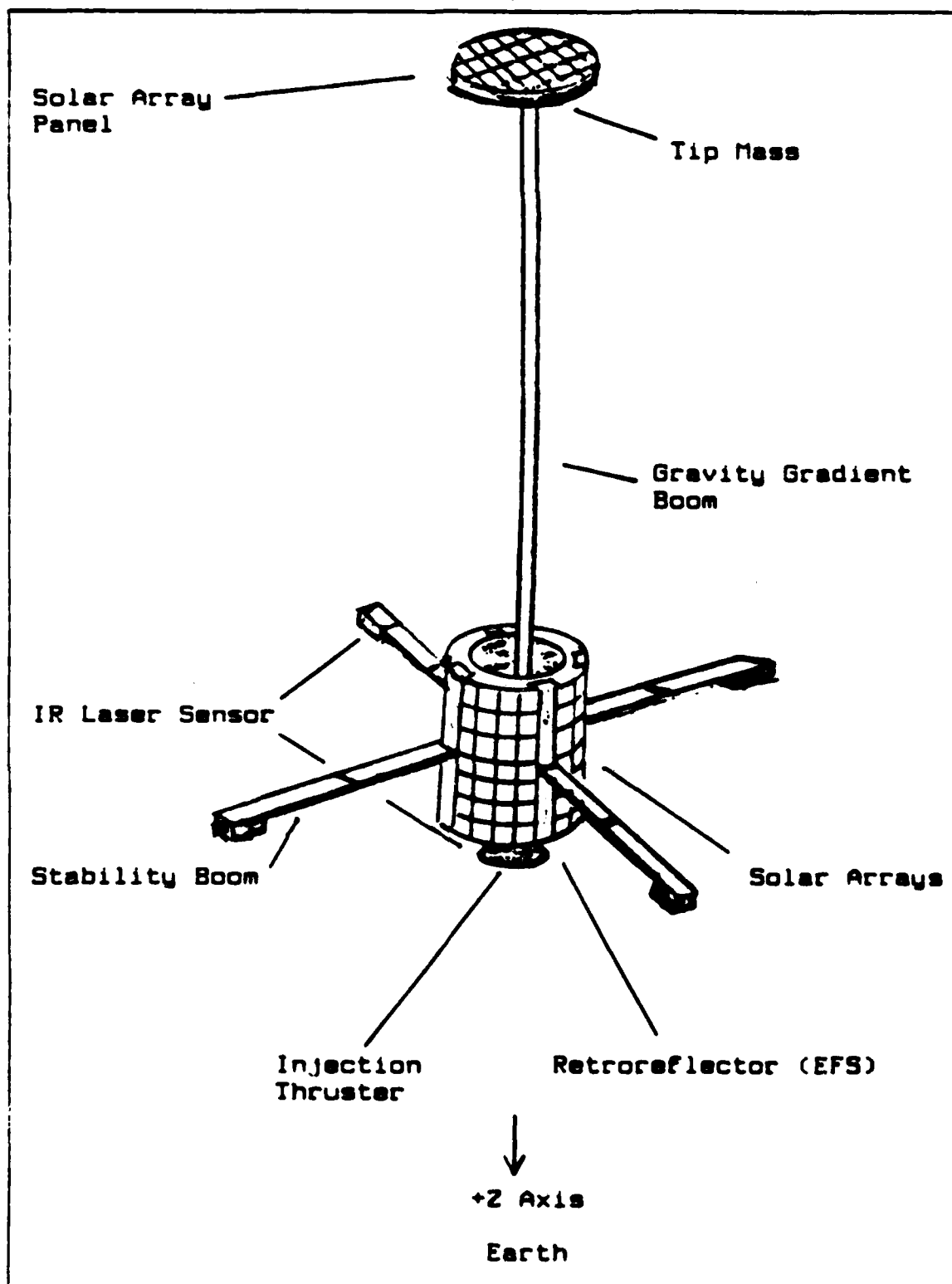


Figure 2.1 SKYLITE Spacecraft Flight Configuration.

A telemetry, tracking, and command subsystem (TT&C) provides operational control of the satellite. It is commanded by uplink commands and onboard stored commands. The TT&C subsystem supports the mission function by telemetering the IR sensor data from the sensor array subsystem to the ground in near real time, and providing command and verification capability for deploying the gravity gradient boom and capture of the spacecraft into gravity gradient stabilization. The TT&C also performs a housekeeping function by providing real time equipment fault monitoring and it collects and conditions telemetry from the spacecraft subsystems while performing this function.

A radio frequency subsystem provides communication between the SKYLITE satellite and the ground station via a 1.0 KBPS S-band command link and a 1.0 MBPS S-band data link. The White Sands Missile Range or a designated SGLS site will provide communications with the SKYLITE spacecraft. It is intended that the communications system will be SGLS compatible.

C. SKYLITE LAUNCH PROFILE

The SKYLITE satellite is designed to be launched from the extended GAS Can onboard the Space Shuttle into a circular parking orbit between 400 and 1400 kilometers at an inclination angle between 28.5 and 37.5. The separation point has not yet been determined. The satellite will extend four arms in each of the x and y directions for stabilization and then spin up using four one pound thrusters. The satellite will then burn a five pound kick motor and make an altitude and plane change into an operational orbit of 700 kilometers and to an inclination of 33 degrees. Once operational orbit is obtained the spacecraft will despin. The gravity gradient boom will be deployed to capture the satellite into gravity gradient stabilization. Provisions have been made to retract the boom and re-attempt capture if the first attempt fails. The SKYLITE satellite is designed to be operational for 36 months.

D. MISSION OPERATION SUMMARY

The tracking of the spacecraft can be performed at certain times during a pass by the Alexandrite tracking laser. The spacecraft's retroreflector will be illuminated by the tracking laser beam, and by means of a ground based receiver, observe its reflected beam of light.

During experimental operations, the Alexandrite illuminating beam is turned on and aimed at the satellite using the spacecraft ephemeris data and the precomputed

trajectory as the satellite ascends above the 45 degrees elevation angle from White Sands. At 60 degrees elevation angle the MIRACL laser is turned on, and the IR beam strikes the satellite. The IR sensor array measures the incident beam's energy. Background measurements are taken just prior to and immediately after the experiment. A single pass will typically last less than fifteen minutes, but the experimental portion of a pass when the MIRACL laser is fired will last no longer than one minute. Experiments using different power levels will be attempted. The power incident on the satellite will range from 0.25 milliwatts per square centimeter to 4.0 watts per square centimeter. The laser beam power will remain constant during each experiment.

Onboard the satellite, the IR sensor array subsystem receives the IR beam and measures its intensity distributed across the sensor array. Signal strength at each sensor location is measured nearly simultaneously, then encoded and sent directly to the wideband downlink formater. The output is modulated onto the S-band carrier in the S-band transmitter, along with housekeeping data. This combined signal is radiated from the satellite S-band cross-dipole antenna to the ground stations receiving dish at 1.0 MBPS. The ground station demodulates the data and sends near real time data to the experimenter for analysis.

III. THE ORION CONCEPT

The basic spacecraft bus selected for the SKYLITE design is a variant of the Orion spacecraft. Orion is the program name assigned to a collective project begun at the Naval Postgraduate School (NPS) in the fall of 1985. The program's focus is the design and construction of a satellite. NPS students provide most of the engineering and design effort, with the remainder subcontracted as funds allow. Each engineering discipline at NPS would concentrate on pertinent spacecraft design problems. For example, mechanical engineering students will concentrate on structures, response to vibration, and thermal control. All Orion design considerations emphasize low cost access to space. This satellite will fill a current industry wide void by providing a common bus to transport a variety of mission oriented hardware.

The Space Transportation System (STS) has the ability to launch small spacecraft by placing them into small canisters secured in the cargo bay. Payloads launched by this method are called Get Away Specials (GAS), and the launching canisters acquired the name GAS Can. This dispenser attracted enough interest to warrant the design and development of a slightly larger receptacle, called the Extended GAS Can. The Extended Gas Can, illustrated in Figure 3.1, has an inner diameter of 19 inches and length of 35 inches. The Orion spacecraft selected for the SKYLITE experiment will be deployed via the Extended GAS Can, and must adhere to these volume constraints. As of August, 1987, the Extended GAS Can was under design, with an anticipated first flight date of late 1989. This date will coincide with the completion of construction on the SKYLITE spacecraft.

The main features of the Orion spacecraft will be presented, with discussion of specific points relevant to the SKYLITE spacecraft. The Orion satellite is designed as a bus to ferry small, relatively simple payloads into low Earth orbit. The payload capability is between 50 and 130 pounds, depending on mission duration and desired propulsion. If the 130 pounds of mission equipment is required the launch weight of Orion will be 275 pounds. Three basic models of Orion are available, with the tradeoffs of propellant versus payload weight. The longer lived and high orbit experiments require the most propulsion, decreasing available payload weight. Conversely, the short lived and low altitude experiments are allowed maximum payload due to the small fuel demands. These tradeoffs are illustrated in Figure 3.2. [Ref. 1: p. 1-32]

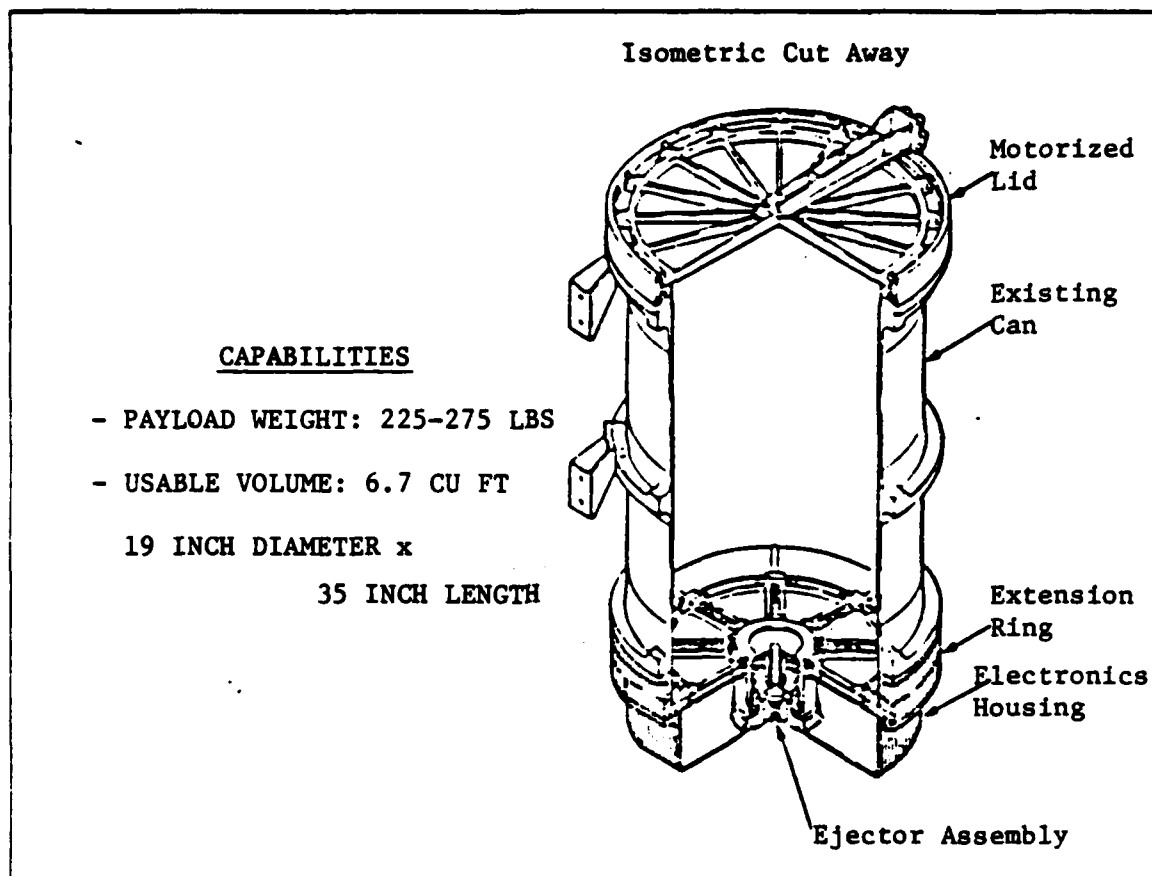


Figure 3.1 Extended GAS Canister.

The Orion satellite has been designed with 7 thrusters. Six thrusters are .1 lb_f rated, and used for spin up and attitude control. The seventh thruster is 12 lb_f and is used for insertion and stationkeeping. Spin stabilization, with appropriate sensors to ascertain attitude, is the method of stabilization. Since the spacecraft is inherently unstable when spinning, a means to introduce stability is necessary. For SKYLITE the extension of four short booms, with masses attached at the end, provide the desired stability. If no additional stabilization method is developed, the majority of Hydrazine fuel will be quickly consumed by Active Nutation Control. The Electrical Power System of Orion will provide 15 watts of continuous power to the payload module. The power supply will be body mounted solar cells supplemented during eclipse by Nickel Cadmium batteries. Although not necessary for the SKYLITE, Orion has a bubble memory data recorder aboard. The satellite will have an inherent SGLS and TDRSS compatible telemetry system as part of the bus support. [Ref. 1: p. 1-32]

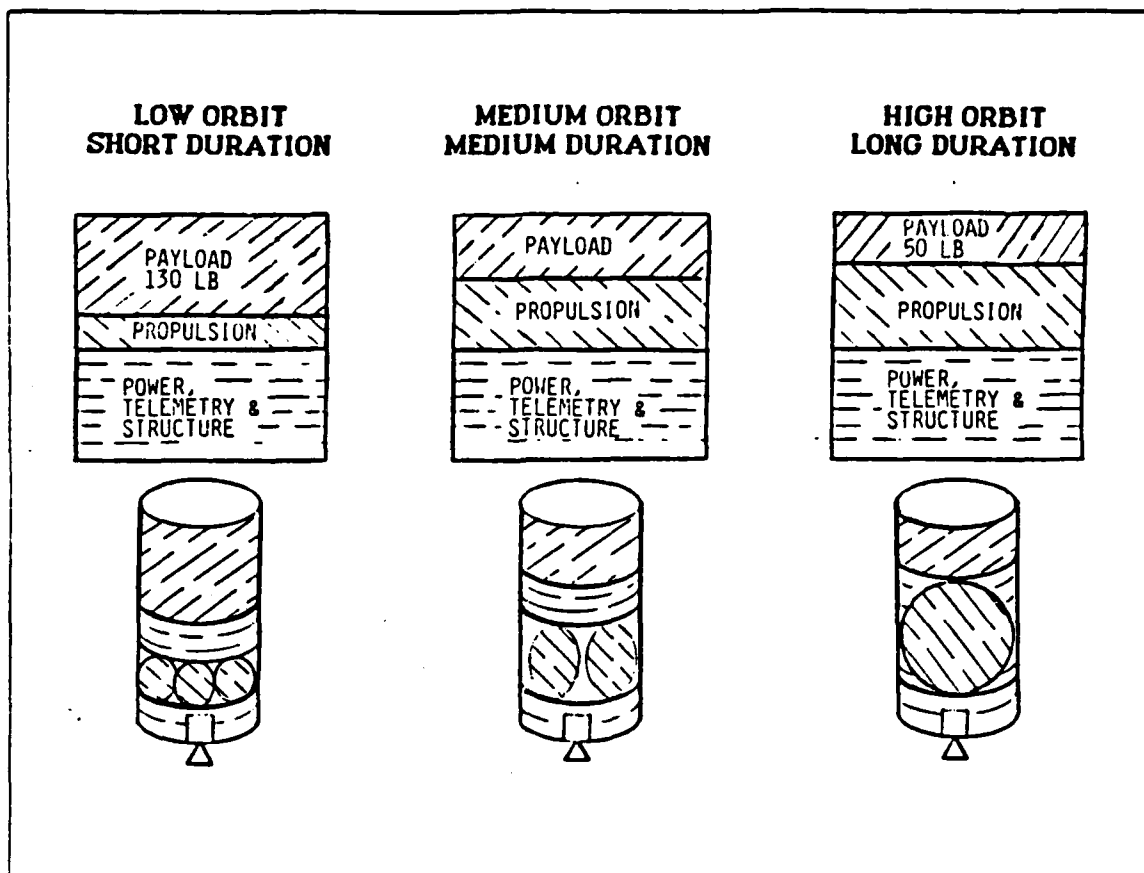


Figure 3.2 Propulsion vs Payload Tradeoffs of Orion.

Two major modifications to the Orion spacecraft will be required for the SKYLITE experiment. These modifications are the addition of several IR sensors on the Earth facing side of the spacecraft and the inclusion of an extendable gravity boom and tip mass. The sensors fulfill the basic experimental purpose, which is measuring the incident radiation from a laser. The gravity gradient boom is necessary to provide a passive stabilization method for SKYLITE, once it arrives on station. If the passive stabilization method was not used, the active method of Active Nutation Control would consume such large quantities of Hydrazine that the experiment lifetime would be significantly shortened.

IV. ORBITAL ANALYSIS

A. INTRODUCTION

Proper orbit selection is the most important aspect of the satellite design process. All other elements in the design process depend upon orbital selection. For example, the particular orbit selected enables the solar panels to achieve their proper orientation with respect to the arriving solar radiation, as well as finely balances the thermodynamic considerations in the thermal design. Typically, the selection of an orbit is a compromise which simultaneously provides for accurate experimental results and creates a healthy environment for satellite operation.

The demands placed on the SKYLITE orbital selection were considerable [Ref. 2]:

- Peak elevation of 80 degrees.
- Laser slew rate of 10-20 mrad/sec.
- Satellite lifetime of 36 months.
- Northward laser firing azimuth.
- Laser firing periods of at least 60 seconds.
- One day revisit time, allowing at least one 60 second lasing period.

Although not specifically requested by the experimenters, an additional requirement became necessary. The satellite exposure to thermal damage by the laser must be minimized. As the orbital altitude increases, laser path loss also increases, thus lessening the laser irradiance at the spacecraft. A baseline value for satellite altitude, and consequently, propagation path loss, would provide a maximum laser irradiance at the spacecraft upon which the thermal design and spacecraft protection could be based. This baseline altitude was selected to be 500 kilometers, and is the minimum altitude allowable for SKYLITE. Should the satellite decay below 500 kilometers, the decreasing laser path loss would raise the irradiance to intolerable values. The spacecraft will be inserted into a 700 kilometer orbit, and subsequent analysis must determine whether compensation is necessary to counteract orbital decay. The requirements listed above were examined for their effect on orbital selection. Their impact is subsequently explained, with elaboration on pertinent phenomena.

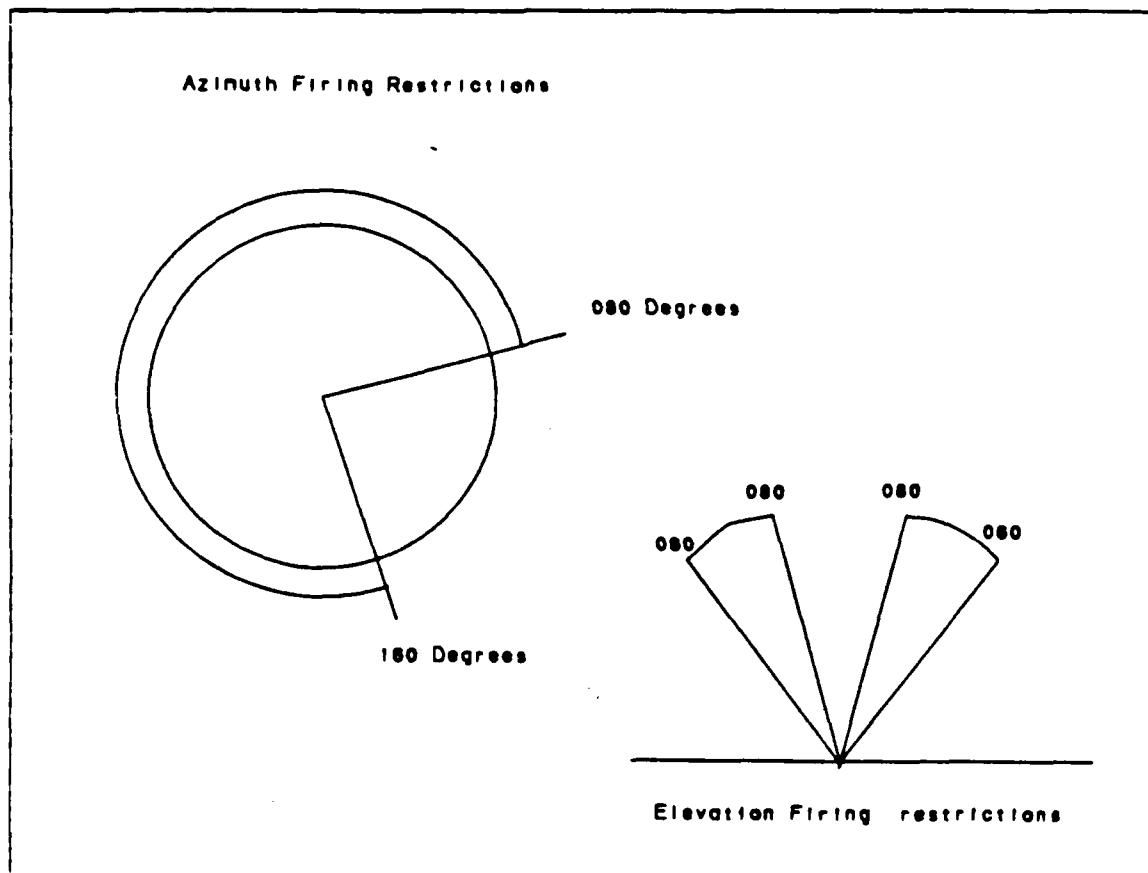


Figure 4.1 MIRACL Laser Firing Limitations, Side and Top View.

restrictions due to construction of the laser are severely limiting. This affects the orbital selection. Since the purpose of the SKYLITE experiment is to measure irradiated power on a spacecraft from the MIRACL laser, the spacecraft must be in a position to be illuminated by the laser beam. If the laser had unrestricted freedom in azimuth and elevation, the selection of a proper orbit would ensure the MIRACL laser site at White Sands Missile Range (WSMR) passed within the satellite swath width. The specific limitations of the MIRACL laser in azimuth are (relative to true north) 160 degrees clockwise to 080 degrees. The elevation limits are 060 degrees to 080 degrees. These restrictions are illustrated in Figures 4.1 and 4.2. The satellite must fly through the annular cone described by the laser firing limitations to adequately sample laser power. [Ref. 2]

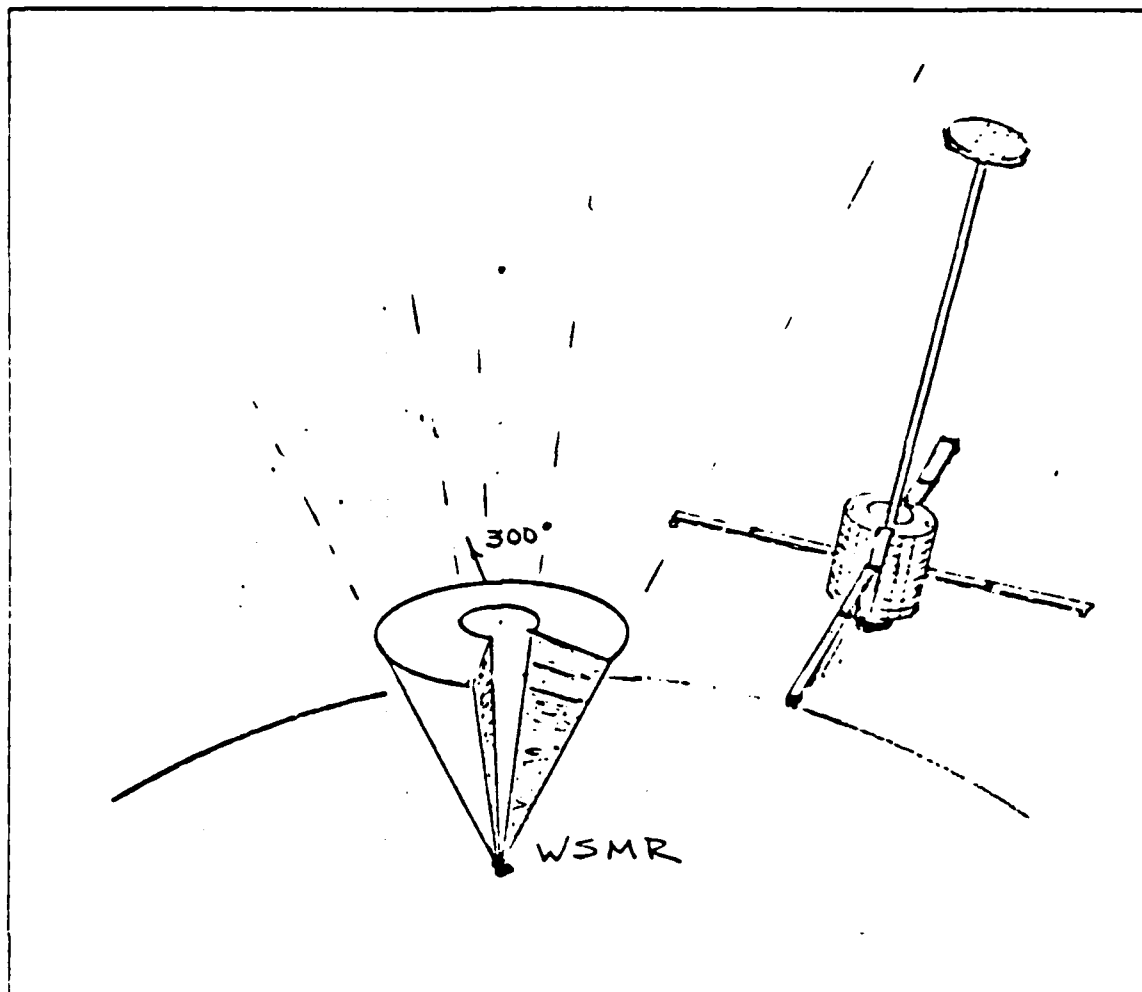


Figure 4.2 Firing Limitation Cone.

B. ORBITAL INCLINATION

The orientation of the azimuthal restrictions affect the selection of the satellite inclination. The specific inclination which maximizes the number of satellite passes through the firing cone must be selected. Except for a firing bearing of 080 to 090 degrees, any pass to the north of the MIRACL site at 60 to 80 degrees elevation provides conditions for a successful shot. The restrictions on a southward firing bearing are more severe. For a southern shot, the restricted azimuth is 080 to 160 degrees, or almost half of the available bearings. Thus, a northern firing bearing was selected which would be satisfied by the satellite deployment into an inclination greater than the latitude of the MIRACL site. Since the MIRACL site is at 32.6 degrees North latitude, a 33 degree orbital inclination was selected for SKYLITE. The dependency of

spacecraft subsystems, such as the propulsion system, on orbital selection becomes immediately apparent. The propellant aboard SKYLITE must be sufficient for orbital injection after deployment from STS. The Propulsion Analysis chapter demonstrates SKYLITE's capability to reach orbits of 33 degrees inclination from a range of STS orbits. Thus, the inclination of SKYLITE, based on MIRACL azimuthal firing constraints, is consistent with the capabilities afforded by spacecraft subsystems.

C. MINIMUM ORBITAL ALTITUDE

The effect of the 36 month orbital lifetime requirement, which is also intimately related to propulsion, is also examined in depth in the propulsion chapter. The altitude requirements were to maintain the satellite altitude above 500 kilometers. At and above 500 kilometers the laser path loss was great enough to reduce laser intensity to a level tolerable by spacecraft hardening. SKYLITE, as is true of all spacecraft, is extremely sensitive to temperature fluctuations. The thermal balance is delicate and precisely controlled. Should the spacecraft descend to an altitude at which the satellite thermal hardening techniques may be overcome by laser irradiance, the thermal balance will be catastrophically upset. Another orbital parameter, the satellite altitude, is now defined, based on the need to lessen the laser's power by increasing its path loss.

D. MAXIMUM ORBITAL ALTITUDE

The minimum satellite altitude was contingent on the need to mitigate laser thermal damage. The upper altitude limit is dictated by the laser slew rate consideration. The MIRACL laser does not have an unlimited train rate throughout its attainable azimuths and elevations. Instead, it must be limited to slew rates of 10 to 20 mrad/sec. The altitude of the satellite affects the slew rate directly. The lower the altitude, the quicker the satellite crosses the field of view. Conversely, the higher the satellite, the slower the satellite traverses the field of view. At geosynchronous altitude of approximately 36,000 kilometers, the period of satellite revolution equals the rotation of the earth, and the satellite appears stationary. An approach was required to refine the upper altitude between 500 and 36,000 kilometers.

The following discussion evaluates the satellite orbital altitudes which correspond to slew rates of 10 to 20 mrad/sec. This slew rate represents the angular velocity of the MIRACL pointing mirror as it tracks and lases SKYLITE. The tendency is to approach the problem and evaluate the slew rate in terms of angular velocity at the Earth's center. Although this approach is considerably simpler, the results would be

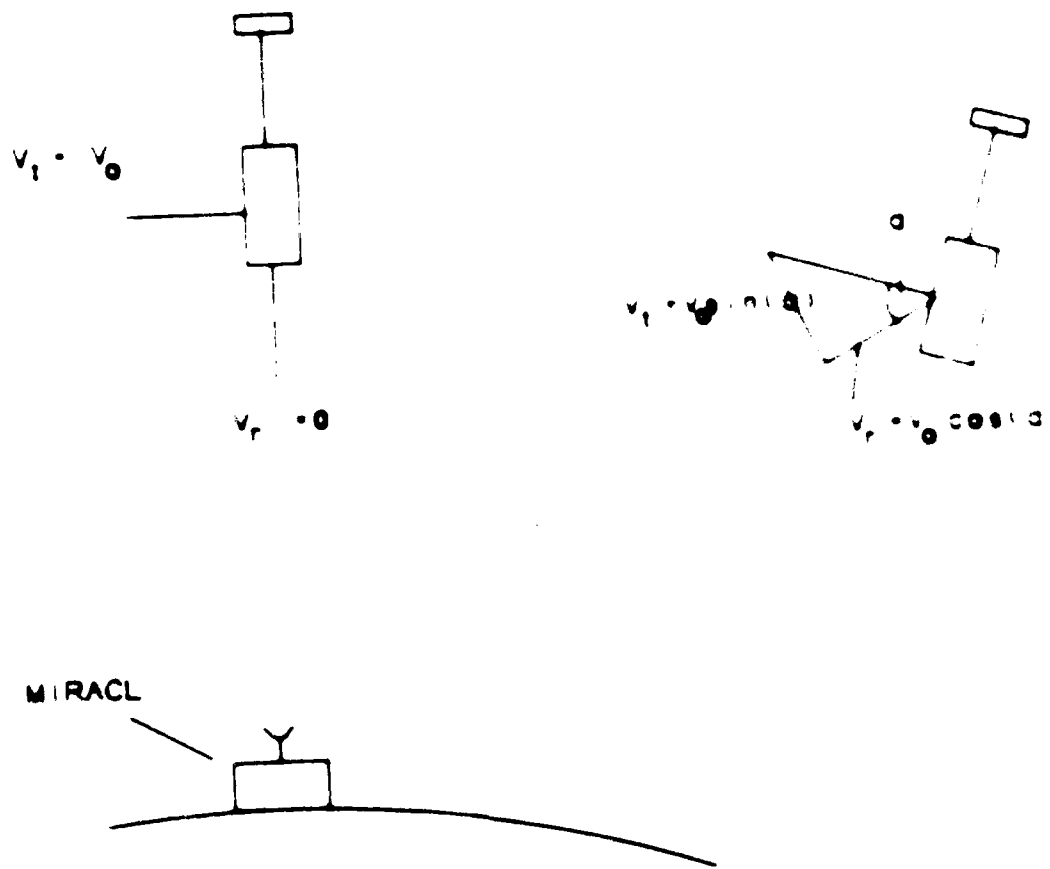


Figure 4.3 Velocity Components of Spacecraft Depend on Elevation

erroneous. To illustrate this problem Figure 4.3 is used. A means is necessary to relate the altitude of the satellite to the angular velocity of the MIRACL pointing mirror. The elevation of the mirror, due to previously discussed limitations, is restricted to between 60 and 80 degrees. For a point on the Earth's surface the slew rate becomes maximum at the point of maximum tangential velocity. The spacecraft velocity vector can be divided vectorially into a tangential and radial component. The absolute velocity of the satellite is given by the basic orbital equation listed below

V_0 = Orbital Velocity

$V_0 = \sqrt{k(r_e + h)}$

r_e = Radius of the Earth

h = Altitude of the satellite (m)

The tangential and radial components of the spacecraft velocity will vary as the elevation angle changes. This is illustrated trigonometrically in Figure 4.3. The maximum view rate will occur at the mirror elevation closest to 90 degrees. For the MIRACL mirror, the maximum elevation angle is 80 degrees. At an elevation angle of 80 degrees, the radial and tangential components are indicated in the following equations:

$$V_t = \text{Tangential Velocity}$$

$$V_r = \text{Radial Velocity}$$

$$V_t = V_s \sin 81^\circ$$

$$V_r = V_s \cos 81^\circ$$

At the instant the satellite is at an elevation of 80 degrees, the instantaneous angular velocity is determined in the following equations:

$$V_t = r \omega$$

$$r = \text{Distance from MIRACL to SKYLITE}$$

$$\omega = \text{Instantaneous angular velocity}$$

Since the distance from the laser site to the spacecraft is a function spacecraft altitude, the view rate, which is dependent on distance to the satellite, is also a function of spacecraft altitude. Thus, the view rate will vary as spacecraft altitude varies. The graph in Figure 4.4 illustrates the variance in view rate with changing SKYLITE altitude.

Upon examining Figure 4.4, the altitude for compliance with the experimenter's 10 mrad/sec view rate becomes more definite. At an elevation of 80 degrees, SKYLITE altitude must be less than 200 kilometers to ensure the 10 mrad/sec view rate. The altitude selected for SKYLITE was 200 kilometers. This height satisfies the view rate restrictions by a significant margin. This altitude, as is discussed in the propulsion chapter, also meets requirements for lessening orbital decay and allowing spacecraft injection.

E. FREQUENCY AND DURATION OF LASING PERIODS

The final orbital requirement, determining the frequency of valid firing periods, required sophisticated computer-based iterative solutions. A valid firing period is any time SKYLITE is in the MIRACL firing cone for more than thirty seconds (Ref. 1). A momentary pass of the satellite throughout the laser cone was not sufficient. The facilities at the MIRACL laser site are extremely expensive, requiring

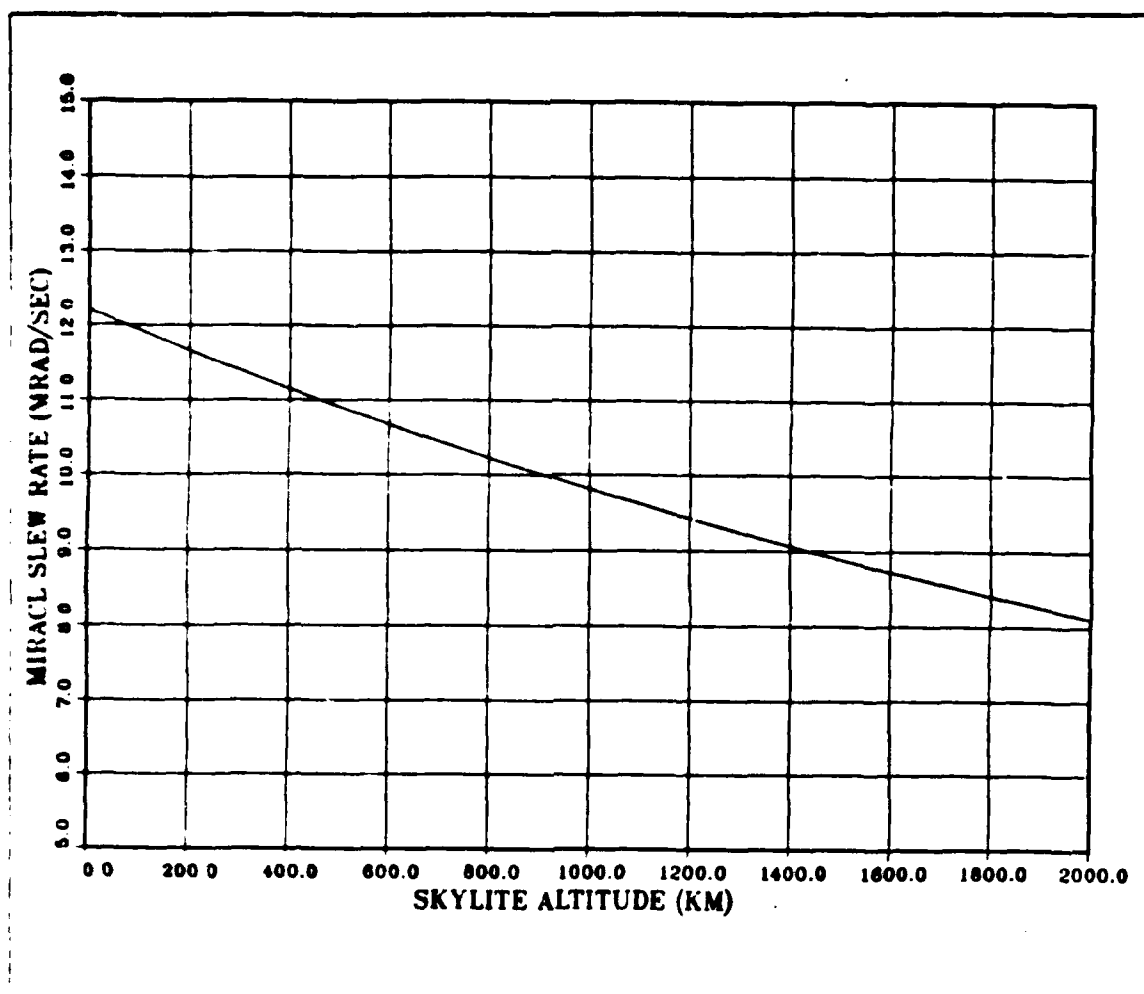


Figure 4.4 MIRACL Slew Rate vs Skylite Alt (elevation = 80 deg).

careful scheduling of sophisticated equipment. To allot the expensive facilities at WSMR to a satellite lasing period, a high degree of confidence that the spacecraft will appear for its prescribed duration is necessary. The solution to the final requirement was not trivial and was prohibitively difficult to solve analytically. The capabilities of two sophisticated orbital computer programs were applied towards an iterative solution of this requirement. The satellite orientation which satisfies all other conditions was selected for analysis by these two programs to observe if it also successfully met the 30 second firing period requirement. SKYLITE's proposed 700 kilometer altitude and 33 degree inclination were investigated to determine if they met the lasing period requirements.

The computer programs used to assist the lasing period study were Amoeba, provided with the assistance of Aerospace Corporation, and the Navy Exercise Support Terminal (NEST). Both programs similarly modeled the flight of SKYLITE through many orbits and counted the number and duration of each pass which entered the MIRACL lasing cone. The pointing angle limitations of the MIRACL laser were adequately modeled, together with SKYLITE ephemeris data. The NEST program was particularly helpful in accounting for the orbital iterations during a long time interval, and the Amoeba program contributed greatly to the analysis of each specific orbit, if desired.

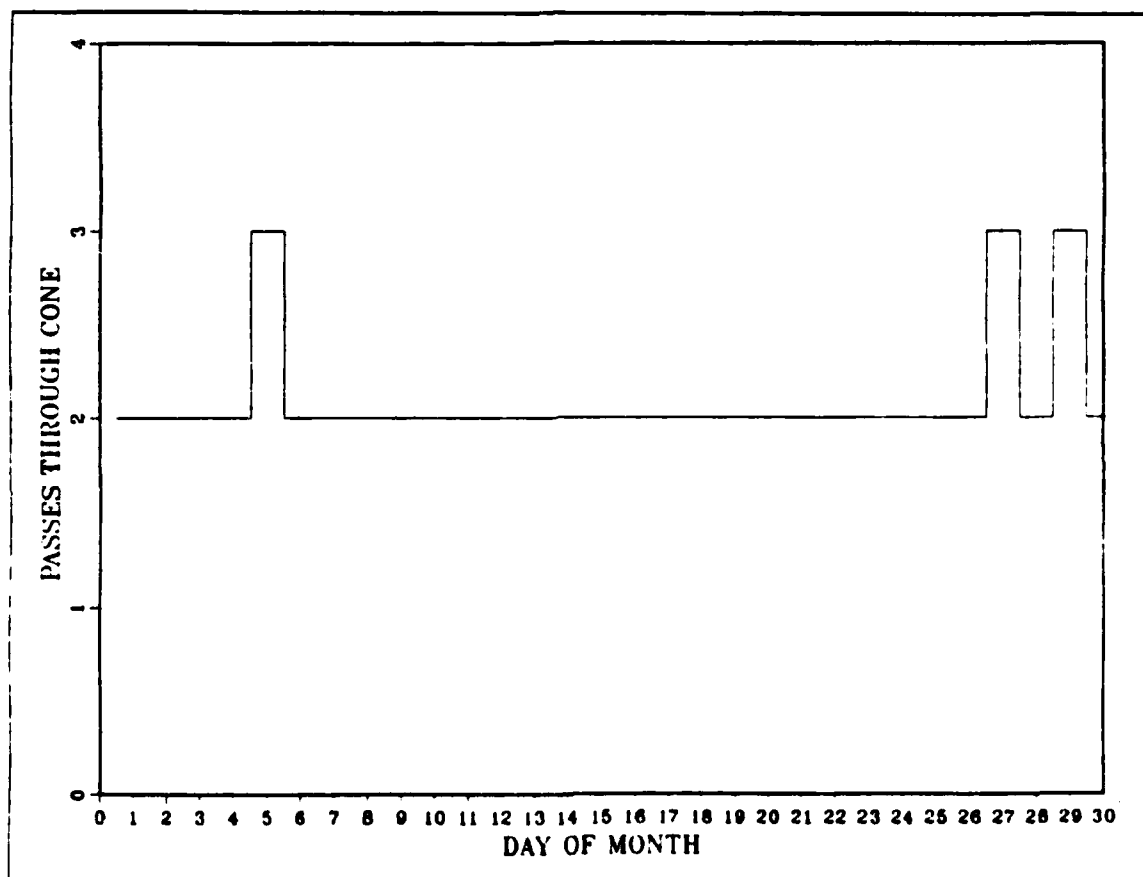


Figure 4.5 Number of Daily SKYLITE Passes Through Laser Cone.

The results of each program were coincident. They agreed in both periodicity and duration of lasing periods. The trend of lasing periods, as illustrated in Figures 4.5 and 4.6 demonstrated that the proposed orbit of 700 kilometers and 33 degrees, was

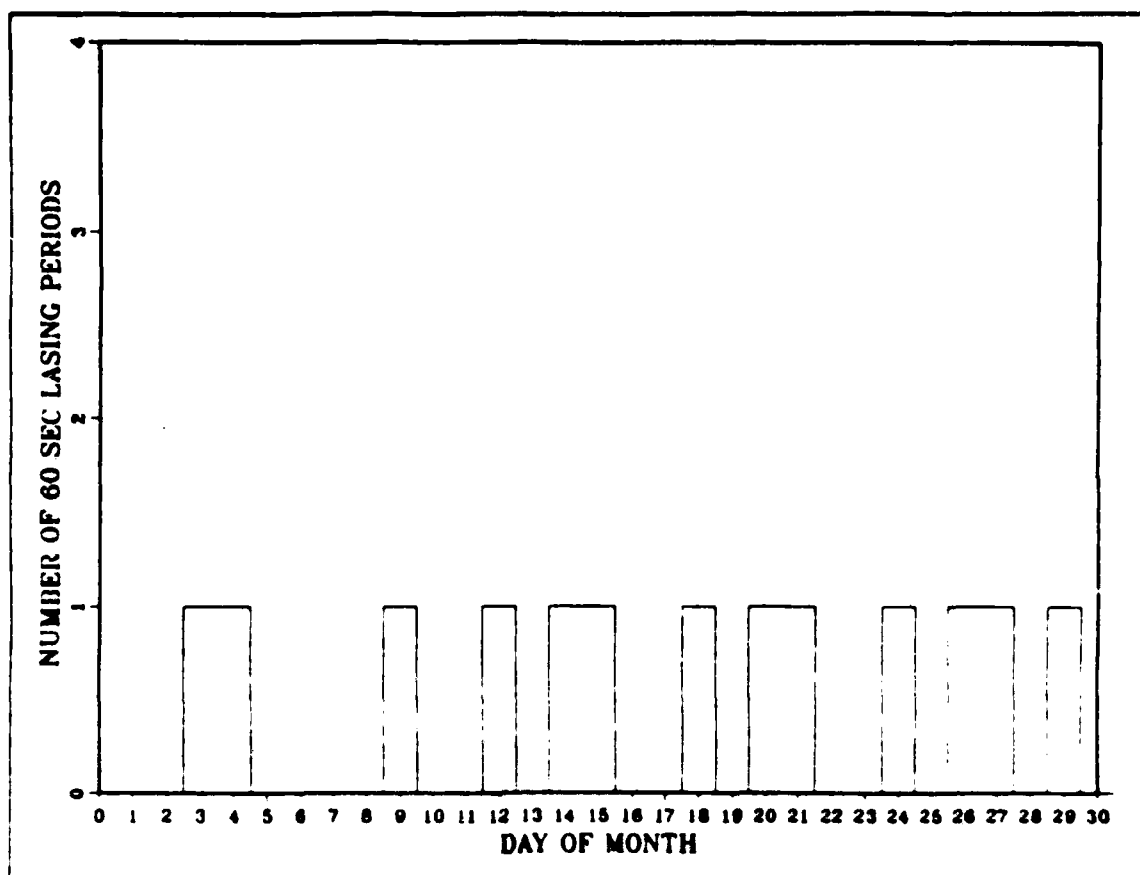


Figure 4.6 Number of Daily 60 Second Lasing Periods Available.

adequate for the lasing period requirements. Although the 60 second lasing period did not appear daily, it was available on approximately half of all the days analyzed. The MIRACL laser will actually illuminate SKYLITE at a frequency of 6 times per year for the satellite lifetime of 3 years [Ref. 2]. At peak lasing periods the spacecraft may be lased approximately once per week for six weeks. The 50 percent daily availability of 60 second lasing periods was judged sufficient for the SKYLITE mission, given the relative scarce number of illumination periods. A lasing period occurring every other day is more than sufficient to meet anticipated MIRACL laser demands.

The previous analysis must be repeated for the orbital altitude at the end of the satellite's lifetime. Atmospheric drag may cause the orbital altitude to decay to a point that the periodicity requirements will no longer be met. A decay analysis, as explained in the Propulsion chapter, indicated the orbital decay, after 36 months would be approximately 20 kilometers, leaving SKYLITE at an altitude of 680 kilometers. The

analysis on the frequency and duration of lasing periods was repeated for an altitude of 680 kilometers. No substantial change in either frequency or duration of lasing periods was noted.

F. CONCLUSION

The difficulty of selecting an orbit which satisfies all restrictions was evident in the described analysis. The selected orbit satisfies the orbital requirements listed by PMW-145, with the exception of frequency of firing periods. The chosen orbit provides a 60 second laser firing period approximately every other day, vice daily, as PMW-145 specifications required. Given the few lasing periods per year (approximately six), the need to wait an additional day does not inhibit laser operations sufficiently enough to warrant expenditure of more funds (for one or two more satellites) to meet the initial PMW-145 laser period requirement.

The selected orbit at 33 degrees inclination and 700 kilometers altitude successfully meets the specifications regarding thermal damage mitigation, satellite lifetime, laser slew rate, and firing duration. The ability to meet all requirements, save one, with a single satellite provides great operational flexibility. The laser experiment can be adequately conducted once a single spacecraft is orbiting, instead of waiting for two or three satellites to achieve successful orbit.

V. PROPULSION ANALYSIS

A. INTRODUCTION

The Orion propulsion system will be implemented into the SKYLITE design with no modifications. The outlined propulsion components are ideal for combining the high reliability of the Orion concept with the long lifetime required in the SKYLITE experiment. However, although SKYLITE will use the same propulsive elements as Orion, they will be employed differently due to the differences in stabilization techniques. The Orion concept provides for spin stabilization, with Active Nutation Control based on the differences between spin and transverse moments of inertia. The fuel consumed would be distributed among the requirements for spacecraft insertion, nutation control, and orbital decay compensation. For the SKYLITE spacecraft, the use of gravity gradient stabilization eliminates the consumption of fuel for attitude control and makes the surplus available for other uses. The significant amount of fuel saved by using passive stabilization then becomes available for satellite insertion, thus expanding the range of STS orbits allowing successful injection to the SKYLITE station. Fuel aboard SKYLITE, not used for insertion, will be used to spin up and retard the satellite as it proceeds to station.

The propulsion system designed for Orion offered three basic configurations. One of the options was to be selected for each Orion variant, optimizing the tradeoffs between payload weight and lifetime. The selection differences presented a choice between taking a large amount of fuel with a small payload or, conversely, a small amount of fuel creating space for a large payload. The equipment and volume constraints for the SKYLITE payload offered the situation that, due to the relatively undemanding volume constraints, no tradeoff between payload and fuel became necessary. This advantage is considerable. The SKYLITE spacecraft has a long lifetime, is insertable from a wide envelope of STS orbits, and allows all experimental instrumentation to be placed on board for the duration of the experiment.

The Orion propulsion system, as selected for the SKYLITE satellite consists of a 16 inch (O.D.) spherical hydrazine storage tank, 6 thrusters rated at .1 lb_f, 1 main thruster rated a 12 lb_f, and piping connecting the thrusters with the tank. The propellant used for all thrusters is Hydrazine, rated at a specific impulse of 220

seconds. The small thrusters are designed for spin up and spin down, and the large thruster is used for spacecraft insertion. Although the specific impulse of Hydrazine could be boosted substantially with thruster heaters, the electrical draw to sufficiently power these heaters is prohibitive. The propulsion design takes great advantage of the ability to turn the thrusters on and off repeatedly, providing great flexibility over the use of solid fuel. [Ref. 1: p. 1-32]

The fuel contained in the storage tank is balanced against the requirements for the SKYLITE flight profile. The sequence of fuel consumption is as follows. The STS orbiter will eject the SKYLITE satellite into a position from which the spacecraft can reach operational altitude and inclination. Once the shuttle is safely clear of the spacecraft, the SKYLITE will be directed to deploy its short stabilizing booms and begin spin up. Once a rotational velocity of 100 rpm is reached, the attitude control thrusters will turn the satellite and the main thruster will fire, beginning the journey to station. Two major main thruster burns will occur. The first burn happens at perigee, commencing a Hohmann transfer ellipse to the orbital altitude. The second burn begins at apogee and circularizes the orbit at operational altitude. The inclination change angle will be divided into a plane change at perigee together with a plane change at apogee. A program exists, which will be subsequently explained, that determines the optimal plane change at perigee and apogee giving the least required delta velocity and fuel consumption. Once station altitude and inclination is attained, SKYLITE is despun, eliminating all rotation about the longitudinal axis. The conditions for gravity gradient capture are examined, and if they are found satisfactory, the boom will be extended. If the capture is unsuccessful, the gravity gradient boom will be retracted and stabilization will be reattempted. This last feature is an advantage of retaining the Orion's attitude control thrusters for SKYLITE, when at first examination, they appeared extraneous for gravity gradient stabilization. The presence of the attitude control thrusters will provide the means for reorienting the spacecraft should the spacecraft be captured upside down or if capture is unsuccessful. As evidenced by several capture attempts and subsequent mission aborts, the process of capturing spacecraft stabilization with the gravity gradient method is extremely tenuous. Any means to provide several attempts at capture raises the reliability of the mission.

Thoughtful evaluation of the fuel demands throughout the mission will provide a plan for fuel consumption. The largest fuel demand will be that necessary to place the

spacecraft into its desired orbit. The priorities impacting the decision for a specific orbit will be explained. The experimental considerations which indicated the optimum orbit follow. The Navy office directing the SKYLITE experiment outlined the physical firing constraints on the MIRACL site at White Sands Missile Range. For reasons evaluated in the Orbital Analysis chapter, an orbit of 33 degrees inclination and 700 kilometers was selected. Thus, the satellite is given an orbital requirement based on experimental constraints. The propulsion system must move the satellite from the STS orbit to the operational orbit, and satisfy these orbital requirements. Also, the SKYLITE altitude is governed by the need to mitigate thermal damage due to MIRACL's irradiance. An altitude region between 500 and 700 kilometers provides sufficient laser path loss to prevent laser damage to satellite components. This altitude requirement places a demand on the propulsion system to compensate for orbital decay of the spacecraft, should it descend below 500 kilometers.

The envelope of operation for the SKYLITE and its propulsion system is now defined. The Orion propulsion system, as applied to SKYLITE, must insert the satellite from as wide a shuttle envelope as possible. It must also compensate for orbital decay, should the satellite altitude wither to less than 500 kilometers and it should provide fuel for spin up and spin down as station is attained. The following calculations figure the amounts of fuel consumed by each of these three requirements and show the best distribution of available fuel in meeting these requirements.

B. TOTAL FUEL AVAILABLE

The Orion variant selected for SKYLITE provides the most fuel available of any Orion design. The fuel is contained in a large spherical tank located in the lower half of the bus. All the Hydrazine available for any propulsion application resides in this tank. The total fuel available to SKYLITE during its three year mission can be calculated given the density of Hydrazine and the internal volume of the sphere.

$$\rho \text{ of Hydrazine at } 68^\circ \text{ F} = 1.0085 \text{ g/cm}^3$$

$$\rho \text{ of Hydrazine at } 32^\circ \text{ F} = 1.0256 \text{ g/cm}^3$$

The volume of the tank is computed from its internal radius of 7.76 inches.

$$\text{Volume} = (4/3)\pi r^3$$

$$\text{Volume} = (4/3)\pi(7.76 \text{ in})^3(2.54 \text{ cm/in})^3$$

$$\text{Volume} = 32118.4 \text{ cm}^3$$

The density of the hydrazine at 68° will be selected to compute the fuel available as this quantity is conservative and more accurately reflects the operating temperature of the Hydrazine propellant when used in the space environment.

$$M_p = \rho \times V = 1.0085 \text{ g/cm}^3(32118.4 \text{ cm}^3) = 32.4 \text{ kg of fuel}$$

TABLE 1
POTENTIAL FUEL REQUIREMENTS FOR SKYLITE

DECAY COMPENSATION FUEL	--- kg
SPIN UP / SPIN DOWN	--- kg
INSERTION FUEL	--- kg
TOTAL FUEL AVAILABLE	--32.40 kg

The total fuel available for all activities is 32.4 kg of Hydrazine. A propellant budget appropriately assigns fuel to each demand to meet mission demands. The fuel allotment must be separated into the categories listed in Table 1.

C. FUEL REQUIREMENTS

1. Orbital Decay

SKYLITE will be initially inserted into a circular orbit of 700 kilometers. The orbit, once established, will begin to decay. The amount of decay is estimable each orbit, based on the properties of atmospheric density (which is low but affecting at LEO altitudes), cross sectional area, spacecraft velocity and the coefficient of drag. If the satellite descends to 500 kilometers a major burn will be necessary to reestablish a 700 kilometer orbit. Although equations exist to predict the decay for a specific spacecraft at a given altitude, the latitude of ranges available for the variables in the equation make the calculations approximate. For example, the values for atmospheric density depend on many factors such as solar activity and orbital altitude. Initial calculations using nominal values provide insight into the magnitude of the decay. Following this, the maximum and minimum decay possible can be explored, using the limiting quantities for all variables. This final approach will give a range of orbital decay that can be anticipated and countered, if necessary. The graph of these calculations is shown in Figure 5.1

The decay per orbit can be calculated [Ref. 3: p.8-28 - 8-31]:

$$\Delta h = 2(\rho/m)\pi(R_e + h)^2 C_d A$$

The variables in the equation apply as follows:

ρ = atmospheric density (kg/m^3)

m = spacecraft mass (kg)

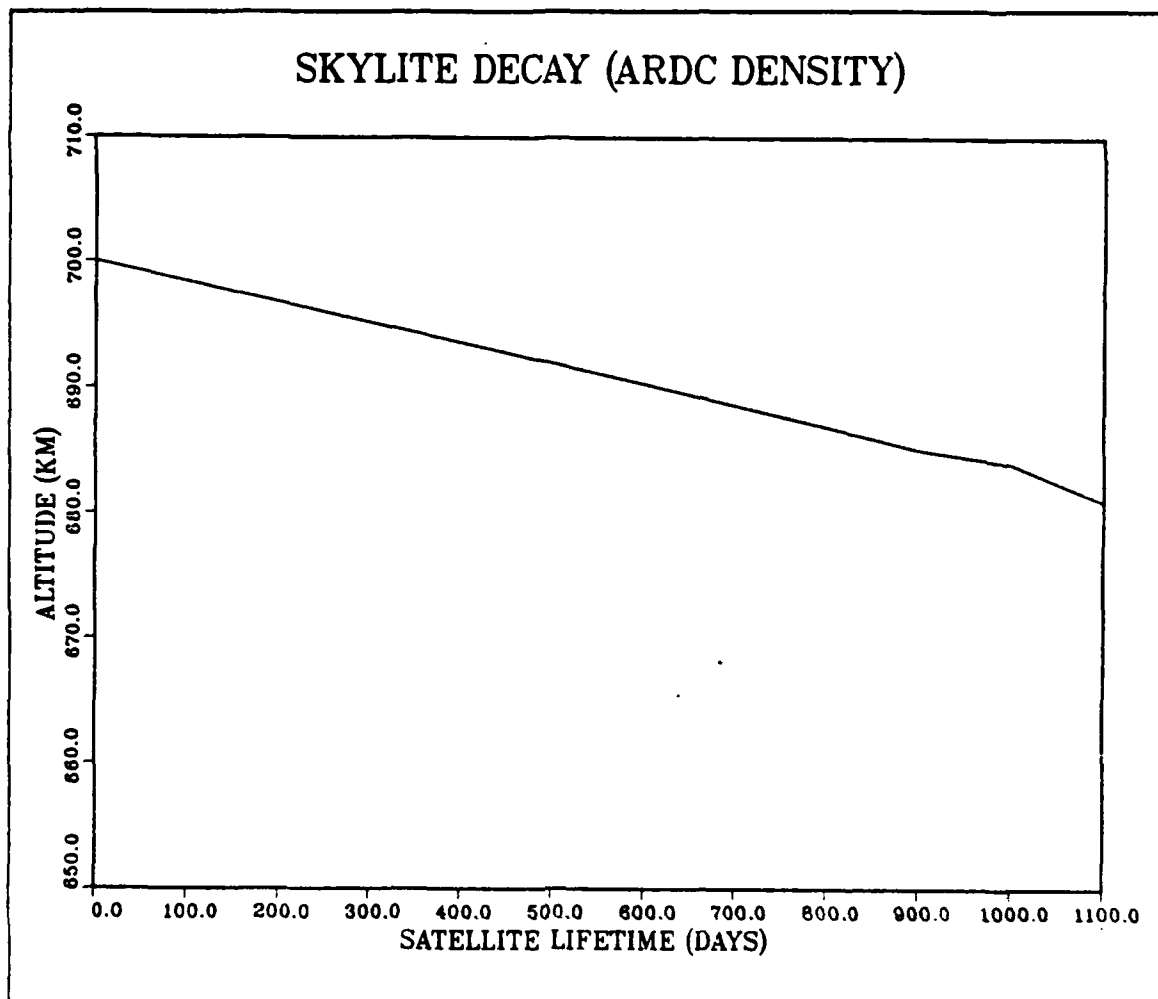


Figure 5.1 Orbital Decay Based on Atmospheric Density.

m = spacecraft mass (kg)

h = altitude (m)

C_d = coefficient of drag

A = cross sectional area (m^2)

Assumptions:

- (1) 30 kg of propellant was consumed during original insertion. This value is conservative because it provides the lightest satellite configuration on orbit. Since lifetime is proportional to spacecraft weight, the lowest weight will give the shortest lifetime.

- (3) An atmospheric density of $\rho = 3 \times 10^{-13} \text{ kg/m}^3$ was used. This figure is extracted from the ARDC model which provides atmospheric density which is higher than median values [Ref. 10: p. 77-93]. Since decay is proportional to ρ , a higher value will cause more decay. Thus if decay requirements can be satisfied at the ARDC values for ρ , they will be more easily satisfied at lower values for atmospheric density.

$$\Delta h = 2(3 \times 10^{-13} \text{ kg/m}^3)(6.378 \times 10^6 + 700 \times 10^6 \text{ m})^2(3)(.429 \text{ m}^2)\pi/(105 \text{ kg})$$

$$\Delta h = 1.157 \text{ m/orbit}$$

Orbital decay will be allowed until SKYLITE altitude is 500 kilometers. At 500 km, as indicated previously, the satellite will be configured for a major thruster burn, and reinsertion will be resumed at 700 kilometers. Computing the number of times that SKYLITE must compensate for decay is extremely important. This will determine the fuel reserved for decay compensation and the remaining fuel may be used for original orbit insertion.

The time period required for SKYLITE to decay from 500 to 700 kilometers must be computed.

$$\text{Total } \Delta H = (700-500)\text{km} = 200 \text{ km}$$

$$\Delta H/\Delta h = (200 \text{ km})/(1.157 \text{ m/orbit}) = 172860 \text{ orbits}$$

$$\text{Total decay time} = 172860 \text{ orbits} \times (98.7 \text{ min/orbit}) = 11848 \text{ days}$$

The time to decay to 500 kilometers exceeds the 3 year desired orbital lifetime. Thus, a nominal atmospheric density does not create enough friction and decay to require a counteracting thruster burn. If this statement is true of all possible values for ρ , the requirement to reserve fuel for countering orbital decay may be eliminated.

Assume the launch and deployment of SKYLITE is delayed from the 1990 date to a time when solar activity is at a peak. During a period of intense solar activity the atmospheric density increases substantially. Historical atmospheric density values, obtained from Marshall Space Flight Center upper atmosphere models [Ref. 4: p. 5], indicate that ρ_{atm} maximum for 700 kilometers is approximately $3 \times 10^{-12} \text{ kg/m}^3$. The time to decay from 700 to 500 kilometers, given this increase in atmospheric density, must be recalculated.

$$\Delta h = 2(\rho/m)(R_e + h)^2 AC_d$$

$$\Delta h = 2(3 \times 10^{-12} \text{ kg/m}^3)(7.078 \times 10^6 \text{ m})^2(.429 \text{ m}^2)\pi(3)/(105 \text{ kg})$$

$$\Delta h = 11.57 \text{ m/orbit}$$

Again, the number of orbits and time required to decay from 700 to 500 kilometers must be calculated.

$$\text{Total orbits} = \Delta H / \Delta h = 200 \text{ km} / (11.57 \text{ m/orbit}) = 17279 \text{ orbits}$$

$$\text{Total time} = 17279 \text{ orbits} \times (98.7 \text{ min/orbit}) = 1184 \text{ days}$$

The period required to decay from 700 to 500 kilometers, even during solar active periods, exceeds the planned experimental lifetime of the spacecraft. The calculations, as outlined above, indicate that reserving fuel for counteracting orbital decay is not necessary.

2. Spacecraft Spin Up and Spin Down, and Boom Length Determination

The SKYLITE spacecraft will have one occasion when it must be spun for stability. This occurs after STS drops the satellite into the parking orbit. Spinning the satellite will provide gyroscopic stability as it transits to station. The fuel required to complete the spin up evolution depends on the thrust of the rockets providing rotational motion, the moment of inertia of the spacecraft about the axis of spin, and the time required to attain the desired angular velocity.

The small thrusters, rated at .1 lb_f , will provide the spin up torque. These thrusters are located at the satellites periphery and are perpendicular to the spin axis. Prior to spin up four stabilizing booms will be deployed, giving SKYLITE inherent spin stability by satisfying the requirement that the moment of inertia about the spin axis (I_s) is greater than the transverse moment of inertia (I_t) [Ref. 5: p. 117-118]. To determine angular acceleration, and additionally, fuel consumed during spin up, the moment of inertia must be determined.

The booms must be a minimum length to provide inherent spin stability. Built into the side of the Orion bus are four channels providing recesses to shelter the booms prior to extension. The boom length must exceed a certain critical length to provide spin stability. The length of these booms will be determined in the following calculations. The Orion configuration is described in Figure 5.2.

The moments of inertia about the transverse and spin axes must be computed. The boom must be lengthened or the ball masses made heavier so I_s will be greater than I_t .

About the spin axis:

$$I_{\text{balls}} = 4m_{\text{ball}}L^2$$

$$I_{\text{total}} = 4m_{\text{ball}}L^2 + (1/2)Mr^2$$

About the transverse axis:

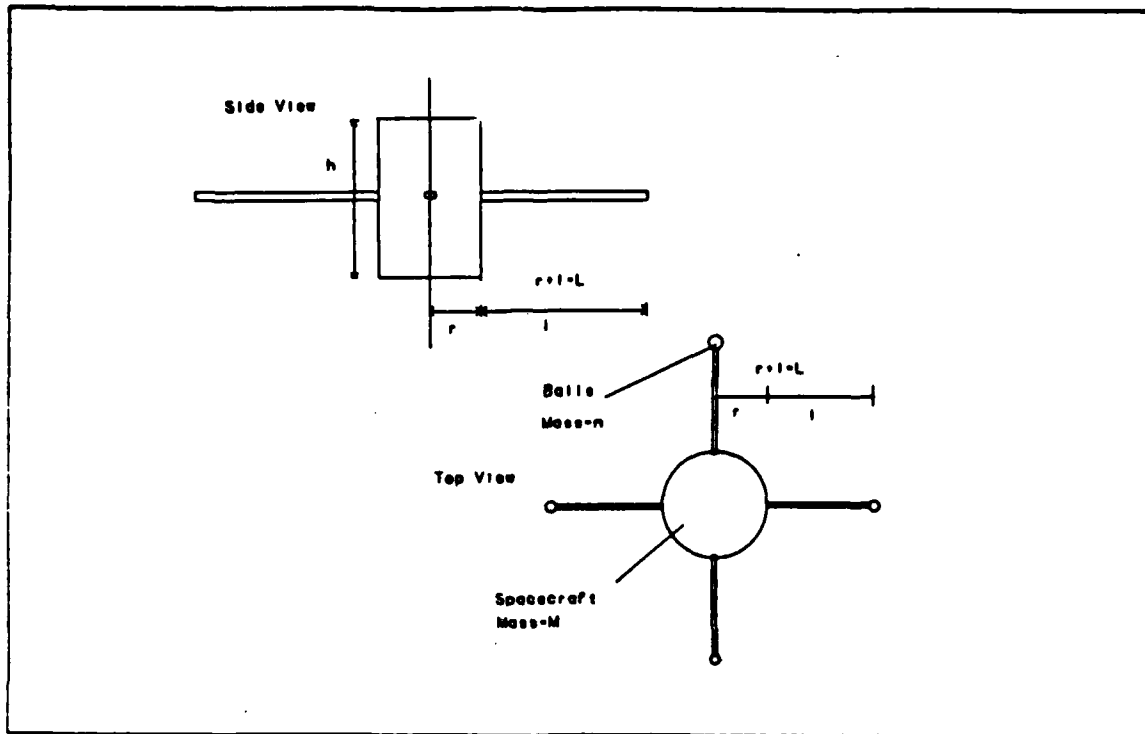


Figure 5.2 ORION with booms deployed, front and top view.

About the spin axis:

$$I_{\text{balls}} = 4m_{\text{ball}}L^2$$

$$I_{\text{total}} = 4m_{\text{ball}}L^2 + (1/2)Mr^2$$

About the transverse axis:

$$I_{\text{balls}} = 2m_{\text{ball}}L^2$$

$$I_{\text{total}} = (1/12)M(3r^2 + h^2) + 2m_{\text{ball}}L^2$$

To achieve stability the ratio of I_s and I_t must be greater than or equal to one.

$$\text{Let } h' = h/r \quad L' = L/r \quad m' = m_b/M$$

Place these substitutions into the ratio of I_s to I_t :

$$I_s/I_t = 1 = 6(1 + 8m'L'^2)/(3 + h'^2 + 24m'L'^2)$$

Solve for $m'L'^2$:

$$m'L'^2 = (1/24)(h'^2 - 3)$$

$$h'^2 - 3 = 0$$

$$h = h r = (35 \text{ in}) (9 \text{ in}) = 3.684$$

$h > \sqrt{3}$ balls will be required for stabilization

Take the above value for h and insert into the equation relating I_t and I_r

$$m L^2 = (1.244 h^2 - 3) = (1.244 (3.684^2 - 3) = .441$$

Now, there is a tradeoff between m and L . The balance between m and L must be resolved. The stability booms must fit into the longerons channel recesses, so 2 lengths of boom material, fitted into the longerons is a good assumption for maximum length. Also, the PMW-145 experimenters stated that siting and sampling sensors at greater than 1.5 meters from the center of the bottom of the spacecraft would be of value to the experiment [Ref. 2]. An interval for L is thus given, together with the indication that the mass placed in the balls will be used productively. Assume that the length of boom is one and a half times Orion's length. This boom would extend a distance from the spin axis equal to the radius plus the length of the boom.

$$L = (1.5 \times 35 \text{ in} + 9.5 \text{ in}) = 62 \text{ in}$$

$$L' = L r = (62 \text{ in}) (9.5 \text{ in}) = 6.526, \text{ using the equation above}$$

$$m L^2 = .441, m = (.441) (6.526^2) = .010$$

$$m = m M = .010, M_b = M(m) = 1.25 \text{ kg}$$

The general shape and mass contained in the stabilization booms has been driven by the above approach. Given the constraints of boom lengths, the minimum mass necessary in the boom's end is 1.25 kg. If the mass is greater for this boom length, the gyroscopic stiffness for spin stabilization will be greater. However, if the mass in the boom ends increases considerably, the moment of inertia about the spin axis will rise, increasing the amount of fuel necessary for spin up and spin down.

As discussed previously, the fuel required for spin up and spin down is dependent on the size of the spin up thrusters, the satellite moment of inertia about the spin axis, and the final angular velocity. SKYLITE will use an angular velocity of 100 rpm. This figure was discussed with engineers at John Hopkins Applied Physics Lab. They felt 100 rpm was a good compromise between the extreme gyroscopic stiffness provided by higher angular velocities and the more affordable fuel consumption involved in attaining lower angular velocities [Ref. 6]. The thruster size of .1 lb_f will act at a distance from the spin axis of 9.5 inches. This distance is coincidentally the

spacecraft radius. The moment of inertia for the satellite will be computed based on assumptions made in the preceding text.

The basic equation relating torque to moment of inertia and angular acceleration is listed:

$$T = I\alpha \quad \text{also, } T = F \times d$$

The variables in the equation are as follows:

T = torque (N-m)

I = mass moment of inertia about the spin axis (kg-m^2)

α = angular acceleration about the spin axis (rad/s^2)

d = distance from the thruster to the spin axis (m)

F = the force of the thruster (N)

Calculate I for the spacecraft when the total satellite mass is 125 kg. Assume the mass of each ball is 1.5 kg, the booms are massless, and the distance from each ball to the spin axis is 62 inches (1.575 m).

$$I_s = (1/2)Mr^2 + 4m_bL^2$$

$$I_s = (1/2)(119 \text{ kg})(.2413 \text{ m})^2 + 4(1.5 \text{ kg})(1.575 \text{ m})^2$$

$$I_s = 3.464 \text{ kg-m}^2 + 14.879 \text{ kg-m}^2$$

$$I_s = 18.34 \text{ kg-m}^2$$

Determine the torque produced by the thrusters and substitute the value for moment of inertia into the equation relating torque, moment of inertia and angular acceleration.

T = radius of spacecraft \times force of thrusters

$$T = r \times F$$

$$T = 9.5 \text{ in} \times .1 \text{ lbf}$$

$$T = .1073 \text{ N-m}$$

α = (Torque)/(Moment of inertia)

$$\alpha = T/I$$

$$\alpha = (.1073 \text{ N-m})/(18.34 \text{ kg-m}^2)$$

$$\alpha = .00585 \text{ rad/s}^2$$

Given an angular acceleration of .00585 rad/s^2 how long will the satellite take to attain an angular velocity of 100 rpm?

$$t = \text{time} = \omega/\alpha$$

$$t = (10.47 \text{ rad/sec}) / (.00585 \text{ rad/s}^2)$$

$$t = 1790 \text{ sec} = 29.83 \text{ minutes}$$

The time the thrusters must burn during spin up is approximately 30 minutes. This seems like an inordinately long burn until the small thruster and short torque arm is taken into account. The weight of fuel required for spin up can be calculated.

$$W_p = (\text{Thruster force} \times \text{time}) / I_{sp}$$

$$W_p = (.1 \text{ lbf} \times 1790 \text{ s}) / 220 \text{ s}$$

$$W_p = .37 \text{ kg of Hydrazine}$$

The fuel required for despin is equal to that consumed during spin up. The total fuel thus burned during a single spin up and despin cycle is approximately .75 kg. This portion of fuel is a minimal amount, particularly considering only one such evolution is necessary.

Thus far the demands on the propulsion system have been small. No propellant reserve is needed for countering orbital drag, and only 1-2 kg will be used to spin the spacecraft. This circumstance provides the opportunity to expand the insertion envelope as much as possible by making almost all the propellant available for the transfer evolution.

3. Spacecraft Insertion

The previous calculations concerning fuel expenditures have left an allowance of 31 kg to be used for orbital insertion. A determination of shuttle orbits which allow insertion of Orion to 700 km and 33 degrees inclination must be made. Nominal STS orbits extend from 400-1400 kilometers in altitude and from 28-56 degrees in inclination. The higher altitudes and inclinations come at the expense of reduced payload and higher propellant fraction. The 31 kg of fuel does not provide enough ΔV to attain SKYLITE's operating station from the entire shuttle orbit envelope.

The approach taken to solve this problem was to divide the STS orbital envelope into a grid and compute the ΔV from each point in the grid to SKYLITE's operating altitude and inclination. The fuel consumed during this maneuver was calculated using $W = W_p(1 - \exp(-\Delta V / I_{sp}g))$. Except from orbits of 33 degrees inclination, all insertion maneuvers involved a change of altitude and inclination. The evolution is completed with two burns. The first burn occurs at perigee and initiates a Hohmann transfer ellipse to SKYLITE altitude. The second burn simultaneously circularizes the orbit and completes the plane change. The range of STS orbits from which SKYLITE can be injected is shown in Figure 5.3.

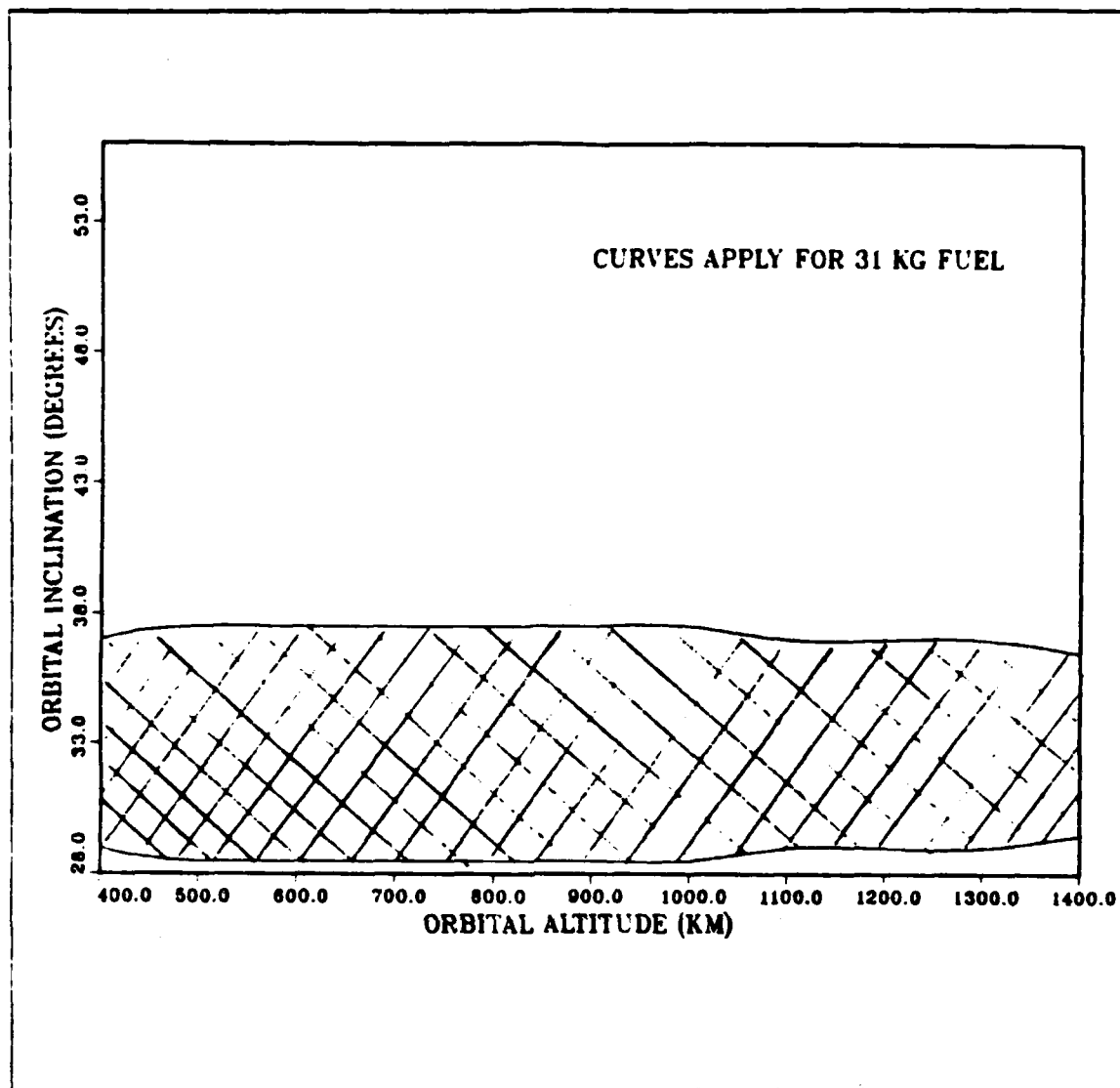


Figure 5.3 STS Orbits Allowing Skylite Injection with 31 kg.

$W = W_p(1 - \exp(-\Delta V/I_{sp}g))$ Except from orbits of 33 degrees inclination, all insertion maneuvers involved a change of altitude and inclination. The evolution is completed with two burns. The first burn occurs at perigee and initiates a Hohmann transfer ellipse to SKYLITE altitude. The second burn simultaneously circularizes the orbit and completes the plane change. The range of STS orbits from which SKYLITE can be injected is shown in Figure 5.3.

A means was necessary to determine how much of the inclination plane change should be attempted at perigee and how much would remain at apogee. The US Space

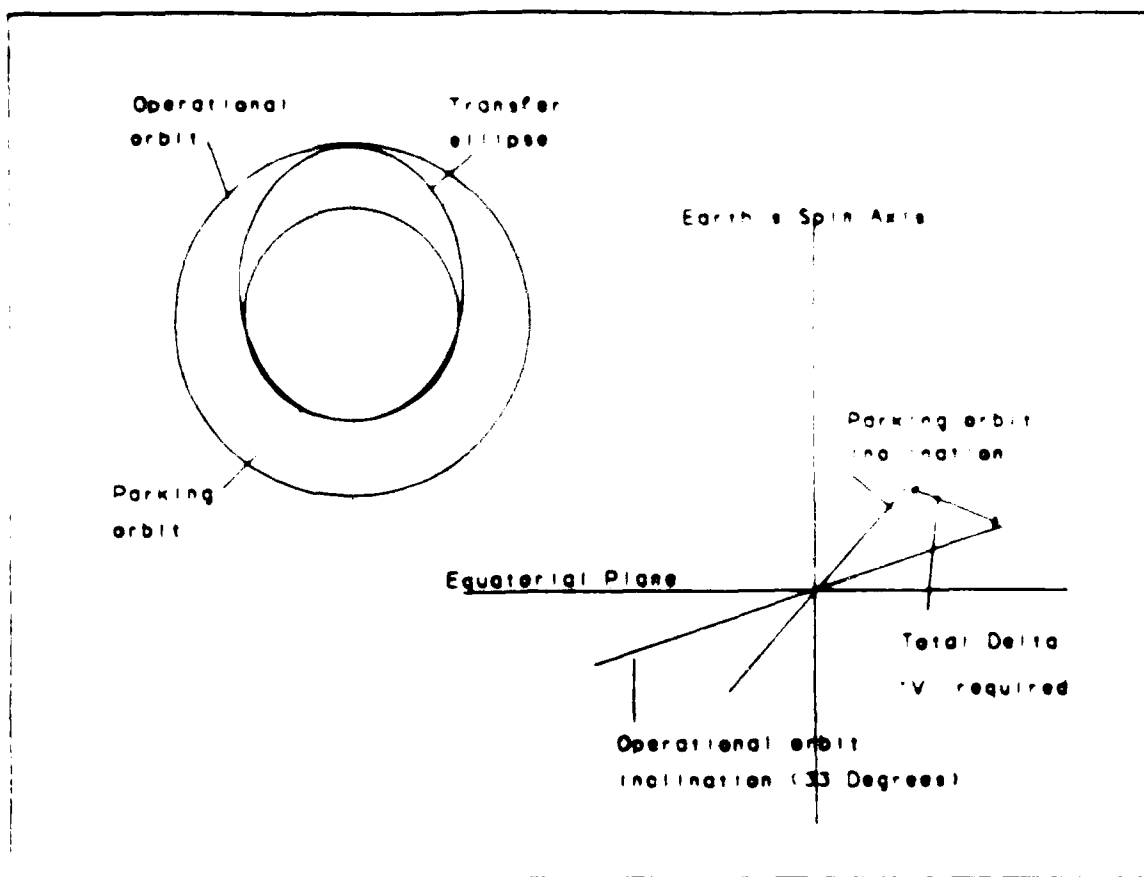


Figure 5.4 Depiction of ΔV at Perigee and Apogee.

Launch Systems Handbook took the simplifying approach that the perigee burn would involve no plane change and the apogee burn would both circularize the orbit and complete the entire plane change [Ref. 7: Appendix A-2]. This method was initially used to gain an appreciation of the fuel quantity involved. However, engineers at Aerospace Corporation mentioned that this simplified approach would provide fuel estimates about ten percent too high [Ref. 8]. They provided an algorithm, to be entered on a computer, that would calculate the most efficient division of plane change at perigee and at apogee, minimizing fuel expended. The algorithm was iterative, beginning with no plane change at perigee and total plane at apogee and proceeding to the inverse, when all the plane change is done at perigee and none at apogee. The program will generate a curve whose minimum is the lowest ΔV available. This minimum value was evaluated as the fuel necessary to transfer SKYLITE from its parking orbit to its operational orbit. This geometry of this approach is illustrated in Figure 5.4. [Ref. 9: p. 72]

The ΔV necessary at both perigee and apogee can be calculated as a function of inclination change at each point [Ref 9 p 72]

The total plane change = 0

Plane change at perigee = α_1

Plane change at apogee = α_2

$$\theta = \alpha_1 + \alpha_2$$

$$\Delta V_1^2 = V_{Pr}^2 + V_{Cl}^2 - 2V_{Pr}V_{Cl}\cos\alpha_1$$

$$\Delta V_2^2 = V_{C2}^2 + V_{Ar}^2 - 2V_{C2}V_{Ar}\cos\alpha_2$$

$$\Delta V_T = \Delta V_1 + \Delta V_2$$

To minimize the total ΔV the values for α_1 must be varied from zero to the entire plane change. An iterative solution, using the above equations, indicated the minimum ΔV possible

D. CONCLUSION

TABLE 2
PROPELLANT BUDGET FOR SKYLITE MISSION

DECAY COMPENSATION FUEL	0.0 kg
SPIN UP - SPIN DOWN	1.4 kg
INSERTION FUEL	31.9 kg
TOTAL FUEL AVAILABLE	32.4 kg

The propellant budget for SKYLITE is summarized in Table 2. The significant advantage of fuel conservation due to selecting gravity gradient stabilization becomes apparent in the previous analysis. Gravity gradient stabilization, requiring no fuel expenditure for active control, increases the total propellant available for other uses. Except for one spin up and despin maneuver, all the fuel aboard Orion is allotted to insertion. This creates noticeable operational flexibility to deploy SKYLITE from a larger portion of the STS orbital regime. Also, the optimized method of calculating ΔV during the insertion phase uses ten percent less fuel making the operational orbit attainable from an even larger portion of the STS operating regime. This provides planning flexibility which gives mission planners the option of launching SKYLITE on shuttle mission profiles deviating considerably from the heart of the envelope.

VI. THERMAL ANALYSIS

A. INTRODUCTION

One pervasive requirement in the design of a spacecraft is thermal control. Each component in the satellite must remain within operating or survival temperatures at all times. Once the satellite is operating successfully in space, the thermal system must operate for the duration of the mission. The thermal control system must satisfy a number of various conditions both internal and external to the satellite. For instance, it must operate in the vacuum of space and in the presence of the many types of radiation. This may seem like a difficult condition to meet requiring much time, personnel and money but the alternative will prove disastrous for the mission.

To design the proper thermal control system a thermal analysis must be performed on various nodes in the satellite. The thermal analysis enables designers to predict temperatures at various points in the satellite allowing for early implementation of active or passive cooling or heating techniques. This also allows for the proper selection of components and materials with specifications that meet the temperature ranges predicted for the operational lifetime of the satellite.

The analysis is performed in various stages. Initially, a coarse estimate is done to find the overall average temperature of the spacecraft and to appraise the relative magnitude of heat inputs from the various thermal sources. This analysis is then advanced to a meticulous and complex study of hundreds of nodal points located throughout the satellite.

To perform the initial thermal analysis of SKYLITE, the satellite will be considered an isothermal body. The approach taken here is one of simplicity and approximation which is not the least trivial. Simple and approximate calculations can provide excellent introduction to more complex calculations and serve as a valuable check on more accurate computation [Ref. 11: p. 1-1].

The calculations for this analysis are applicable to computing the average temperature of the satellite. The average temperature is actually the fourth power average, taken over the satellite surface, but weighted by the emittance of the various surface elements. The average temperature obtained represents a number that will be the temperature of some point within the satellite. This fairly simple calculation

determines the temperature of the satellite, even though the location of this particular temperature may be unknown. It represents a goal that can often be achieved for any desired internal point, if suitable insulation or heat transfer paths are provided. [Ref. 11: p. 1-17]

The average satellite temperature for SKYLITE is given by Equation 6.1 [Ref. 11: p. 2-14].

$$\sigma T^4 = (\alpha/\epsilon) (a/A) (S) (\psi) + (\alpha/\epsilon) (\rho) + \mu + (Q/\epsilon A). \quad (\text{eqn 6.1})$$

where

σ = Stefan Boltzmann constant ($5.66 \times 10^{-8} \text{ W/m}^2 \cdot \text{K}$)

T = temperature ($^{\circ}\text{K}$)

α = absorptivity of surface (or absorptance)

ϵ = emissivity of surface (or emittance)

a = projected area (m^2)

A = surface area (m^2)

S = solar constant (W/m^2)

ψ = fractional sunlight

ρ = reflected sunlight on plane, averaged over all orientations, and over all points equidistant from earth (W/m^2)

μ = earth-emitted radiation for plane, averaged over all orientations (W/m^2)

Q = internally generated heat, usually electrical dissipation (watt)

It can be seen that there are four principle factors involved in calculating the average temperature. These four factors are solar radiation, earth's albedo, earth's blackbody radiation and internal heat. These factors are the maior contributors of heat which effects the average temperature of the satellite. Each factor will be analyzed during this thermal analysis as it pertains to PROJECT SKYLITE. A fifth factor, unique to this design, that accounts for the heat produced during the lasing experiment, will also be discussed.

The average temperature calculations will be performed for both hot and cold orbits. The cold orbit temperature occurs when various orbital conditions minimize the

heat contributions from each factor of equation 6.1 The hot orbit condition is just the opposite - when conditions maximize thermal inputs. These conditions will be discussed as each factor of equation 6.1 is analyzed and average temperature calculations are performed for the hot and cold orbits.

In addition to the hot and cold orbit average temperature calculations a maximum and a minimum temperature will be computed. This calculation will provide an upper and lower temperature boundary that the satellite will experience during its lifetime.

The document used as a reference for this thermal analysis is titled *Spacecraft Thermal Design* by Dr. Gary D. Gordon [Ref. 11]. All theory, equations and guidance was provided through the use of this document.

B. SATELLITE TEMPERATURE FLUCTUATIONS

Before each factor of Equation 6.1 is analyzed it is important to understand three phenomena that occur to satellites orbiting the earth.

- 1) Thermal transients occur when a satellite is in sunlight for a fraction of the orbit and in eclipse for the rest of the orbit. While the satellite is eclipsed it begins to cool but before it can settle at some temperature equilibrium it emerges into the sunlight and begins to heat. This cycle of heating and cooling repeats itself each orbit.
- 2) Temperature variation occurs because of the earth's rotation around the sun. As the earth reaches various positions in its orbit around the sun the value of S , the solar constant, changes.
- 3) As the satellite decreases in altitude because of orbital decay the values of many of the variables in equation 6.1 change.

Each of these phenomena will cause a variation in satellite temperature. For this reason it is important to consider each of these problems when calculating the average hot and cold orbit temperature and the maximum and minimum temperatures of the satellite in order to determine the temperature regime the satellite will encounter during its lifetime.

Figure 6.1 shows the cycle of fluctuations in temperature as the satellite is eclipsed by the earth and then emerges into sunlight [Ref. 11: p. 9-12].

C. EFFECTS OF DIRECT SUNLIGHT ON THE SATELLITE

The largest source of constant heat for SKYLITE is direct sunlight. This is represented by the first term in equation 6.1, $(\alpha/\epsilon)(a/A)(S)(\psi)$. This term contains two important properties, surface absorptance, (α) and emittance (ϵ) , which are key factors in determining satellite temperature.

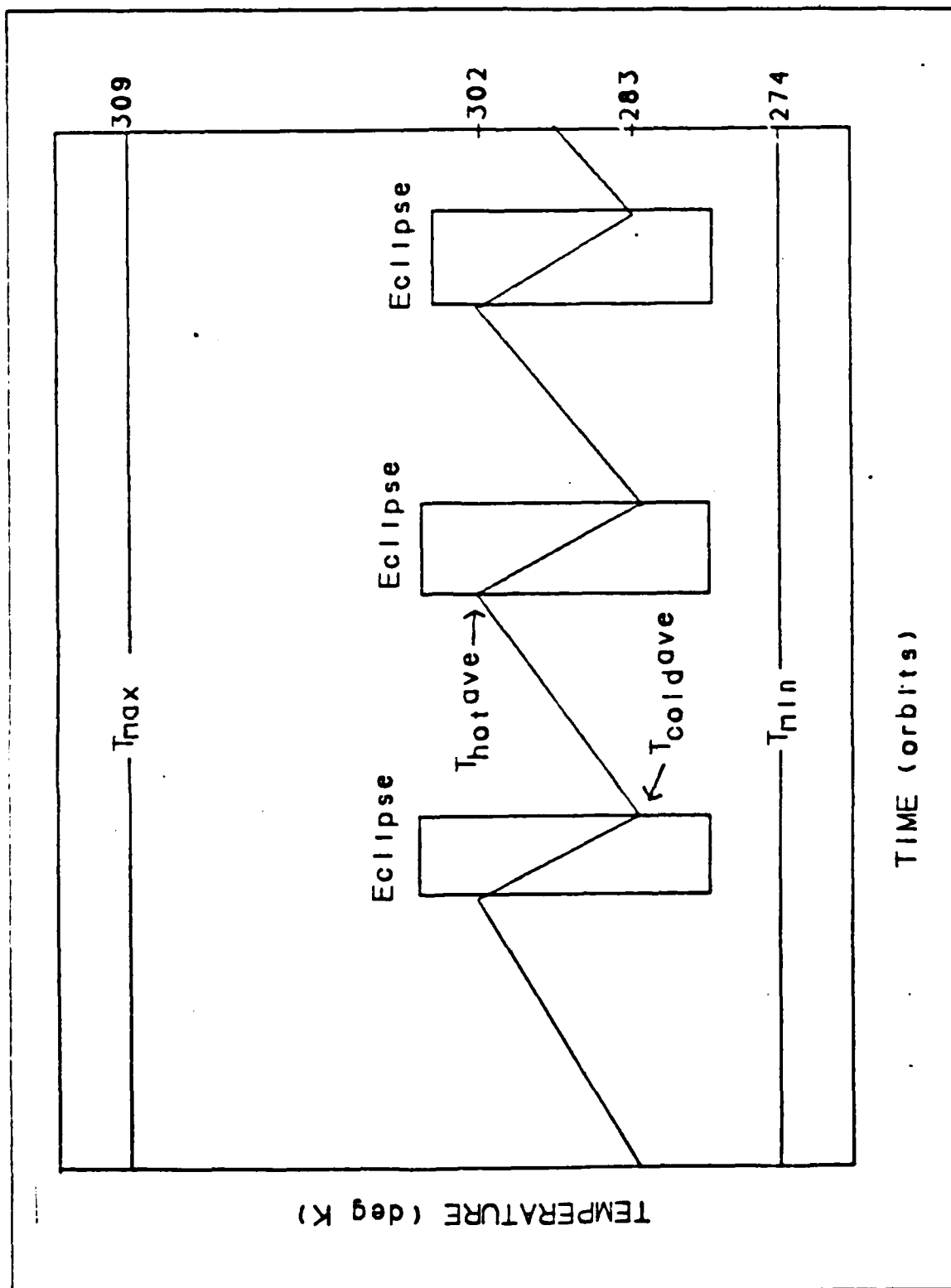


Figure 6.1 Eclipse and Sunlight Temperature Fluctuations.

The absorptance is defined as the fraction of incident radiation which the surface will absorb. This ratio will vary with the type of radiation. For this case, sunlight is the most predominate radiation and the absorptance with respect to sunlight is assumed. For satellites, the absorptance refers to the solar radiation with wavelengths from 0.3 to 3.0 microns. [Ref. 11: p. 1-8]

The emittance or emissivity of the satellite's surface is defined as the ratio of radiation intensity from a surface to the radiation intensity at the same wavelength from a blackbody at the same temperature. In essence, it is the medium's efficiency for blackbody emission. An ideal blackbody has an emissivity of 1.0. For satellites, the emittance refers to wavelengths from 5.0 to 50.0 microns. [Ref. 11: p. 1-8]

The absorptance-emittance ratio (α/ϵ) is critical in determining satellite temperature. For example, doubling this value will increase the absolute temperature by approximately 20 percent. Consequently, by varying the value of the absorptance-emittance ratio the temperature of the spacecraft can be passively controlled. For instance, an increase in solar intensity, such as the occurrence at winter solstice, can be compensated by using a low ratio. A decrease in solar intensity, such as the occurrence at summer solstice, may be compensated by using a higher ratio.

Most materials have an absorptance to emittance ratio from 0.3 to 10.0. For example, white paint has a low absorptance and a high emittance with a ratio of 0.3 to 0.5; black paints have a ratio near 1.0. [Ref. 11: p.1-8]

The second variable in the solar radiation term, a/A , takes into account the shape of the satellite. The variable, a/A is the ratio of projected area "a" to total area "A". This ratio has a similar effect on the satellite's temperature as the absorptance-emittance ratio. Because of the difficulty in precisely calculating this ratio, a simple approach will be taken. The following rule is germane for this approximation:

For any convex solid - one in which any straight line will not intersect the surface at more than two points - the average projected area is equal to one fourth of the total surface area. [Ref. 11: p. 1-15]

The average ratio for most satellites is therefore 0.25 or

$$a_{ave} = .25(A)$$

The third variable, S , is the total direct sunlight, or the solar constant. This value varies between 1311 W.m^2 at summer solstice and 1397 W.m^2 at winter solstice [Ref. 5: p. 348].

The fourth variable, ψ , is the fraction of time that the satellite spends in sunlight during each orbit. This is termed the fractional suntime. For example, if ψ equals 0.70, the satellite would spend seventy percent of its time in the sunlight and thirty percent in the earth's shadow. Subsequently, in calculating the average temperature of the satellite, the term due to direct sunlight is reduced by the time the satellite is in eclipse. [Ref. 11: p. 2-3]

The fractional suntime is a function of the distance from the spacecraft to the earth's center, r , and of the angle θ between the sun's rays and the orbit normal. This is depicted in Figure 6.2 [Ref. 11: p. 2-3].

Computing the fractional suntime is often difficult and is usually done by computer. However, the fractional suntime for a circular orbit like SKYLITE's can be computed using the following formula: [Ref. 11: p.2-5]:

$$\psi = 1/2 + 1/\pi * \tan^{-1} \sqrt{1 - (R/p)^2} / (R/p)^2 - \cos^2 \theta$$

where

R = the earth's radius ($6.378 \times 10^6 \text{ m}$)

p = orbital radius (SKYLITE is $7.078 \times 10^6 \text{ m}$)

θ = the angle between the orbit normal and the sun's rays.

The following values will be used to compute the heat input from direct sunlight for both the hot and cold orbits.

The ratio $\alpha \epsilon$ will be given the value 1.3, used for both orbits. The initial value used for $\alpha \epsilon$ was 1.1, a measurement taken from an RCA listing for glass covered, silicon solar cells, [Ref. 11: p. 1-10] which make up a large portion of the outer surface of the satellite. This ratio was increased to 1.3 for passive thermal control purposes which will be discussed later in the chapter.

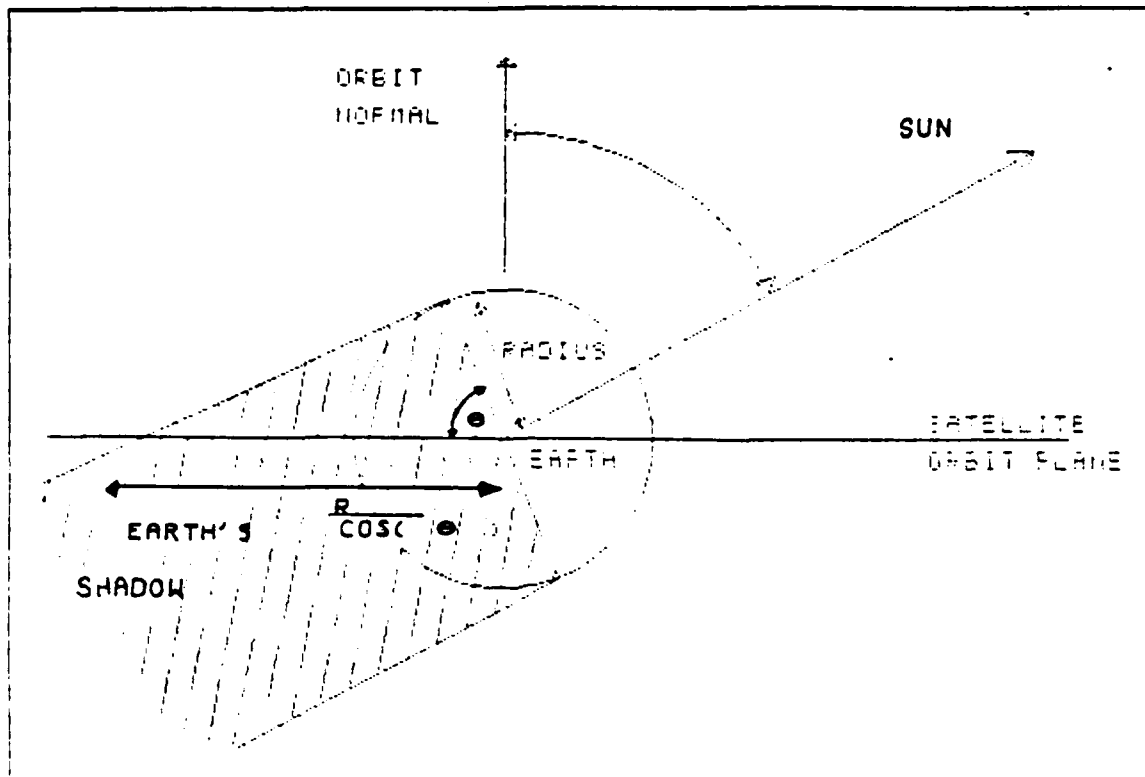


Figure 6.2 Configuration of Fractional Suntime Variables.

As discussed previously, the value for a/A is 0.25. The summer solstice value of 1311 W m^{-2} will be used for the cold orbit solar constant. 1397 W m^{-2} , the winter solstice value, will be used for the hot orbit. The fractional suntime, ψ , as computed by the respective formula, for the hot and cold orbit of a satellite at 700 kilometers equals 0.78247 and 0.64275 respectively. The value for ψ changed because the value for θ varied as the earth's inclination changed relative to the sun. Thetas of 90 degrees and 146 degrees were used for the cold and hot orbits respectively. Replacing the four variables with these hot and cold orbit values yields the following heat input from direct sunlight:

$$\begin{aligned} Q_{\text{sunlight hot}} &= (1.3)(.25)(1397 \text{ w/m}^2)(0.78247) \\ &= 355.3 \text{ W/m}^2 \end{aligned}$$

$$\begin{aligned} Q_{\text{sunlight cold}} &= (1.3)(.25)(1311 \text{ w/m}^2)(0.64275) \\ &= 273.9 \text{ W/m}^2 \end{aligned}$$

D. EFFECTS OF THE EARTH'S ALBEDO ON SATELLITE TEMPERATURE

The second term of equation 6.1, $(\alpha/\epsilon)(\rho)$, takes into account the average reflectivity of the earth or the earth's albedo, a_e . This value does vary, however, most of the measurements fall between 0.35 and 0.40. This is to say that if the albedo equals 0.35, thirty five percent of the sun's radiation striking the earth is immediately reflected from the earth. [Ref. 11: p. 2-12] Consequently, this reflected solar radiation is incident on the satellite and must be accounted for when performing the thermal analysis.

The amount of reflected radiation incident on the satellite is a function of the satellite's position, orientation of the sun, and satellite altitude. ρ , defined as the reflected sunlight equidistant from the earth, can be calculated using the following formula [Ref. 11: p. 2-13]:

$$\rho = (S)(a_e)/8 * (1 - \sqrt{1 - (R/\rho)^2})$$

where

S = solar constant

R = earth's radius

ρ = orbital radius

a_e = average reflectivity of earth (earth's albedo)

This second term not only takes into account the reflected solar radiation from the earth, ρ , but also uses the absorptance-emittance ratio to calculate temperature of the satellite attributed to the earth's albedo.

The following values will be used to calculate the hot and cold orbit heat inputs from the earth's albedo. The ratio, α/ϵ as previously discussed remains at 1.3. The cold orbit value for ρ , the reflected sunlight, equals 18.5635 for a solar constant of 1311 W/m^2 and an a_e of 0.20. The value 0.2 is at the lower end of measurements for a_e and will be used as a conservative value. The hot orbit value for ρ equals 39.5621 for a S of 1397 W/m^2 and an a_e of 0.40. Replacing the two variables with these values yields the following heat input from the earth's albedo effects for the hot and cold orbit.

$$\begin{aligned} Q_{\text{albedo hot}} &= (1.3)(39.5621 \text{ W/m}^2) \\ &= 51.4 \text{ W/m}^2 \end{aligned}$$

$$Q_{\text{albedo cold}} = (1.3)(18.5635 \text{ W/m}^2) \\ = 24.1 \text{ W/m}^2$$

E. EFFECTS OF THERMAL RADIATION FROM THE EARTH ON THE SATELLITE

The third term, μ , of equation 6.1 accounts for the heat radiated into space by the earth. The lower the orbit of the satellite, the more the radiation emitted by the earth contributes to the heat input.

μ is a function of the total radiation incident on the satellite from the earth's emission and the total satellite area. μ can be calculated using the following formula [Ref. 11: p. 2-11]:

$$\mu = 1/2 \sigma T_e^4 * (1 - \sqrt{1 - (R^2/\rho^2)})$$

where

σ = Stefan Boltzmann constant

T_e = the total power that is emitted by the earth expressed in terms of equivalent temperature for the earth.

R = radius of the earth

ρ = orbital radius

The thermal radiation from the earth, μ , was calculated for both the hot and cold orbits using the following values. 250°K was used as the average total power that the earth emits in terms of an equivalent temperature [Ref. 11: p. 2-8]. R/ρ for an orbital altitude of 700 kilometers equals 0.901102. Replacing the variables with these values yields the following heat input from the earth's thermal radiation for both the hot and cold orbit.

$$Q_{\text{earth}} = (0.5)(5.66 \times 10^{-8} \text{ W m}^2 \cdot \text{K}^4)(250 \cdot \text{K})^4 (1 - \sqrt{1 - (0.901102)^2}) \\ = 62.6 \text{ W m}^2$$

F. EFFECTS OF INTERNAL HEAT DISSIPATION

The fourth term of equation 6.1, $(Q/\epsilon A)$ accounts for Q , the internally generated heat of the satellite. There are many ways to evaluate Q . The standard method is to determine the power that each component in the satellite dissipates and sum the individual amounts. This is not feasible at this stage of SKYLITE's design because the power dissipation of many of the components and electronic circuits is difficult to calculate and the duty cycle of each is uncertain. A simple yet reliable approach can be used however, which is to determine the electric power available to the satellite and assume that this power will be in some way utilized during the mission. [Ref. 11: p. 2-1]

This power, Q , is then divided by the emittance of the satellite and the total area of the satellite over which the radiation of heat takes place.

Care must be taken when using this approach to evaluate the amount of internal heat dissipated. Energy cannot be created. This fact is important. When the satellite is in sunlight the power utilized by the equipment was originated by the solar cells. The solar cells utilize some percentage of solar radiation to create a voltage and provide a current to the various electrical components of the satellite. This energy, measured in the form of heat, could mistakenly be counted twice during the analysis. Care must be taken to guard against this problem. If 100 percent of the solar radiation incident on the solar array is used to calculate Q_{sunlight} then the power received by the electrical components which is transformed into heat cannot be used to calculate Q_{internal} . The heat input from Q_{internal} can come from frictional heat developed by some moving parts, propulsion elements or from electrical components powered by the battery during eclipse.

To account for these various heat inputs internal to SKYLITE, a value of 5 watts will be used for Q . The total area of the satellite, A , is 1.7136m^2 using the dimensions for SKYLITE of 19 inches diameter and 35 inches in length. ϵ , the emittance, is 0.8. The values yield the following internal heat input.

$$\begin{aligned} Q_{\text{internal}} &= 5.0 \text{ W} / (0.8)(1.7136\text{m}^2) \\ &= 3.6 \text{ W/m}^2 \end{aligned}$$

G. EFFECTS OF INCIDENT LASER ENERGY ON THE SATELLITE

One significant radiation factor not found in equation 6.1 is the heat input caused by the radiation incident on the satellite during the lasing experiment. Equation 6.1 accounts for the classical contributors to the average spacecraft temperature. The heat caused by the lasing of the satellite is unique to this mission and the thermal design must account for this fifth factor. To plan for the worst case, the high energy experiment power must be used in the calculation. The value used for the high energy experiment will be 4.0 watt/cm^2 . This heat input will be transient in nature in that the longest lasing time will be approximately one minute in duration occurring on the average of once every four to six weeks. However, it is important to calculate the heating effects from the incident radiation of the laser to assess the relative magnitude of heat generated. A maximum temperature during lasing can then be calculated that will enable the proper selection of hardware and structural materials that can withstand this temperature.

The value for laser heat input can be calculated by using a formula similar to that of direct sunlight.

$$Q_{\text{laser}} = (\alpha \epsilon) (a/A) (S) (\psi)$$

The value for $\alpha \epsilon$ will change to 0.5. As discussed in the Q_{sunlight} section, the absorptance of a satellite is measured at the 0.3 to 3.0 micron region. The wavelength used for the MIRACL laser is 3.6 to 4.2 microns which nullifies the $\alpha \epsilon$ value that was used for the sunlight calculations. The solar cells will be coated with a highly reflective material that has a 95 percent efficiency in the 3.6 - 4.2 micron region for protection against overheating the solar array. However, the reflective properties will not be fully attained due to the high grazing angle (60 - 80 degrees) of the laser energy striking the satellite. The reflective effects of the coating somewhat diminished by the high grazing angle should provide an absorptance of approximately 0.4. ϵ will remain at 0.8. This results in a α/ϵ ratio of 0.5.

The value for a/A will have to change to account for the projected area that the laser energy will be incident on the satellite. The laser's minimum elevation firing angle is 60 degrees. Because of SKYLITE's gravity gradient stabilization method, the base of the satellite will be pointing at nadir. If the laser is fired at 60 degrees elevation, it will give the greatest projected area with the lowest grazing angle on the satellite, with radiation striking both the base and along one side. The projected area can be calculated giving an (a/A) ratio of 0.35.

The "S" term will be the amount of laser power incident on the spacecraft during the high power test, this being 40,000 W/m².

ψ in this case will equal 1. This is to say that the satellite will be in the laser radiation for the full period of laser firing - worst case is one minute. If these values are substituted into the formula the resultant heat input from the laser energy at high power will equal:

$$\begin{aligned} Q_{\text{laser}} &= (0.5)(0.35)(40000 \text{ W/m}^2)(1.0) \\ &= 7000 \text{ w/m}^2 \end{aligned}$$

H. CALCULATING THE AVERAGE HOT AND COLD TEMPERATURES

When all the terms of the heat equation are placed together the average spacecraft temperature is given by

$$\sigma T^4 = Q_{\text{sunlight}} + Q_{\text{albedo}} + Q_{\text{earth-thermal}} + Q_{\text{internal}}$$

As discussed throughout this chapter these are the most important contributions to the average spacecraft temperature. In order to calculate the average hot or cold orbit temperature prior to the lasing experiment, each of the heat source values must be summed. This total is then divided by the Stefan Boltzmann constant and the fourth root taken. Substituting the cold orbit values gives

$$\sigma T^4 = 273.9 + 24.1 + 62.6 + 3.6 = 364.2 \text{ W/m}^2$$

$$T_{\text{coldave}} = ((364.2 \text{ W/m}^2) / (5.66 \times 10^{-8} \text{ W/m}^2 \cdot \text{K}^4))^{1/4}$$

$$T_{\text{coldave}} = 283.2 \cdot \text{K}$$

Entering the values for the hot orbit, the average temperature rises to

$$\sigma T^4 = 355.3 + 51.4 + 62.6 + 3.6 = 472.9 \text{ W/m}^2$$

$$T_{\text{hotave}} = 302.3 \cdot \text{K}$$

These two temperatures are computed without the laser heat input. To find the actual rise in temperature during the lasing experiment a separate equation must be solved that will show the rise in temperature per unit time (dT/dt). This calculation will be discussed in the next section.

I. CALCULATING THE MAXIMUM AND MINIMUM TEMPERATURES

Thus far, the average hot and cold orbit temperatures of the satellite have been calculated. But in order to find the upper and lower temperature limits that the satellite will experience, the value of several variables in Equation 6.1 must be changed to reflect the hottest and coldest conditions in the satellite's lifetime.

To calculate the maximum temperature the following equation must be solved using the proper hot orbit conditions [Ref. 11: p.9-13].

$$mc(dT/dt) = \epsilon A (\sigma T_H^4 - \sigma T^4)$$

where

m = the mass of the body (grams)

c = the specific heat of the body (J g \cdot °C)

T_H = the maximum Hot Orbit Temperature

T = Average Hot Orbit Temperature

In order to find T_H , the hot orbit temperature, the value for ψ and S in equation 6.1 must be changed to 1.0 and 1397 w/m² respectively to maximize the heat input from sunlight. All other values remain the same as the average hot orbit temperature values. Replacing these values in equation 6.1 yields a value for T_H of 317°K. Now dT/dt can be calculated. The following values will be used:

m = 95,000 grams (mass of satellite after orbit and plane change)

c = 0.226g-cal/g \cdot °C (value for Aluminum)

ϵ = 0.8

A = 1.7136 m²

T_H = 317°K

T = 302°K (from previous calculation)

The units for specific heat can be changed to $0.946 \text{ J/g}\cdot\text{C}$ to simplify calculations. Substituting in these values gives

$$mc(dT/dt) = (.8)(1.7136\text{m}^2)(\sigma 317\cdot^4 - \sigma 302\cdot^4)$$

$$dT/dt = 138.1 \text{ mc}$$

$$dT/dt = 138.1(95000)(.946)$$

$$dT/dt = 1.5\cdot \text{ sec}$$

To find the rise in temperature during the sunlight portion of the orbit dT/dt can be multiplied by the number of minutes that the satellite is in sunlight. The period of SKYLITE'S orbit is 98.7 minutes. Multiplying 98.7 by ψ of 0.78247 equals 77.23 minutes. dT can now be figured.

$$dT = (1.5367\cdot \text{ sec})(60\text{sec/min})(77.23\text{min})$$

$$dT = 7.1\cdot$$

This value can now be added to the average hot orbit temperature to give the maximum temperature the satellite will experience during its lifetime excluding the transient temperature increase during the lasing experiment.

$$T_{\text{MAXsun}} = 302.3\cdot\text{K} + 7.1\cdot\text{K} = 309.4\cdot\text{K}$$

Although $309.4\cdot\text{K}$ is normally the highest temperature that the satellite will experience there will be times during the laser experiment that it will be subject to an intense transient heat input. It is necessary to calculate the transient rise in temperature that will occur during the high energy lasing experiment to find T_{MAXlaser} .

Q_{laser} has already been calculated as 7000 W/m^2 . This amount of energy from the laser has been mitigated by losses due to the 60 to 80 degree grazing angle of the radiation striking the satellite and the highly reflective coating which will be applied to the solar cells.

When Q_{laser} is added to equation 6.1 the average temperature rises to $758\cdot\text{K}$. This will be used for the value of T_H . $758\cdot\text{K}$ is the temperature that the satellite will tend to if the laser energy was incident on the satellite for infinity. All of the other values will remain the same as those used for the average hot orbit calculations.

dT/dt for the hot orbit during the experiment equals $2.8 \times 10^{-1} \text{ }^\circ/\text{sec}$. The experiment will have a maximum duration of one minute. Multiplying dT/dt by 60 seconds yields a change in temperature during the experiment of 16.8 ° .

Now the maximum temperature that the satellite will experience at any time throughout its life can be figured by adding 16.8 degrees to the average hot orbit temperature of 302.3 degrees .

$$T_{\text{MAX hot+laser}} = 302.3 \text{ }^\circ\text{K} + 16.8 \text{ }^\circ\text{K}$$

$$T_{\text{MAX hot+laser}} = 319.1 \text{ }^\circ\text{K}$$

The final temperature to determine will be T_{MIN} . This temperature occurs as the satellite is just emerging into sunlight after its pass through eclipse. This is calculated using minimum heat contributions. It is the coldest temperature that the satellite will experience. The following equation is used to calculate this temperature [Ref. 11: 9-13].

$$mc(dT/dt) = \epsilon A (\sigma T_L^4 - \sigma T^4)$$

T_L can be calculated by eliminating the sunlight and albedo factors from equation 6.1. This will leave only the earth's blackbody radiation and internal heat inputs. This will give a T_L value of $185 \text{ }^\circ\text{K}$. The value for T will be the average cold orbit value of $283.2 \text{ }^\circ\text{K}$. All other values will remain the same as those in the average cold orbit calculation. Substituting these values into the equation yields a dT/dt for the cold orbit of $-4.5 \times 10^{-3} \text{ }^\circ/\text{sec}$. This value is multiplied by the satellite's time in eclipse to compute the minimum temperature that the satellite will experience. The period of the orbit multiplied by $(1-\psi)$ will give the satellite's time in eclipse. This value equals 35.26 minutes. Multiplying eclipse time by dT/dt yields a decrease in temperature during eclipse of -9.6 degrees . Subtracting this value from the average temperature of the cold orbit will result in the minimum temperature that the satellite experiences.

$$T_{\text{MIN}} = 283.2 \text{ }^\circ\text{K} - 9.6 \text{ }^\circ\text{K}$$

$$T_{\text{MIN}} = 273.6 \text{ }^\circ\text{K}$$

J. PASSIVE THERMAL CONTROL

For reasons of reliability, weight, simplicity, and cost, SKYLITE will rely entirely on passive thermal control. There will be no moving parts. The thermal control of the satellite will depend on thermal surface properties, thermal insulation, thermal mass, thermal heat paths, etc. to maintain desirable temperatures.

The typical goal for a satellite's average temperature is 0°C to 40°C . However, the component equipment must pass qualification tests with wider temperature limits, with 10°C being the usual overstress criteria. This puts limits of -10°C to 50°C for the equipment tests.

For the first iteration of SKYLITE's thermal analysis an overall α/ϵ of 1.1 was used. This produced a temperature range from -3°C , during the coldest conditions to 37°C during the lasing experiment. The lower limit was deemed undesirable, specifically for the hydrazine fuel which freezes at 0°C . The α/ϵ ratio was increased to 1.3 which yielded a range in temperature between 1°C and 46°C . This ratio produced an increase in temperature for the cold orbit but may be unacceptable for the maximum temperature allowable. The optimum ratio will probably fall between 1.1 and 1.3. Further study is required to determine the possible passive thermal techniques necessary to meet temperature criteria. It may be necessary to have different surfaces having different α/ϵ values to raise and lower temperatures at specific points on the surface of the satellite.

K. CONCLUSION

The preceding thermal analysis was simple and direct. The entire satellite was assumed to be isothermal, and all temperatures are bulk temperatures. This initial step determines an approximate operating range for spacecraft temperatures. Due to thermal coupling, and radiation effects, the temperature variations within the satellite may be extreme, particularly during periods of laser illumination. For subsequent and more precise analyses, the temperature at discrete points within the vehicle must be ascertained with extremely complex programs and algorithms, using nodal analysis. However, for a concept analysis, the isothermal approach is sufficient, demonstrating considerable accuracy for previously designed spacecraft. The passive thermal design for SKYLITE maintains a temperature range of -6°C to 36°C during orbit, with transient temperature increases to 46°C during lasing periods.

Two critical areas that must be analyzed during subsequent nodal analysis are the solar cell and gravity boom temperature gradients during lasing periods. The

temperature effects of both the hot and cold orbit and the laser radiation on the solar cells must be determined as a function of time, since the design and impedance for the solar array is critically dependent on the temperature profile. The gravity gradient boom, the tip mass and the solar array on the tip mass are sufficiently separate from the satellite to require a separate thermal design.

VII. SPACECRAFT POWER ANALYSIS

A. INTRODUCTION

The satellite power analysis is often one of the most exhaustive in the design process. This is due to the wide variety of equipment requiring power as well as the fluctuating power sources. The approach that follows details an analysis of the electrical power capabilities of the solar cells and batteries, followed by an examination of types of equipment and loads drawing on these sources.

For spacecraft in low earth orbit (LEO) the requirement of providing power to satellite equipment is satisfied with solar arrays and batteries. The solar arrays supply all necessary power except during eclipse periods. During eclipse there is no solar power incident upon the solar panels and the batteries supply all the required power. This is done by allowing the solar panels and the batteries to power a common bus. If either of the supply sources is unavailable, the other will assume the entire load. A prime consideration in this arrangement is that, since the batteries do not have unlimited power, the solar panels must be able to recharge the batteries as well as power the spacecraft, during the time the orbit is sunlit. If the solar array is not well designed in this area, the batteries will be drawn down to a point when they cannot fully power the spacecraft during eclipse.

The load conditions that face the power sources are complex. The power demands are a combination of steady state, transient and one time loads. An example of a steady state load is a transponder that must be continuously powered. A transient power requirement may occur during random periods in the orbit. For example, a spacecraft may have a sensor that must be turned if another vehicle flies into its field of view. An instance of a one time load is presented as a spacecraft is deployed and many arrays are deployed by electric motors. Once the arrays are erected the electric motors may never operate again. So, the power sources must be matched against all steady state loads, as well as transient and one time loads. Load budgets, which sum the power requirements during different operating are prepared. These budgets are compared against the available power at that particular time. If a power surplus is not evident, then reevaluations become necessary.

The initial calculations for power sources available to SKYLITE involved an assessment of power provided by the body mounted solar panels. The calculated solar power available will give an estimate of how much equipment can be powered as the batteries are recharging, as the spacecraft is in the sunlit portion of the orbit. Once the solar array was evaluated, the battery necessary during eclipse was sized. These evaluations are discussed in the section on power sources. The electrical demands of the satellite equipment and the load diagrams are explained in the section on electrical loads.

B. POWER SOURCES

1. Solar Array

Solar arrays are an accommodating means of supplying power to a spacecraft as it proceeds through its orbit. They provide virtually an infinite source of energy. Although batteries and propellant are also available as power sources, they have finite limits and their weight requirements become more prohibitive as the spacecraft design lifetime lengthens. The approach taken towards ensuring a power source is available aboard SKYLITE, was to supply the primary power bus from the solar panels at all times except eclipse and periods when the electrical demand may exceed the solar array supply. During such times of peak demand the solar power will be supplemented with battery power. An analysis was done regarding the power supplied by the solar panels aboard SKYLITE. This analysis is subsequently discussed, illustrating the variations in potential solar power throughout an orbit.

The arrays which convert solar power are composed of strings of solar cells. These cells are approximately 2 cm by 4 cm, although their size is variable to create the most efficient array possible. The two primary chips mass produced for solar panels are Silicon (Si) and Gallium Arsenide (GaAs). The silicon type cells have been used since the infancy of the space age and provide efficiencies of approximately 9-15 percent at a reasonable cost. The Gallium Arsenide cells, which attain efficiencies between 15-20 percent, may also be purchased, although their cost is prohibitive for use in the SKYLITE design. Thus, Silicon cells were selected for use aboard SKYLITE, and the efficiency of these particular cells range from 9.5 to 14.5 percent, based on the cell temperature. [Ref. 5: p. 342]

The solar power converted to electricity by a solar panel is dependent on three attributes. These attributes are solar array area, cell efficiency and solar irradiance. Their relationship is illustrated in the following equation [Ref. 5: p. 347].

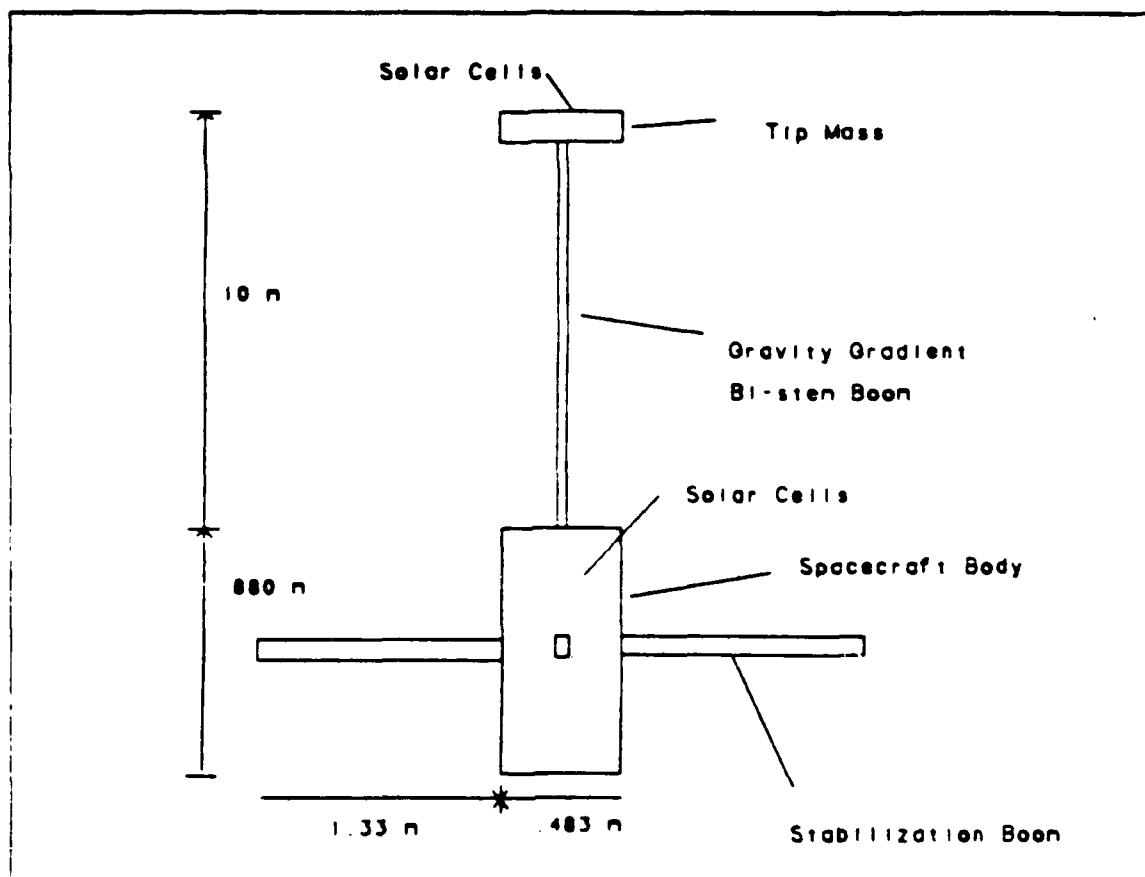


Figure 7.1 Solar Array Arrangement on SKYLITE.

$$P = \eta \times A \times S$$

η = solar cell efficiency (%)

A = solar array area perpendicular to the Sun's rays (m^2)

S = solar illumination value (W m^2)

For a spin stabilized or three axis stabilized spacecraft the calculation for power converted from a solar array is straightforward. The ease of calculation arises from the fixed position of the solar arrays with respect to the incident radiation. The projected area of the solar panel available for collection is unchanging, making the power output of the array almost constant and very predictable. However, for a gravity gradient stabilized satellite, such as SKYLITE, the procedure is much more difficult. The solar array on SKYLITE is body mounted, with additional cells on the top of the gravity boom tip mass. The arrangement is depicted in Figure 7.1. Since the bottom of SKYLITE always points to the Earth, the orientation of the solar panels

and the sun continuously changes as the satellite orbits. As the power available from an array is a function of its projected area, the array power to the bus will also constantly change. The spacecraft power analysis requires a precise assessment of minimum and maximum power, so the solar array's varying output due to changing geometry must be evaluated for averages as well as low and high power points.

2. Minimum Power Orbit

The orbital parameters impacting solar power collection were analyzed to determine particular orbits when the array will produce its maximum and minimum available power. Since collected power is proportional to projected area and solar illumination, the least power will be collected when these values are minimum and the most power is available when these values are maximum. If the electrical demands can be satisfied under these limiting conditions, they can be satisfied at all the ranges in between.

Unfortunately, the entire surface area of SKYLITE is not available for mounting solar cells. There must be room provided for other items such as thrusters, sensors, antennae, and structural fixtures. A reasonable approximation is that 95 percent of the surface area will contain solar cells. This value applies both to the cells on the top of the tip mass and the cells on the outside of the spacecraft body. This evaluation leaves the following area available for collecting solar power.

$$\begin{aligned} \text{Area}_{\text{spacecraft}} &= 2rh = 2(.2413 \text{ m})(.889 \text{ m}) = .429 \text{ m}^2 \\ \text{Area}_{\text{tip-mass}} &= \pi r^2 = \pi(.2413 \text{ m})^2 = .183 \text{ m}^2 \end{aligned}$$

Both of these areas must be decreased by five percent for the spacing reason discussed above.

$$\begin{aligned} \text{Area}_{\text{tip,eff}} &= .183 \text{ m}^2 \times .95 = .174 \text{ m}^2 \\ \text{Area}_{\text{s/c,eff}} &= .429 \text{ m}^2 \times .95 = .4076 \text{ m}^2 \end{aligned}$$

The reason the area available for solar collection on the spacecraft body is not equal to the cylinder surface area becomes apparent only after consideration. The total circumferential area is never visible to the sun at an instant. Instead, the apparent area available for collection is the projected area of a cylinder. This area is equal to the product of the diameter and height. The area provided by the tip mass and spacecraft cannot be algebraically summed as they never present their maximum collection area to the sun simultaneously. When the tip mass cells are perpendicular to the solar rays the

cylinder face is parallel (collecting no energy) and visa versa. The difficulty of determining solar power available increases due to this situation.

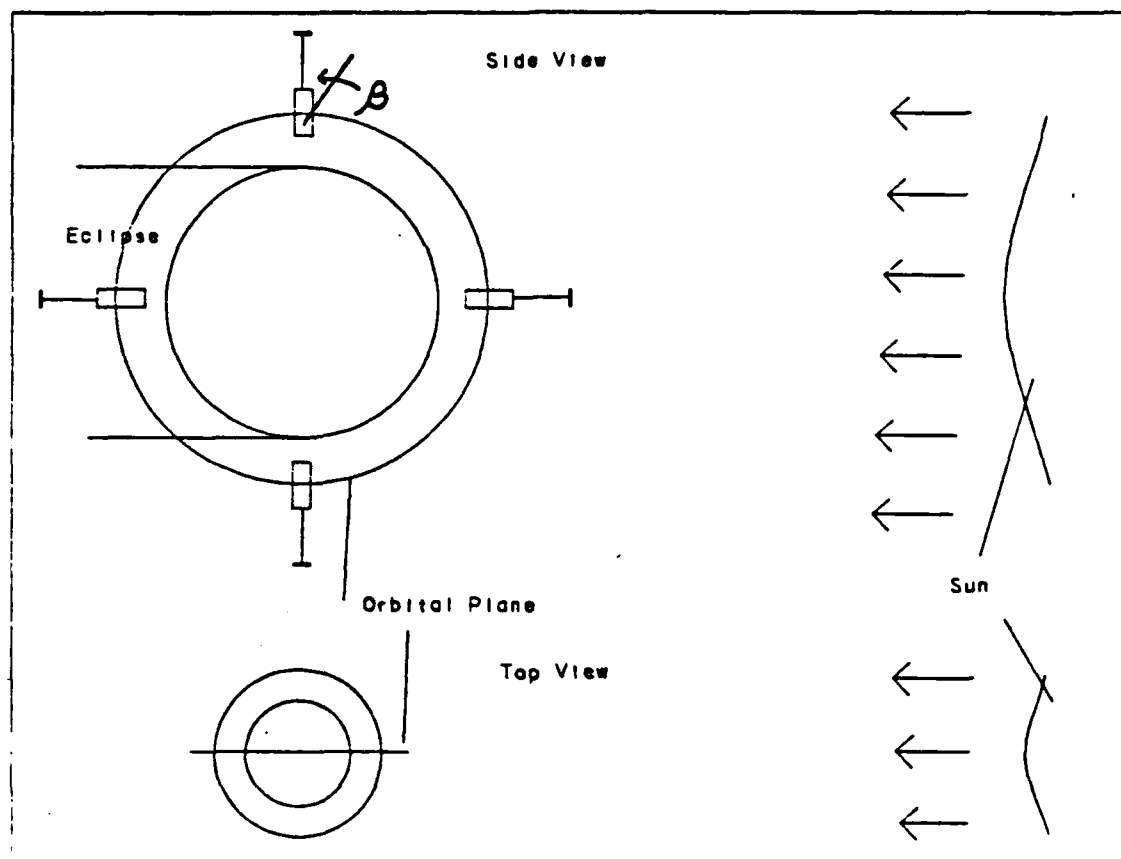


Figure 7.2 Orbital Position Causing Minimum Solar Array Power.

The relative position of the sun, earth and spacecraft causing the solar array output to reach a minimum is illustrated in Figure 7.2. This orientation may occur periodically throughout the year. However, the particular orientation resulting in minimum array output takes place during the summer solstice. The Sun and Earth are furthest separated at the summer solstice, causing the solar constant to reach its minimum value of 1310 W/m^2 [Ref. 5: p. 348]. Also, another factor minimizing the solar array power output is the regression of the orbital plane to a position that is parallel to the arriving solar rays. This orientation provides two minimum power values, minimum instantaneous power and minimum average power in an orbit. The minimum instantaneous power available in any orbit occurs when the spacecraft axis is

pointed directly at the sun. At this position, the only solar array area used for collection is that on the top of the tip mass. The average power is minimum throughout the orbit because of the low average area presented to the solar rays and the high eclipse time. The orientation described in Figure 7.2 creates the longest eclipse of any possible orbit. The lengthy eclipse reduces the sunlit time, which the array depends on for power collection.

The minimum instantaneous power available is a straightforward calculation using previously defined equations. As the tip mass cells become perpendicular to the solar rays the solar array area reaches a minimum and all solar power is collected by the tip mass solar cells.

P_i = Instantaneous Power

$P_i = A_{tip} \times \eta \times S$

$A_{tip,eff} = .174 \text{ m}^2$

$\eta = 12 \%$

$S = 1310 \text{ W/m}^2$ during summer solstice

$P_i = (.174 \text{ m}^2)(.12)(1310 \text{ W/m}^2) = 27.4 \text{ W}$

An additional concern to be discussed at this point is the solar cell efficiency decrease due to radiation damage by trapped radiation at low Earth altitudes. The radiation effects are cumulative over the lifetime of the orbit. The radiation damage factors were calculated for SKYLITE orbit at 700 km and 33 degrees inclination throughout a three year life. The radiation damage factor is .89. This value means that the solar cell effectiveness decreases by eleven percent after three years. Since the electrical demands of the satellite must be satisfied at the end of life (EOL) as well as beginning of life (BOL), all subsequent solar calculations will account for the decrease in efficiency caused by trapped radiation. [Ref. 5: p. 336]

The minimum instantaneous power, at the end of life is given by the following equation.

$P_i(EOL) = P_i(BOL) \times D$

D = solar cell derating factor due to radiation damage = .89

$P_i(EOL) = .89 \times 24.34 \text{ W}$

The minimum average power throughout an orbit is a more difficult calculation. The solar cell area available for solar power collection is a function of the

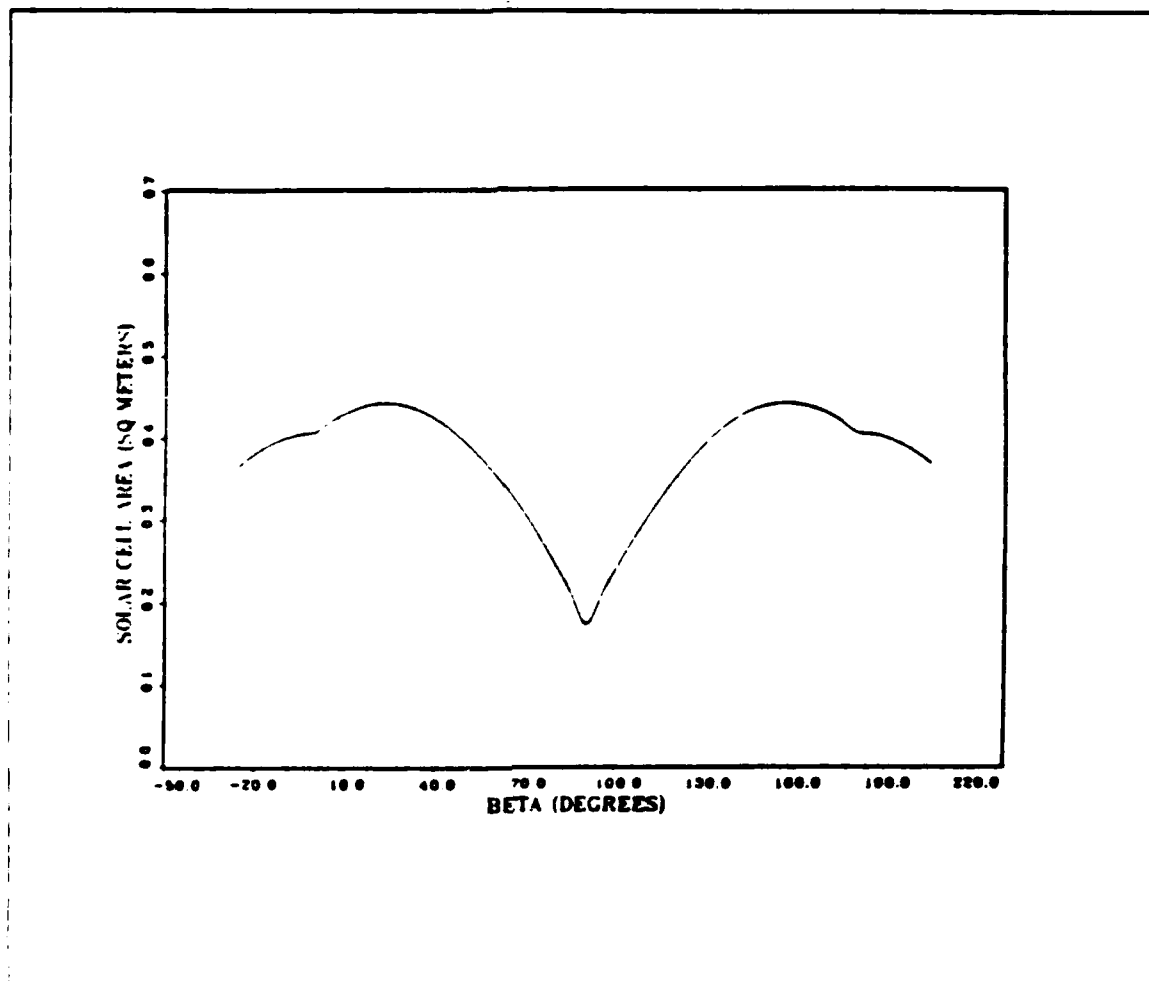


Figure 7.3 Projected Area Available-Minimum Power Orbit.

sum of the disc area presented and the cylinder area presented. The cylinder area presented will range from a maximum near its northernmost and southernmost points and a minimum as the cylinder becomes perpendicular to the sun's rays. The projected area of the cells on the disc, because it is ninety degrees off of presentation from the cylinder, varies inversely. The disc has minimum projected area at the northernmost and southernmost points, with a maximum when the spacecraft axis is perpendicular to the sun's rays. The following comments refer to Figures 7.2 and 7.3. Using the angle β as the angle between the spacecraft longitudinal axis and an axis perpendicular to the sun's rays, the area available in this orbit can be described by Figure 7.3. The area varies as depicted in the graph with the eclipse region defined as β values from 206.5 to 333.5 degrees. The average projected area during the sunlit portion of the orbit, when

entered in the solar cell collection equation, will provide the average power available by the solar array. The average area is calculated by integrating the area under the curve in Figure 7.3 and dividing by the time the spacecraft is exposed to the sun. These calculations result in an average area of .3753 m². The average solar power provided in this orbit can be determined.

$$P_{avg} = \eta \times A_{avg} \times S \times D$$

$$P_{avg} = .12(.3753 \text{ m}^2)(1310 \text{ W/m}^2)(.89)$$

$$P_{avg} = 52.5 \text{ W (EOL)}$$

The minimum average value of 52.5 W is the least amount of average power that will ever be supplied by the solar array during an orbit. If the spacecraft load is designed so that it can be satisfied by this minimum value, then all other spacecraft orientations, all with higher average power, will sufficiently supply this load.

3. Maximum Power Orbit

The previous procedure used for evaluating the conditions of minimum solar array output power must be repeated to determine the maximum solar array power. The same variables whose combination created the conditions of minimum power, also cause periods of maximum power generation. These variables, projected array area and solar constant, combine to generate this maximum at a different point of the orbit. The specific orbital arrangement creating maximum power is illustrated in Figure 7.4. During this orbit the projected area of the spacecraft solar array will be less varying than in the minimum power orbit. Also, because the solar angle is fifty six degrees, the eclipse will be considerably shorter. The eclipse during the maximum power orbit is 21.4 minutes, versus 35 minutes for the minimum power orbit. The short eclipse period and greater cross sectional area, combine to provide substantial increase in both maximum instantaneous and maximum average power.

The maximum instantaneous power occurs when the top of the spacecraft has rotated to a position when it points towards, though not directly at, the Sun. At this point the total projected area is a sum of the apparent area from the disc solar cells and the cylinder solar cells. The maximum instantaneous power is calculated using the previous equations.

$$P_i \text{ (EOL)} = \eta \times A \times S \times D$$

$$S = \text{Maximum solar constant (winter solstice)} = 1390 \text{ W/m}^2$$

$$A = \text{Peak sum of the disc and cylinder projected area} = .4624 \text{ m}^2$$

$$D = \text{Derating factor (EOL)} = .89$$

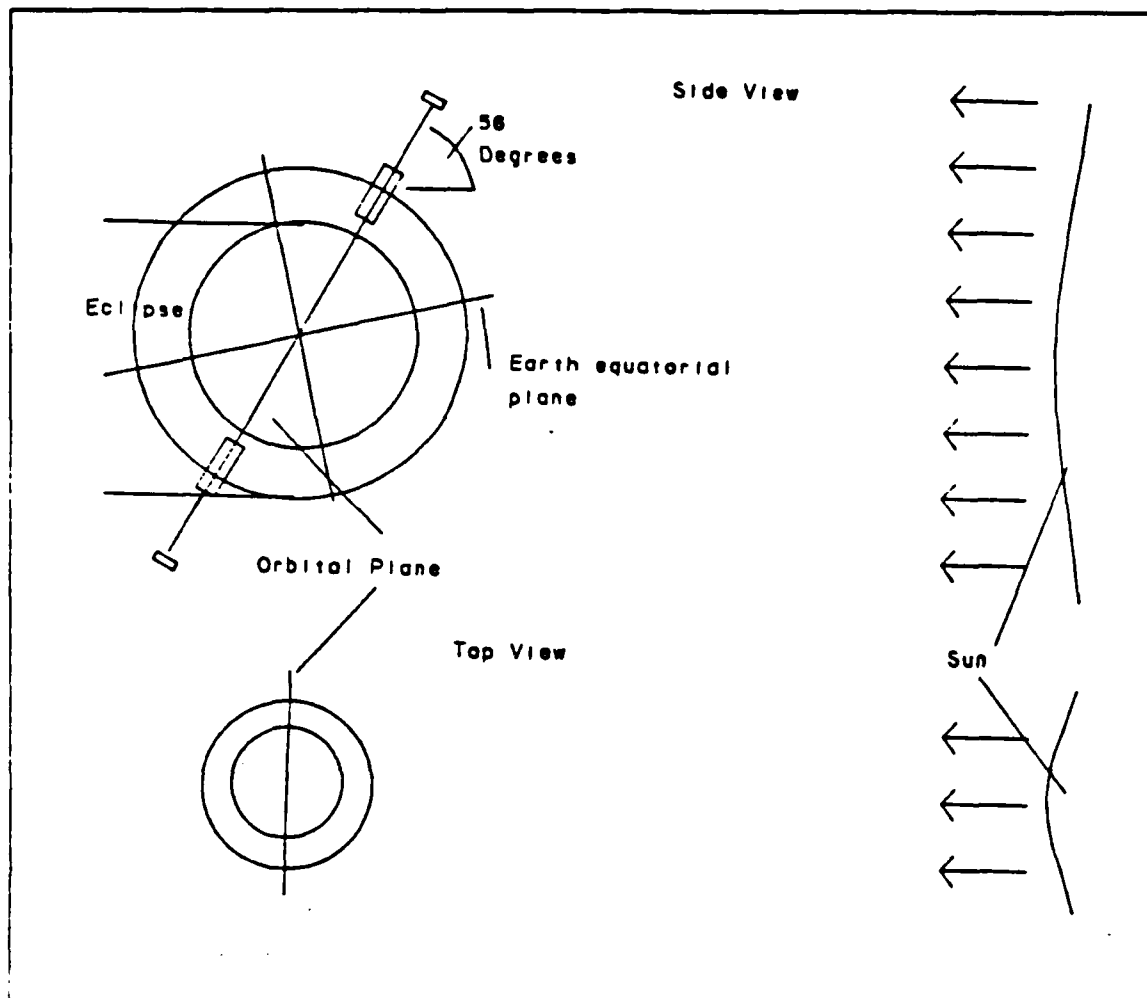


Figure 7.4 Orbital Geometry Creating Maximum Power Output.

$$\eta = \text{Solar cell efficiency (\%)} = 12\%$$

$$P_i = .12(.4624 \text{ m}^2)(1390 \text{ W/m}^2)(.89)$$

$$P_i = 68.64 \text{ W}$$

As seen in Figure 7.5, the projected area available as a function of β does not vary as severely as that in the minimum power orbit. This feature will manifest itself in the computation of average power in the maximum power orbit. The average maximum power, since the projected area is relatively constant, will approach the maximum instantaneous power. Again, the average projected area was determined by integrating the area under the curve in Figure 7.5 and dividing by the time the spacecraft is illuminated by the Sun. The average maximum power is calculated in the following equations.

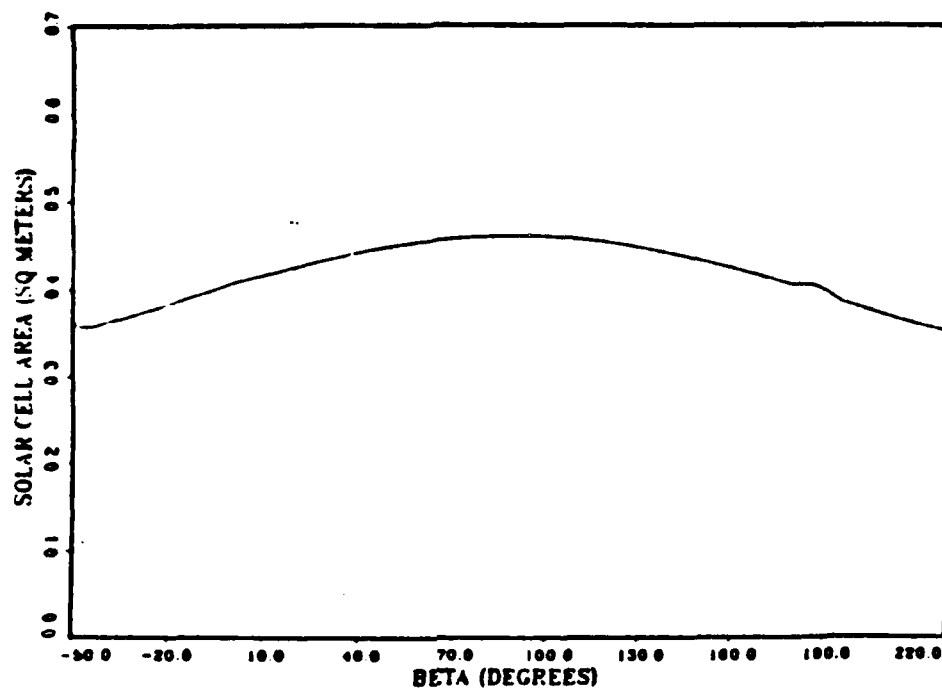


Figure 7.5 Projected Area Available-Maximum Power Orbit.

$$P_{avg} = \eta \times A_{avg} \times S \times D$$

$$P_{avg} = .12(.423 \text{ m}^2)(1390 \text{ W m}^{-2})(.89)$$

$$P_{avg} = 63.83 \text{ W}$$

The approach just developed provides limiting power boundaries that must now be considered as electrical equipment is selected for the spacecraft. The average minimum and maximum power limits are physical restrictions imposed by the orbit and spacecraft selection. If more array power is desired the options are: change the orbit, make more area available for mounting solar cells, or use more efficient, albeit more costly, solar cells. The power source for SKYLITE has been examined. Whether or not the source is sufficient will be decided in the next step in the electrical power analysis, matching the power source with the battery and electrical loads.

4. Battery

The battery chosen for SKYLITE was a type that has been particularly important in space related applications. The Nickel-Cadmium battery was selected because of its dependability, acceptable power rating and cost. The main purpose of the battery aboard a long life spacecraft is to provide electrical power as the spacecraft passes into eclipse. Once the solar arrays become sunlit again they resume their role as prime power source and battery recharging begins. A significant feature of the SKYLITE regarding battery allocation is the relatively low power demands required of the battery. SKYLITE is a transportation bus for an array of IR sensors. The sensors require power only when the MIRACL laser is illuminating the satellite. At all other times the sensors are dormant and the spacecraft reverts to a hibernation state, with only the minimum essential components receiving power.

TABLE 3
POWER BUDGET FOR SKYLITE (WATTS)

Sun sensors (pkg)	0.5
Magnetometer	0.5
Rcvr Demodulator	2.0
Signal Switcher	0.5
Transmitter	5.0
Stable Clock	1.0
Clock P S	1.0
TT&C Signal Proc	2.0
Charging Equipment	1.0
Downlink Formatter	1.0
Timing Distributor	0.5
TX Signal Routing	0.5
RX Signal Routing	0.5
Power Margin	4.0
TOTAL	20.0 Watts

TABLE 4
SKYLITE EQUIPMENT POWERED DURING EXPERIMENT (WATTS)

IR Detectors	1.0
Detector Signal Proc	1.0
Power Margin	1.0

The loads listed in the Table 3 and 4 must be sustained with batteries only when the satellite is in eclipse. The means to determine the proper amount of batteries necessary is to relate the power, battery depth of discharge (DOD), eclipse time and eclipse load in the following manner. [Ref. 5: p. 347-350].

$$P = L \times T / DOD$$

P = Total rating of all batteries (W-h)

L = Electrical load requiring power (W)

T = Time the spacecraft is in eclipse (h)

DOD = Allowable depth of discharge (%)

The terms in the equation were selected with consideration. The electrical load determination was the most straightforward. The satellite operates in two basic regimes; dormant and experimental. The experimental regime occurs six times yearly, when the sensors are activated and SKYLITE is lased by MIRACL. The dormant period includes all other time periods. The load demand for each period is listed in Tables 3 and 4. Due to the relatively rare occurrence, and the low additional power requirement during each experiment, the power load on the battery was assessed as that existing during the dormant state. The duty cycle of the experiment is so low that battery charge and discharge for these periods is lost in the noise. The battery must supply 20 watts of power during periods of eclipse. The eclipse period was the next factor considered. Because of the satellite regression about the Earth, and the Earth's rotation about the Sun, the period of the eclipse will vary from a low of 21 minutes to a high of 35 minutes. Obviously, the electrical draw on the battery must be sustained for a greater period during the longer eclipse. The more conservative figure of 35 minutes was used in determining necessary battery size. The batteries appropriate for a period of 35 minutes will be excessive for a period of 21 minutes, but this allows a margin of safety in the design. The final factor that was decided to size the battery was the allowable depth of discharge. The depth of discharge is the degree that the battery may be depleted before recharging commences. For relatively short missions or few battery charge/discharge cycles (geosynchronous altitude) the depth of discharge can exceed that which is allowed for a mission requiring more cycles. The number of charge/discharge cycles is calculated by the number of orbits during the satellite lifetime, since each orbit has an eclipse. Although true of SKYLITE, not all satellite orbits have one eclipse every orbit. Given the 98.7 minute orbit for SKYLITE's

altitude, there will be 15,986 orbits in the 3 year mission. A table provided by Hughes Aircraft Company was used to ascertain the depth of discharge available for 16,000 orbits [Ref. 12: p. 1-7.21]. The depth of discharge determined with this chart was 9 percent. The quantity of batteries was then calculated.

$$P = L \times T / \text{DOD}$$

$$P = (20 \text{ W})(.5833 \text{ h}) / (.09)$$

$$P = 129.62 \text{ W-h}$$

The rating of the batteries must be provided by Nickel Cadmium batteries with a capability of 10 W-h/lb. [Ref. 5: p. 350]. Thus, 12.96 pounds, or 5.9 kilograms of Ni-Cd batteries will be placed in the satellite to satisfy the eclipse power demands. These figures are very conservative, given the power margin listed in the loading table and the shorter actual eclipse intervals.

The batteries will be recharged once the solar cells are again illuminated by the sun. At this time, the solar cells will charge the batteries and provide power to the spacecraft. The charging rate will depend on the spacecraft power load and the power generated by the solar array. Any surplus will be applied to recharging at a rate above .025 C [Ref. 5: p. 352].

The preceding explanation has indicated how the battery for a certain spacecraft and mission is sized. The battery size depends heavily on several unrelated issues, such as orbit attitude and inclination. For SKYLITE, although the total power requirement is not overwhelming, meeting the power loads is not trivial, given the low volume available for battery storage and small area for solar array mounting.

Electrical loads that must be satisfied throughout the satellite lifetime are listed in Table 3. Additional loads that arise during experimental periods are listed in Table 4. The loads faced when experiments occur are unnoticeable when the duty cycle is viewed from a year's perspective.

C. SOLAR CELL PROTECTION

The solar cells surrounding the SKYLITE spacecraft will be subjected to a relatively intense irradiance at IR wavelengths for periods of up 60 seconds. If the solar cells are not sufficiently protected during this period, the temperature rise of the cells will be sufficient to cause the adhesive to break down or fog. Should the adhesive fail, the cells and cover glass would not be bound to the spacecraft, ceasing further solar power. If

the adhesive fogs, the cells will be opaque to visible light, effectively stopping the conversion of sunlight to spacecraft power. Either event will prevent further experimental activities. Thus, the solar cells must be protected from damage due to high temperature.

The Thermal Control Chapter analyzed the temperature response of the spacecraft throughout the orbit as a function of season, sun angle and laser irradiance. However, the temperature evaluated was body averaged and was referred to as bulk temperature. The actual temperature of a spacecraft component can be substantially larger or smaller than the bulk temperature when a steep temperature gradient is present. The illumination of the spacecraft by a laser can create such a temperature gradient if no protection is implemented. To protect the SKYLITE solar cells from failure due to high temperatures, two methods will be used. The first method involves the design of highly conductive thermal paths through the satellite. A conductive thermal path dissipates the heat on the satellite's periphery into the spacecraft interior as soon as a surface temperature rise begins. If the thermal paths are extremely conductive, the spacecraft temperature will be uniform throughout, preventing temperature extremes at any particular point. The second method of protection will involve covering all solar cells with a thin cover glass. This glass has high reflectance at IR wavelengths and high transmittance at visible wavelengths. The presence of the glass reduces solar cell efficiency to 95-97 percent of its prior value. The slight reduction in solar cell output will not affect electrical system operation. The protective glass has a reflectance of 96 percent when the laser path is normal to the surface and decreases to a minimum of 60-70 percent when the laser path is 60 degrees from the normal. Unfortunately, the spacecraft and laser site geometry dictate lasing angles between 60 and 80 degrees so the cover glass IR reflectance will be minimum. However, even 60 percent reflectance, combined with conductive thermal paths, should prevent high spacecraft surface temperatures. [Ref. 13]

The measures anticipated for solar cell protection are currently available. Several complex computer programs, using nodal analysis can calculate the temperature at thousands of points within the spacecraft. Thermal paths can be designed and controlled using the results of the programs. The technology necessary to manufacture a cover glass with high transmittance at visible wavelengths and high reflectance at IR wavelengths is mature. However, the specific substance causing high reflectance in the 3.6-4.2 μ band is unknown. A research effort of approximately six months is required

to develop and produce the needed substance. The risk in implementing both measures for solar cell survivability is low and would significantly increase the reliability of the experiment.

D. CONCLUSION

Body mounted and tip mounted solar arrays, covering .407 m² and .183 m², respectively, will provide primary power to the SKYLITE satellite. The power available from the solar arrays varies from a minimum of 52.5 W to a maximum of 63.83 W. During periods of eclipse the power requirements will be supplemented by a 6 kg Nickel Cadmium battery, rated at 129.62 Watt-hours. Due to the very low experiment duty cycle, the battery discharge during experimental periods is easily resupplied. These power sources will provide the necessary power during launch, insertion and experiments. Protection of the solar arrays with IR reflective materials and careful thermal conduction will protect the array and enhance the mission with relatively low risk.

VIII. SPACECRAFT STABILIZATION

A. INTRODUCTION

The stabilization analysis for the SKYLITE satellite required a careful survey of available stabilization methods. The three primary stabilization methods used in spacecraft design are three axis, spin (dual or single), and gravity gradient stabilization [Ref. 15: p. 147-150]. For the SKYLITE design gravity gradient stabilization was selected. Three axis stabilization, although capable of providing extremely accurate pointing angles, was thought too complex and expensive for the SKYLITE mission. Spin stabilization, attractive due to its simplicity, was discarded since it provides stabilization in inertial coordinates, not earth pointing coordinates, as was necessary for SKYLITE. Spin stabilization did create long intervals of time when an earth facing sensor could be maintained, but there were also large gaps of sensor inavailability that impacted too severely on MIRACL operating schedules. Thus, considering weight, complexity, volume, and firing opportunities, the selection of gravity gradient stabilization was thought most applicable for SKYLITE.

Gravity gradient stabilization is defined as the alignment of one axis of a satellite along the local earth vertical so that a particular end of the satellite is always facing downward, towards earth [Ref. 15: p. 149]. For SKYLITE, the positive z axis, which is the bottom of the satellite, will always point to earth. The advantages of selecting gravity gradient stabilization are : no requirement for active control, no attitude sensors are necessary for control (may be used for sensing spacecraft position), and high reliability. The disadvantages of gravity gradient stabilization are: the satellite is extremely sensitive to disturbing torques, orbital eccentricity is limited to less than .02, and the local vertical accuracy is limited to two or three degrees at an altitude of 500 miles [Ref. 6].

The advantages of gravity gradient stabilization mesh well with SKYLITE's operating requirements. However, the disadvantages must be closely examined. The eccentricity constraint is of no consequence, as a circular orbit was desired. For the mission requirement of attitude knowledge there is room for misinterpretation. The requirement necessitates a measurement of spacecraft attitude that is accurate to five degrees. The demand is not for attitude stabilization within five degrees, but instead

requires attitude knowledge within five degrees. In anticipating the disadvantage of gravity gradient instability due to the motion of components within the spacecraft, once the orbit is captured successfully, there will be no moving parts. The final disadvantage of extreme susceptibility to disturbance torques was difficult to minimize. However, several design techniques were implemented to moderate the effects of these torques [Ref. 17]. The magnetic torques were minimized by placing the wiring for the solar cells immediately below the substrate. This action minimized the area about which the current would travel, thus reducing magnetic torque. Solar pressure torque and torque due to aerodynamic drag were the remaining disturbing forces. At very low earth orbits, the aerodynamic drag dominates gravity gradient stabilization, possibly making it ineffective. The selection of a reasonably high low earth orbit mitigates the degradation of stabilization due to aerodynamic torques and allows the righting moment of the gravity gradient boom to dominate. Finally, the effects of solar pressure cannot be obviated. The solar pressure is constant in all near earth regions. The fluctuations in stabilization created by solar pressure torques can be lessened only by providing an even larger righting moment with the gravity gradient boom [Ref. 14: p. 2-3].

B. GRAVITY GRADIENT BOOM LENGTH DETERMINATION

The use of a gravity gradient boom for attitude stabilization is a fine balance of a minute correcting moment with even more minuscule disturbing forces [Ref. 14: p. 1]. The available orbits for gravity gradient stabilization are limited. The spacecraft must be far enough from Earth to prevent overwhelming aerodynamic drag forces from disrupting balance, yet close enough to the earth for its gravitational field to provide a stabilizing moment.

The general shape of a satellite utilizing gravity gradient stabilization is a long rod whose longitudinal axis aligns itself with the local earth vertical. The stubby ORION bus differs considerably from the preferred shape so a means of distributing a long boom is necessary. The SKYLITE spacecraft is given this long profile by the extension of a boom through its top plate. The material composing the extension will be a tapered boom commonly referred to as a bistem boom. This boom has been successfully employed on many spacecraft throughout the last fifteen years. There have been no known failures of the extension of the bistem boom. It will provide the deployment of the tip mass as well as the structural strength required to support the tip mass against aerodynamic forces.

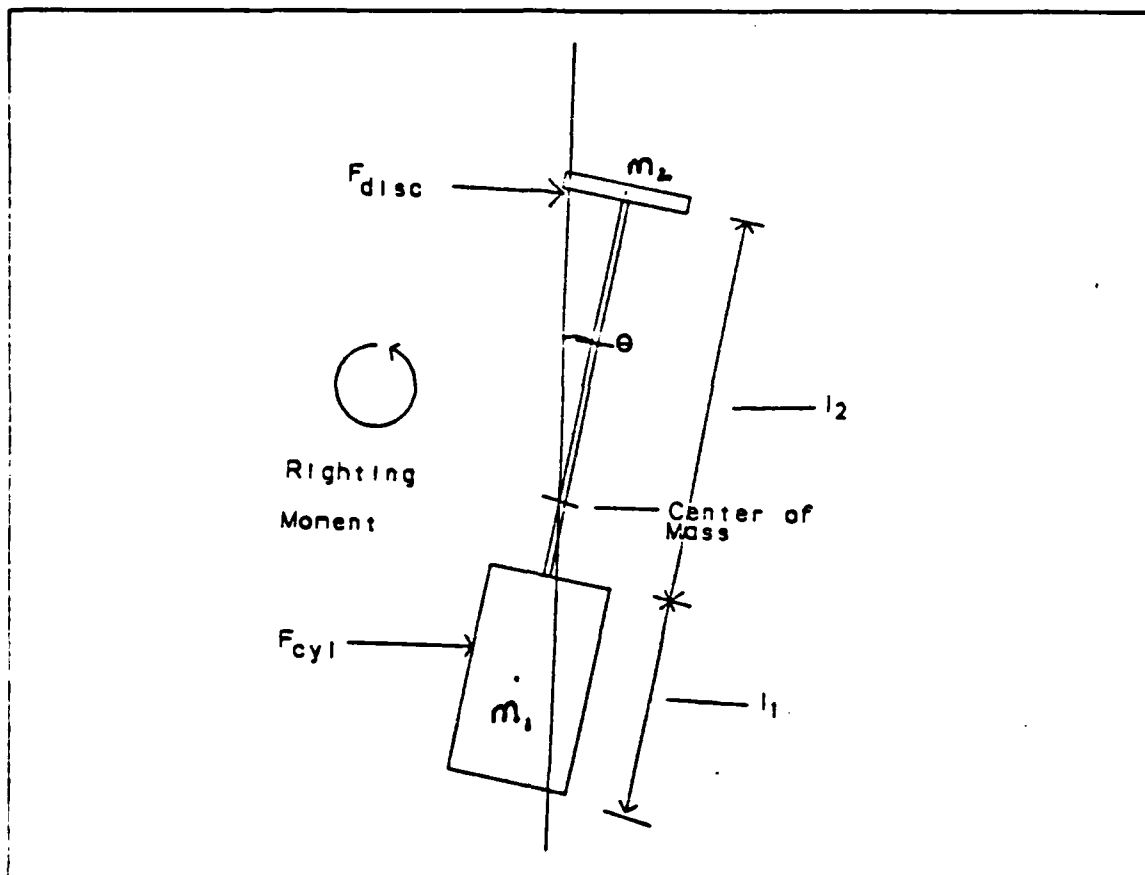


Figure 8.1 Forces Acting On SKYLITE.

1. Boom Length Calculations

To design the boom length and tip mass for the SKYLITE spacecraft, the disturbing forces and righting moments were calculated. The actual configuration of SKYLITE in orbit is depicted in Figure 8.1, with the forces indicated. The following equations were used to evaluate the design [Ref. 15: p. 36-37, 149-151].

$$F_{disc} = F_{aero} + F_{sp}$$

$$F_{aero} = \text{aerodynamic drag force} = (1/2)\rho V^2 C_d A \text{ (N)}$$

$$F_{sp} = \text{Solar pressure force} = PA(1.5) \text{ (N)}$$

$$F_{disc} = (1/2)\rho V^2 C_d A + PA(1.5) \text{ (N)}$$

$$M_{gg} = (m_1 m_2 l^2 k \sin 2\theta) / (m_1 + m_2) 2r_o^3 \text{ (N-m)}$$

The variables in the equations apply as follows.

$$\rho = \text{atmospheric density (kg/m}^3\text{)}$$

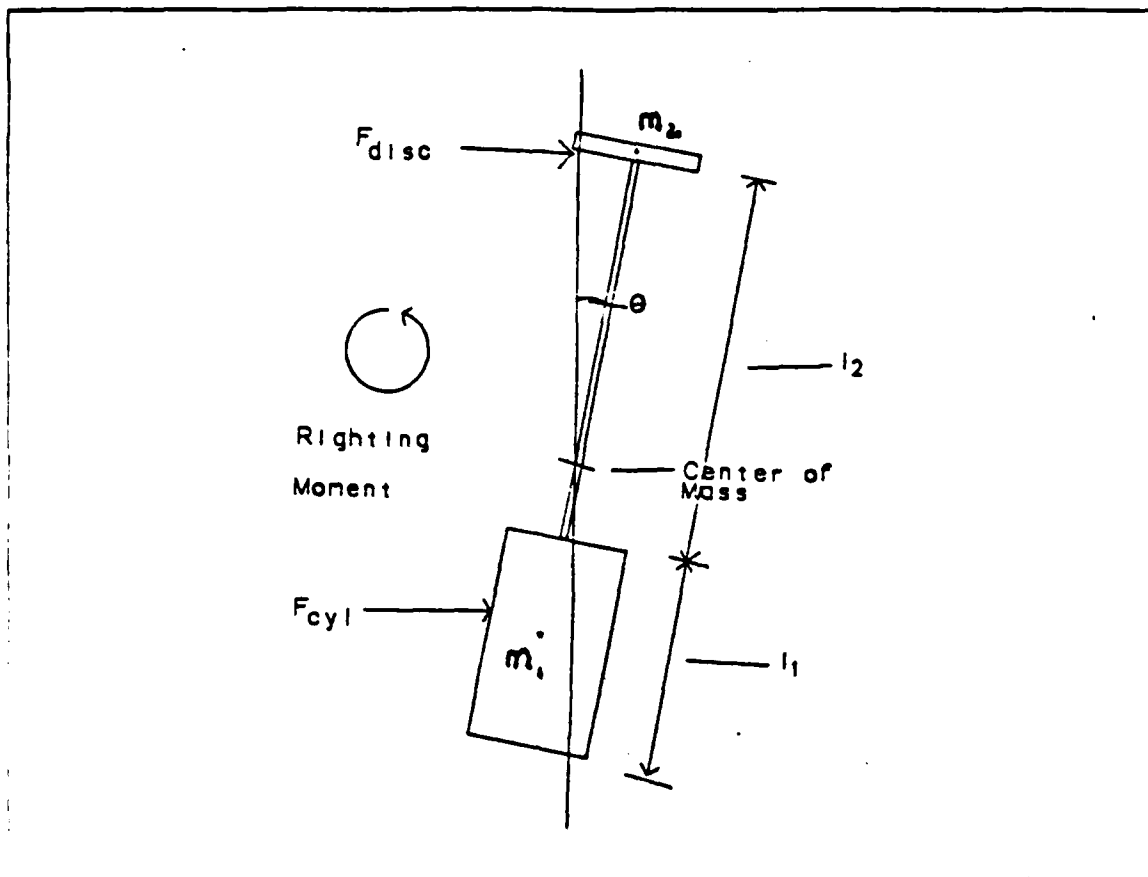


Figure S.2 Free Body Diagram of SKYLITE.

V = spacecraft velocity (m.s)

C_d = coefficient of drag

A = cross sectional area of the spacecraft (m^2)

P = solar radiation pressure at 1 Astronomical Unit

M_{gg} = righting moment of gravity gradient boom (N-m)

m_1, m_2 = masses at the boom ends (kg)

r_0 = orbital altitude of satellite (m)

θ = angle at which righting moment equals disturbing forces

l = boom length (m)

The performance of the gravity gradient boom was evaluated through two orbital stations, each described by altitude, inclination, and atmospheric density. As seen in the above equations, the disturbing torques are a function of satellite velocity and atmospheric density. For a circular orbit, the satellite velocity is computed

directly, using $V_c = \sqrt{k/r}$, with r representing the orbital radius. Thus, the disturbing torques are dependent on orbital radius, and atmospheric density. If either of these quantities changes, the equations governing equilibrium must be reevaluated.

The different orbital stations evaluated were a 700 kilometer and a 680 kilometer orbit, using the appropriate atmospheric density curves as presented in the ARDC model. The ARDC figures are conservative, in that they provide densities higher than normal and generate disturbing forces which stronger than those calculated using median values of atmospheric density. Ideally, if launched on schedule in 1989, SKYLITE will begin orbit during high solar activity at an altitude of 700 kilometers. This orbit will provide disturbing torques that may satisfactorily be corrected by a certain boom length and tip mass. However, if the launch is delayed, the disturbing forces will increase due to the expected peak in solar activity during 1990-1991. The boom length and tip mass must be changed to successfully counteract the larger forces. If the orbit is delayed and solar activity is severe, the orbital decay rate for SKYLITE will increase, lowering it into the second evaluated region at 680 kilometers. The boom length and tip mass used will be the arrangement which adequately maintains stabilization throughout both evaluated orbits.

The equations listed previously were manipulated to give the following equation which solves for boom length.

$$l = \{F_c - F_d(M/m_2 - 1)\} 2r_o^3 / \{(M - m_2)k \sin 2\theta\}$$

The variables apply as follows:

F_d = total force on the disc (N)

F_c = total force on the cylinder (N)

M = total mass of the disc and cylinder (kg)

A critical feature of this equation is the presumption that θ is known. θ is the maximum angle at which the satellite will deviate from the local vertical and is selected during the design based on the collecting requirements of the onboard sensors. Were θ too large, the sensors would not maintain the MIRACL laser in the field of view at critical moments. Ideally, θ would always be zero, which is impossible since at zero degrees no righting moment exists. At the outset of the design, achieving a reasonable θ with an attainable boom length was questionable. Calculations were made to determine how boom length varied with small changes in θ . A value for θ of five

degrees was selected, based on the premise that if the satellite never varied more than this from the local vertical, whenever it flew through the firing cone, sensors would be maintained at appropriate orientations for irradiance sampling.

The assumptions that follow were applied to evaluating both orbital stations and conditions to determine boom length and tip mass.

- (1) Forces opposing gravity gradient stabilization are aerodynamic drag and solar radiation pressure torque.
- (2) ORION configuration can be approximated by a barbell when considering the balance of forces.
- (3) The mass of the spacecraft when it arrives on station is 95 kg. This assumes that 30 kg of fuel was consumed enroute to station.

Several observations were drawn from analyzing the balance of forces on the spacecraft. They were useful in selecting an appropriate boom length and tip mass.

- (1) If the allowable θ is doubled, boom length will be halved. This is important because if the experimenters can accept a larger θ the boom may be significantly shortened.
- (2) Contrary to intuition, as the tip mass (m_2) increases, the length of boom increases. This suggests there is a minimum tip mass that will sufficiently balance the spacecraft without requiring an inordinately long boom.
- (3) The balance is very sensitive to F_d . Since F_d is acquired from the aerodynamic force and solar pressure on the disc, and both of these quantities are functions of the disc cross sectional area, then the cross sectional area is important. If tip shape is changed, the cross sectional area and thus boom length is also changed. If boom length is too high, it may be reduced by substituting a lighter material in the tip mass, which gives the same mass, but provides a larger cross sectional area.
- (4) The equation determining boom length becomes negative and valueless when the term $F_c - F_d(M/m_2 - 1)$ equals zero. This occurred when the tip mass (M_2) was 4.5 kg. Thus, for this tip mass cross sectional area, a mass of 10 kg was selected to avoid the described negative value.

The boom length was evaluated for a tip mass of 10 kg, a θ of five degrees at each of the orbits of interest with the following results.

- (1) 700 km, nominal solar activity ($\rho = 3 \times 10^{-13} \text{ kg/m}^3$)
[Ref. 4: p. 5].

Boom length = 1 meter

- (2) 700 km, severe solar activity ($\rho = 3 \times 10^{-12} \text{ kg/m}^3$)

[Ref. 4: p. 5].

Boom length = 7.8 meters

The boom length from the above calculations must be at least 7.8 meters long to satisfy the desired angle of θ in all regimes. The deviation of the spacecraft from the local vertical will not always be five degrees. The disturbing torques of aerodynamic drag and solar pressure do not always act in the same direction and maximize angular deflection. When the spacecraft is flying away from the sun the solar radiation pressure and aerodynamic drag will act in opposite directions, causing a sufficient righting moment to be obtained with much less than five degrees deflection. Accounting for the absence of magnetic torque and the fluctuations in values for atmospheric density the designed boom length will be 10 meters. This is 2.2 meters above the calculated value and will supply an additional amount of righting moment. Thus, the tip mass for SKYLITE will be a disc with a thickness of 4.4 cm and a mass of 10 kg. The boom length satisfying attitude stabilization throughout all flight regimes is 10 meters.

C. ATTITUDE SENSING

Since SKYLITE employs gravity gradient stabilization, which is a passive method requiring no feedback or control loops, sensing attitude orientation for stabilization is not necessary. However, the experimenters at WSMR need to know the position and orientation of the spacecraft to calculate incidence angles for laser power measurements. The attitude knowledge specifications required accuracy to within three degrees.

To meet the knowledge specifications, an ADCOLE 4π Steradian Sun Sensor assembly will be mounted on the spacecraft. The assembly consists of five identical sun sensors and associated electronics. The function of the sensors is to provide condition data on the telemetry signal from which the direction of the sun with respect to a satellite axis can be determined. Each sensor generates two-axis solar aspect data over its field of view and an analog voltage proportional to the intensity of the incident solar radiation. The electronic components select the sensor most closely facing the sun by comparing analog voltages. The field of view (FOV) of each sensor is 128 by 128 degrees within which sensor resolution is .5 degrees and transmission accuracy is $\pm .25$ degrees. [Ref. 16]

Also contributing to pointing knowledge will be a magnetometer assembly which will provide attitude information by sampling the magnetic field about the spacecraft.

The sampled measurements are also transmitted via the telemetry signal and compared to the NASA magnetic field data base. The NASA file is extremely accurate, and based on the position of SKYLITE, the samplings can be compared to determine the attitude at each position. The magnetometer outputs are also analog voltages from 0 to 5 volts representing a field of ± 500 mgauss along each of the three axes. The magnetometer accuracy is ± 5 mgauss over the entire field range. [Ref. 16]

The use of sun sensors and magnetometers for attitude knowledge will provide information accurate to within 1-2 degrees, thus exceeding the experimental requirement of 3 degrees. Emphasis is placed on the necessity of ground support for both sensors to derive satellite attitude. The spacecraft does not downlink an attitude with respect to a certain reference system, but instead transmits measurements which allow attitude determination at the ground station. The projected schedule is to sample the attitude sensors each orbit as the satellite passes within communications range of the ground station. The precise attitude knowledge designed into the spacecraft system will be essential when boom deployment is performed to capture SKYLITE in gravity gradient stabilization.

The evolution of capturing the spacecraft into a gravity gradient stabilization is tentative and precise. The failure to capture the spacecraft has been the end of several satellite missions. During the infancy of space exploration gravity gradient stabilization was evaluated as very useful due to its simplicity and relatively accurate orientation tolerances. Unfortunately, as with any new scientific endeavor, the moment of capture was elusive and sometimes unattainable. Several experiments failed at their initial capture attempts, and since they did not have fuel or mechanisms for another attempt, the mission was doomed. In SKYLITE, a means for repeated attempts is available. Capture will occur as the boom is extended at the righting moment becomes greater than the disturbing moment. The boom will continue until it reaches a ten meter length. if at any time during the operation the capture fails, the boom can be retracted and capture can be reattempted at a future time.

D. CONCLUSION

The stabilization requirements for SKYLITE are adequately satisfied with the use of a gravity gradient boom. A boom length of 10 meters will stabilize the longitudinal axis of the spacecraft within five degrees of the local vertical. This orientation places the laser site in both the sensor and retroreflector field of view during experimental periods. Knowledge of the spacecraft attitude will be established by magnetometers

and sun sensors to .5 degrees and 2 degrees respectively. These values exceed the experimental attitude knowledge requirement of 3 degrees. Satellite attitude will be calculated at the ground site using transmitted magnetometer data.

IX. STRUCTURAL ANALYSIS

A. INTRODUCTION

Since the spacecraft selected for the SKYLITE mission was a modified version of the ORION bus, the structural analysis closely coincides with that originally done [Ref. 1: p. 19-20]. However, many rough approximations, such as the loading of ORION in its cantilever position inside the STS cargo bay, will be redone based on the loads and forces peculiar only to SKYLITE. The ORION bus was analyzed in its SKYLITE configuration to determine if it satisfactorily meets rigidity, maximum stress, deflection, and vibration requirements. Additionally, the short booms, deployed from SKYLITE to ensure stability during injection, will be evaluated for stress and deflection caused by centripetal acceleration during spin up and spin down. The SKYLITE structural analysis examines the following points, highlighting details and explaining engineering considerations.

- Spacecraft Loading
- Center of Mass Variances
- Moment of Inertia Determination
- Maximum Stress Evaluation
- Maximum Structural Deflection
- Vibration Under Base Excitation
- Maximum Stress and Deflection of Deployed Stability Booms

B. STRUCTURAL LOADING

The arrangement of payload and support equipment throughout the spacecraft significantly affects the spacecraft behavior when deployed as well as the structural performance during periods of high loading. For example, a primary disturbing torque for low Earth orbiting satellites is aerodynamic torque. This torque exists due to the difference in displacement between the center of mass and the center of pressure. Ignoring all other considerations, aerodynamic torque can be minimized by shaping and loading the spacecraft to lessen the distance between center of pressure and center of mass. Also, an example of a structural consideration appears in the case of SKYLITE due to its position in the STS cargo bay. SKYLITE is launched from the extended GAS can aboard the STS. The longitudinal axis of the GAS can, and

SKYLITE, is perpendicular to the longitudinal axis of the STS. This arrangement places SKYLITE in a cantilevered position, rather than an axially loaded position. The point of maximum stress in a cantilevered homogeneous object occurs at its base, and is very sensitive to large loads placed at the free end. Thus, if the stress in a cantilevered orientation is of extreme concern, the loads inside the spacecraft may be redistributed towards the fixed end, reducing the amount of maximum stress. For these two reasons, the dispersion of items and loads inside the satellite must be well considered.

The basic structure of ORION, as initially designed, was selected for the SKYLITE design [Ref. 1: p. 20]. The structure and materials were identical, with major loading variances existing in the payload type and location. These loads and equipment listed in Table 5 were the baseline values used to calculate the center of mass, stress and deflections for SKYLITE [Ref. 1: p. 20]. The loads were distributed as pictured in Figure 9.1. Several assumptions made in developing Table 5 must be explained. Any masses which are evenly distributed along the spacecraft longitudinal axis, such as structural skin, longerons, or miscellaneous materials were considered as acting at the center of mass. This assumption agrees with standard loading analysis concerning evenly distributed loads. Also, all available weight allowances were considered fully utilized. For example, the upper cargo bay has an allowance of approximately 42 pounds for payload. At the outset of SKYLITE's design, the exact payload weights were unknown, so all available weight was assumed to be used. This would result in conservative calculations and an inherent safety factor, should the actual SKYLITE payload not actually equal the maximum payload weight possible. The final point to elaborate upon concerns the fuel contained in SKYLITE. The ORION bus has three variants which tradeoff fuel and payload. Since the SKYLITE payload appeared undemanding, the ORION variant possessing the most fuel aboard was selected. The amount of Hydrazine in the fuel tank at STS liftoff is 77.88 pounds. Even though this fuel load will be consumed during injection and transit to station, it was considered essential to structural calculations since it is present at STS liftoff.

C. CENTER OF MASS VARIANCES

As previously explained, accurate knowledge of the location of the center of mass is essential to accurate structural evaluation. The center of mass of SKYLITE will vary due to fuel consumption. The magnitude of the variance was based on the distance of the fuel tank from the center of the spacecraft and the amount of fuel is consumed. If

TABLE 5
SKYLITE LOADING TABLE (LB)

Weights on the top plate:	
Top plate	1.65
Thruster	.60
SUBTOTAL	2.25
Weights in upper storage bay:	
Support plate	1.65
Batteries	5.85
Data equipment	8.10
Thruster	2.40
Payload	42.00
SUBTOTAL	60.00
Weights through the Center of Mass:	
Structural Skin	8.48
Longerons	5.80
Booms	4.20
Fasteners	3.48
Solar Array	8.00
Wiring, electronics	25.00
Miscellaneous	19.00
SUBTOTAL	73.96
Weights acting through the tank support:	
Tank support members	2.00
Tank strongback	2.20
Fuel	77.88
Piping	4.00
Propellant tank	19.00
SUBTOTAL	105.00
Weights through lower plated support:	
Lower plate	1.05
SUBTOTAL	1.05
Weight acting through bottom plate:	
Baseplate	9.75
IT&C Equipment	8.10
Thrusters	2.00
Stabilization balls	8.00
SUBTOTAL	27.85
OVERALL TOTAL	270.11 Pounds

the spacecraft is deposited by the STS directly into the operational orbit, no fuel will be burned and the center of mass will not change. However, as discussed in the Propulsion chapter, the allowances for insertion indicate that most or all of the fuel will be expended. Knowledge of the position of the center of mass relative to the center of

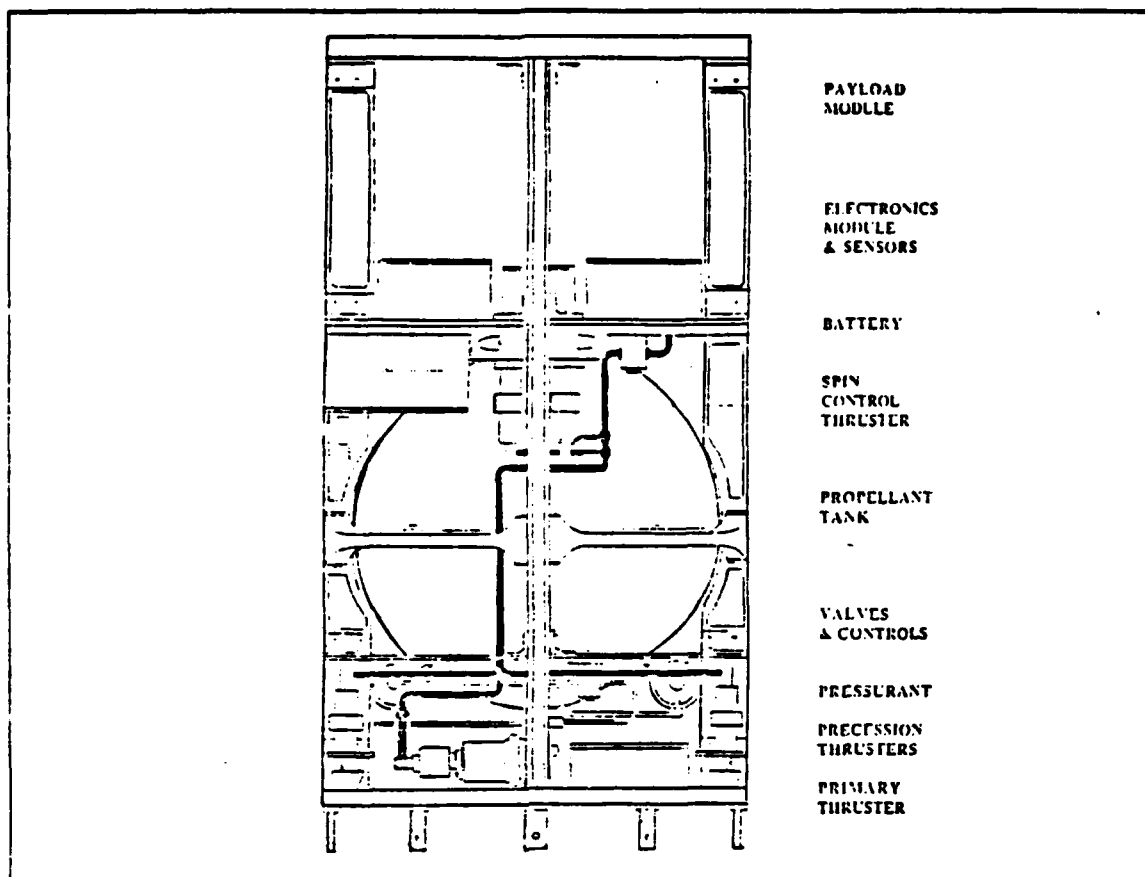


Figure 9.1 Loading and Placement of ORION Components.

pressure was essential to estimating the disturbances torques, and consequently the length of the gravity gradient boom necessary to employ gravity gradient stabilization. The last point must be reemphasized. If the center of mass, and consequently the disturbing torque estimates, were substantially in error, the length of boom allotted for satellite stabilization will not be sufficient, resulting in an uncontrolled spacecraft and an aborted mission.

The table of loading listed in the previous section was used to determine the center of mass prior to any fuel consumption. Although the short stabilizing booms will be deployed prior to spacecraft injection, they will not displace the center of mass since their extended position is perpendicular to the satellite longitudinal axis. The base of the satellite was the origin for calculating the center of mass, with all loads were referenced to this point. The satellite loads listed in Table 5 act through distances listed in Table 6.

TABLE 6
DISTANCE OF SKYLITE LOADS, REFERENCED TO THE BASE

Distance from satellite baseplate to:

Baseplate	0.00 cm
Lower plate support	15.60 cm
Propellant tank support	29.63 cm
Estimated center of mass	44.45 cm
Upper bay support	54.58 cm
Top plate	88.90 cm

The center of mass is calculated using the loads and distances from Tables 5 and 6 [Ref. 1: p. 20]. The following equation, which evaluates the center of mass, was used to sum the product of the distance times the load and divide by the sum of the loads.

$$\text{C.M.} = \Sigma(d \times m) / \Sigma(m)$$

d = Distance from the baseplate to each load (cm)

m = Mass of each load (kg)

C.M. = 36.61 cm from the baseplate.

The calculations were repeated for spacecraft loading with no fuel present, which provided the spacecraft's center of mass as it arrived at its operational station. The difference of the two calculations also yielded the change in the center of mass.

$$\text{C.M.}_{\text{station}} = \Sigma(d \times m) / \Sigma(m)$$

C.M._{station} = 38.97 cm from the baseplate

The spacecraft center of mass rose 2.36 cm as the propellant was burned. This calculation agrees with the intuitive evaluation that the center of mass will rise if a weight low in the body of the spacecraft (fuel) is removed. The distance from the center of mass to the center of pressure when the satellite arrives on station will be 5.476 cm. This value was used in the Stabilization chapter to determine the magnitude of aerodynamic and solar radiation disturbing torques.

D. MOMENT OF INERTIA DETERMINATION

The determination of the moment of inertia about the longitudinal axis is essential to evaluate the magnitude and location of maximum stress. The moment of

inertia is inversely proportional to the stress at any point and the two quantities are related by the following formula [Ref. 18: p. 513].

$$\sigma = My/I$$

σ = Stress at desired location (N m^{-2})

M = Moment at desired location (N-m)

y = Distance from neutral axis to desired location (m)

I = Moment of inertia (m^4)

Since the evaluation of maximum stress is necessary, the moment of inertia for the ORION bus was determined. The moment of inertia was calculated for the base plate attaching the satellite to the STS bay, and for the cylindrical shell of the spacecraft adjacent to the baseplate. The necessity to determine moments of inertia at two positions will be explained.

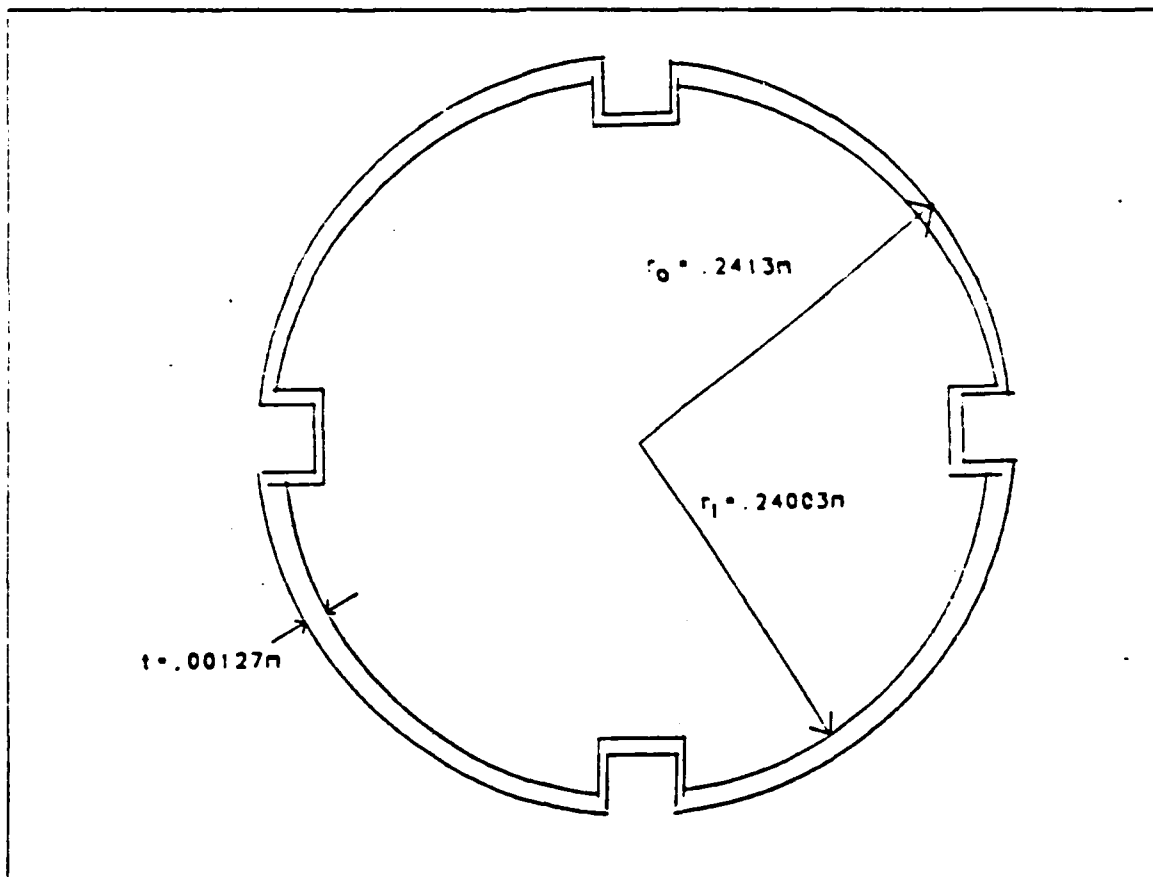


Figure 9.2 Cross Sectional Diagram of the ORION Baseplate.

1. Baseplate Moment of Inertia

The configuration and details of the ORION baseplate are illustrated in Figure 9.2. The item is 24.13 cm in radius and has 4 square cutouts designed to retain the longerons. The depth and width of the cutouts as drawn are 2.54 cm by 5.08 cm [Ref. 1: p. 21]. The moment of inertia calculation became slightly more difficult due to the presence of the cutouts. Whereas the moment of inertia for a disc is direct and simple, the cutouts must be included by means of the Parallel Axis Theorem [Ref. 18: p. 514]. The equations used to describe the calculations follow.

I_d = Moment of inertia for a disc

$$I_d = \pi d^4 / 64$$

$$I_d = \pi (48.26 \text{ m})^4 / 64$$

$$I_d = 2.663 \times 10^{-3} \text{ m}^4$$

The absence of material due to the cutouts reduces the total moment of inertia and must be subtracted from that of the disc [Ref. 18: p. 446].

$$\text{Parallel Axis Theorem} = I_f = I_i + Ad^2$$

I_f = Moment of inertia with respect to the axis of interest (m^4)

I_i = Moment of inertia with respect to a distant axis (m^4)

A = Area of the cutout (m^2)

d = Distance from the axis of interest to the distant axis (m)

Only two of the cutouts as drawn in 9.2 are separated from the neutral axis, the remaining two are accounted for by subtracting their moment of inertia from the disc's moment of inertia.

$$I_{bp} = I_d - I_{co}$$

I_{bp} = Moment of inertia of the baseplate (m^4)

I_d = Moment of inertia of the disc (m^4)

I_{co} = Moment of inertia of the cutouts (m^4)

$$I_{bp} = 2.663 \times 10^{-3} \text{ m}^4 - 1.354 \times 10^{-4} \text{ m}^4$$

$$I_{bp} = 2.527 \times 10^{-3} \text{ m}^4$$

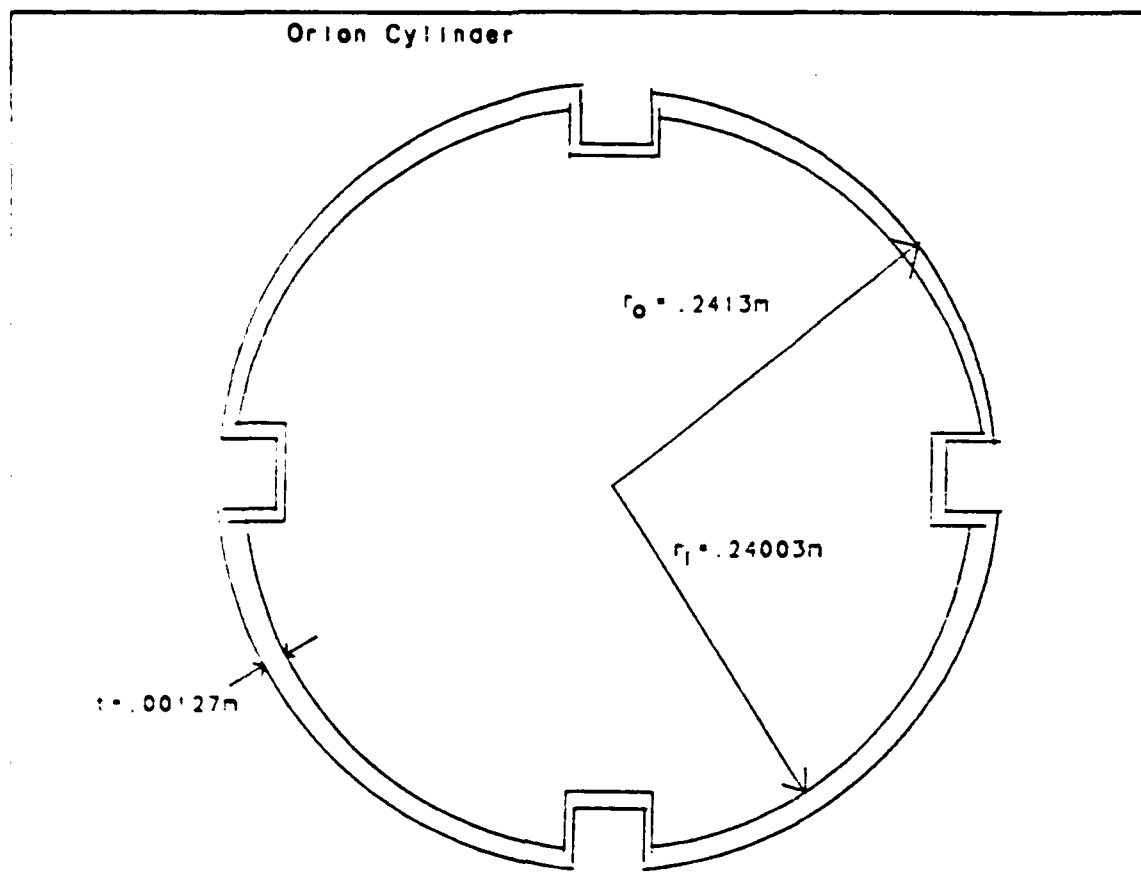


Figure 9.3 Cross Section of the ORION Cylindrical Shell.

2. Cylinder Moment of Inertia

The moment of inertia for the thin walled shell of ORION was next evaluated. The ORION shell is drawn in Figure 9.3. A simple equation exists to calculate the moment of inertia of a thin walled structure. This equation, though not exact, provides an extremely accurate approximation to the true moment of inertia. This equation is explained below [Ref. 18: p. 514].

I_{cyl} = Moment of inertia of a thin walled cylinder (m^4)

$$I_{cyl} = r_o^3 \pi t$$

r_o = Radius to the outside of the cylinder (m)

t = thickness of the cylinder (m)

The equation is evaluated for the 24.13 cm outer radius and .127 cm skin thickness of ORION.

AD-A187 986

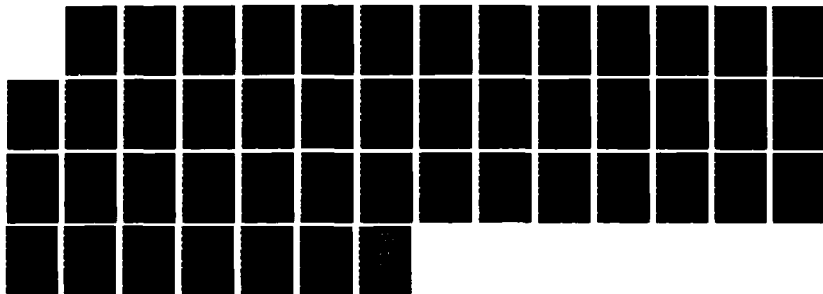
PROJECT SKYLITE: A DESIGN EXPLORATION(U) NAVAL
POSTGRADUATE SCHOOL MONTEREY CA W J WELCH ET AL.
SEP 87

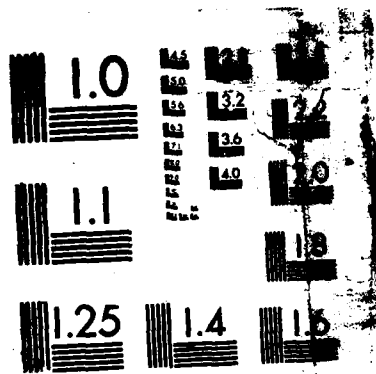
2/2

UNCLASSIFIED

F/G 4/1

ML





MICROCOPY RESOLUTION TEST CHART
NATIONAL BUREAU OF STANDARDS-1963-A

$$I_{cyl} = (.2417 \text{ m})^3 \pi (.00127 \text{ m})$$

$$I_{cyl} = 5.634 \times 10^{-5} \text{ m}^4$$

The moment of inertia calculations were accurately evaluated for use in subsequent analyses concerning stress and deflection. The importance of calculating moments of inertia for the baseplate and the cylinder become apparent when perusing these subsequent analyses.

E. MAXIMUM STRESS EVALUATION

The location and magnitude of maximum stress must be determined to verify that the strength of the material selected for the satellite structure is indeed adequate. The housing of SKYLITE in the extended GAS (Get Away Special) can dispenser poses unusual loading during conditions during the maximum stress interval caused by liftoff. The SKYLITE satellite, because its longitudinal axis is perpendicular to the acceleration vector at launch, experiences lateral or transverse loading conditions. This orientation is different than the typical spacecraft configuration which receives axial loads upon launch. The ORION bus, due to its relatively stubbiness, is not as sensitive to axial loads or transverse loads. Axial loads become critical based on column length, which the ORION bus barely emulates. Also, transverse loads for a base mounted satellite become crucial if the length of the member is unduly long or if an extreme load is placed at the end of the beam. Again, the ORION configuration, because of its short length, mitigates the effects of a high transverse load.

The position of SKYLITE, as it resides in the STS cargo bay during launch is illustrated in Figure 9.4. The base of the satellite is secured via the extended GAS can dispenser to the shuttle. For purposes of analyzing material stress, the ORION bus was considered a cantilevered beam, with several point loads. A simplifying worse case assumption was considering all the loads aboard SKYLITE to be concentrated in the top plate. This evaluation, although very conservative, did not provide for accurate loading representation, should a partial redesign become necessary.

Modeling SKYLITE as a cantilevered beam, for purposes of evaluating the maximum stresses, was very accurate and provided for simple straightforward analysis. Using the loads and distances listed in Tables 5 and 6, the loading diagram in Figure 9.5 was developed. NASA requirements were for the structural members of the satellite in the extended GAS can to withstand acceleration limits of up to five times the force of gravity. These requirements effectively multiply the loads in the spacecraft

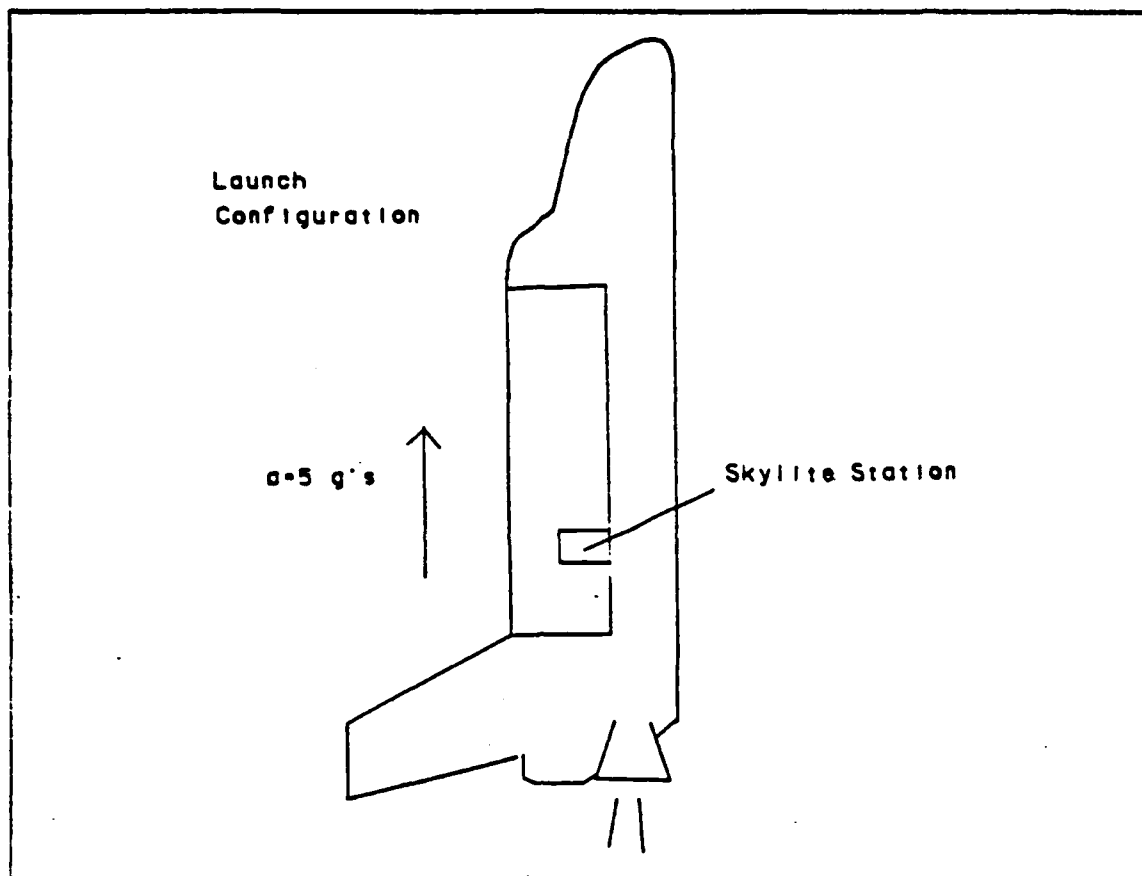


Figure 9.4 SKYLITE Position in the STS Cargo Bay.

by five when evaluating maximum stress at launch. The stress in a cantilevered beam is calculated using the relationship that follows.

$$\sigma = My/I$$

The variables in the equation were previously explained. A cantilevered beam has a resultant force and moment that exists in the attached base that must resist all the forces and moments of loading along the beam. The resultant force and moment calculations are listed.

F_r = Resultant force in SKYLITE base (N)

F_r = Sum of all SKYLITE loads under launch acceleration (N)

$F_r = 5 \times \Sigma(m_i \times g)$

m_i = Mass of each point load (kg)

g = Earth acceleration constant (9.8 m/s^2)

$F_r = 5 \times 122.74 \text{ kg} \times 9.8 \text{ m/sec}^2$

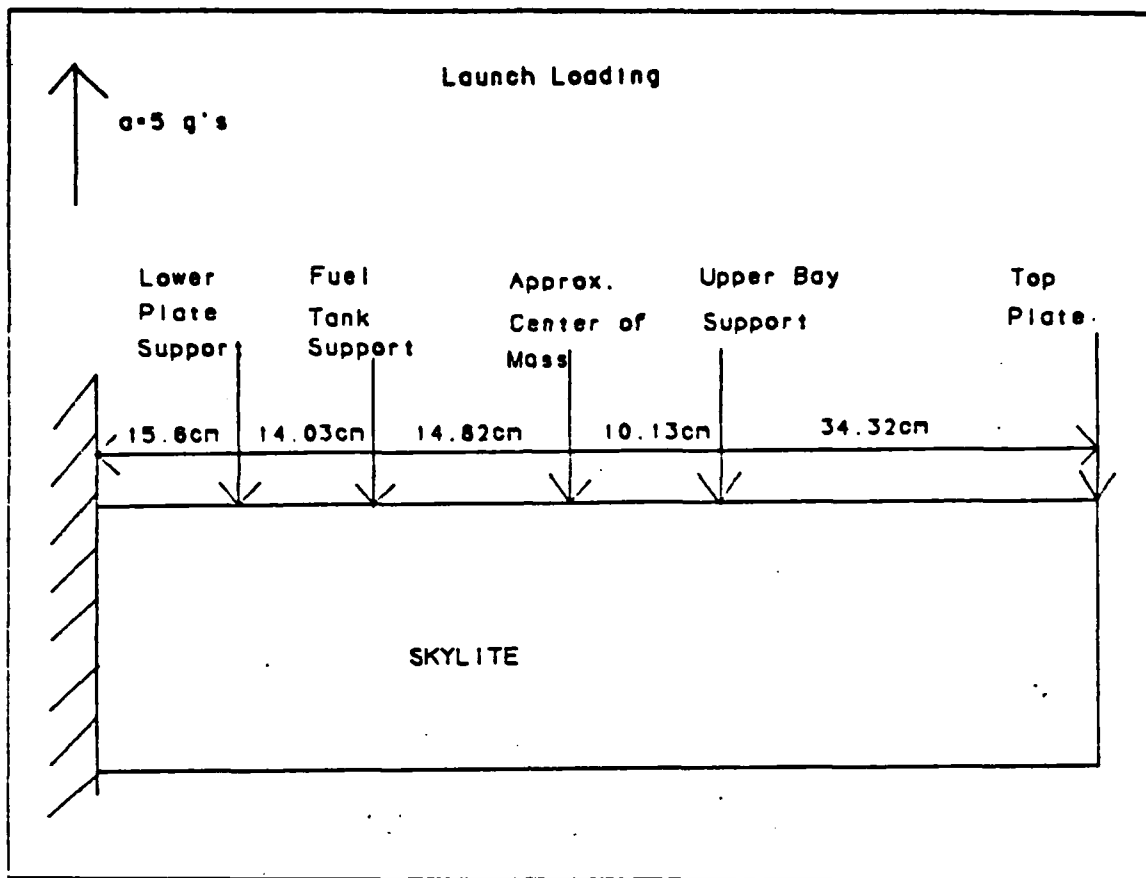


Figure 9.5 Loading Diagram of Skylite At Launch.

$$F_r = 6014.6 \text{ N}$$

The resultant moment at the base was calculated also allowing for five g's of acceleration and subsequent effective loads five times greater than those listed in Table 5.

$$M_r = \text{Resultant moment (N-m)}$$

$$M_r = 5 \times \sum (m_i \times d \times g)$$

$$M_r = 2642.63 \text{ N-m}$$

Determining the point of maximum stress, once the moment of inertia and resultant moment was known, was straightforward. The point of maximum stress occurs at the furthest distance from the neutral axis, which was on the periphery of the structure.

$$\sigma = My/I$$

y = Furthest distance from neutral axis = Radius of satellite

$$\sigma = (2642.63 \text{ N-m})(.2413 \text{ m})/(2.527 \times 10^{-3} \text{ m}^4)$$

$$\sigma = 2.52 \times 10^5 \text{ N/m}^2$$

Since the maximum resultant moment exists at the fixed end for a cantilevered beam, the maximum stress was initially thought to occur also at the fixed end. However, the error in this conclusion became apparent upon closer inspection. A large transition exists between the moment of inertia of the base plate and the moment of inertia of the cylinder adjacent to the baseplate. Actually, the moment of inertia decreases by a factor of 44 at this point. Since the stress is inversely proportional to the moment of inertia, the resulting maximum stress increased by a factor of 44. As a result, the point of maximum stress exists at the cylinder just above the base plate and is calculated using the moment of inertia for the cylinder instead of the base plate moment of inertia.

$$\sigma = My/I$$

$$\sigma = (2642.63 \text{ N-m})(.2413 \text{ m})/(5.634 \times 10^{-5} \text{ m}^4)$$

$$\sigma = 1.13 \times 10^7 \text{ N/m}^2$$

The strength of the material comprising the structure of SKYLITE was evaluated to ascertain its ability to withstand the maximum stress generated during peak acceleration periods. If the material strength does not adequately exceed the maximum stress experienced, the spacecraft may structurally fail upon launch. The material selected to construct the ORION bus was HT 7075-T6 Aluminum. The yield strength of this Aluminum alloy, which is the peak stress possible before plastic deformation occurs, is $5.143 \times 10^7 \text{ N/m}^2$ [Ref. 18: p. 1384]. The safety factor, or margin of safety is computed using the following equation [Ref. 18: p. 493].

$$N = Y/\sigma$$

$$N = \text{Safety Factor}$$

$$Y = \text{Yield strength (N/m}^2\text{)}$$

$$\sigma = \text{Maximum stress experienced by structural member (N/m}^2\text{)}$$

$$N = (5.143 \times 10^7 \text{ N/m}^2)/(1.13 \times 10^7 \text{ N/m}^2)$$

$$N = 4.55$$

The safety factor of 4.55 is more than adequate in terms of structural ability to withstand launch loads. The figure given for this safety factor is not an index, but an approving indication that the configuration of SKYLITE in the STS cargo bay will adequately withstand launch loads. Considerably more statistical analysis, regarding the variance and quality of T6-7075 Aluminum, would further substantiate the confidence. The large safety factor reflects the inherent strength in the ORION cylindrical design due to its large diameter when compared to its short length.

F. MAXIMUM STRUCTURAL DEFLECTION

The deflection of the free end of ORION as is resided in the STS cargo bay was investigated to determine if it was in compliance with the limits set by NASA. The clearance between the sides of ORION and the interior walls of the extended GAS dispenser is slight and any impact between the two surfaces may cause failure in the satellite operation and deployment. With the .2413 cm outer diameter of the spacecraft, the satellite must not deflect more than .9525 cm to remain within space limitations set by NASA. The interior diameter of the Extended GAS can dispenser is 50.8 cm, and NASA requires that all satellite assemblies must remain further than .3175 cm from the dispenser sides during flight evolutions. Maximum deflection of the spacecraft will occur at the free end due to the ORION cantilever configuration. This deflection was again considered using the maximum STS liftoff acceleration and the loads acting at distances indicated in Tables 5 and 6 [Ref. 1: Chap. 2].

The deflection at the free end of a cantilevered beam due to loading by several forces was determined by the principle of superposition. This principle states that the deflection created by each individual load may be summed to provide the total deflection caused by all the loads. The deflection created by individual loads increases as the load increases and also as its position nears the free end of the beam. The specific deflection for each load was calculated using a mechanical engineering table. For the conditions of loading at launch, under an acceleration of 5 g's, the deflection at the free end is calculated in the following equations [Ref. 18: p. 518-519].

$$D_t = \sum D_i$$

$$D_t = \text{Total deflection (cm)}$$

$$D_i = \text{Deflection of caused by individual loads (cm)}$$

$$D_t = .01078 \text{ cm}$$

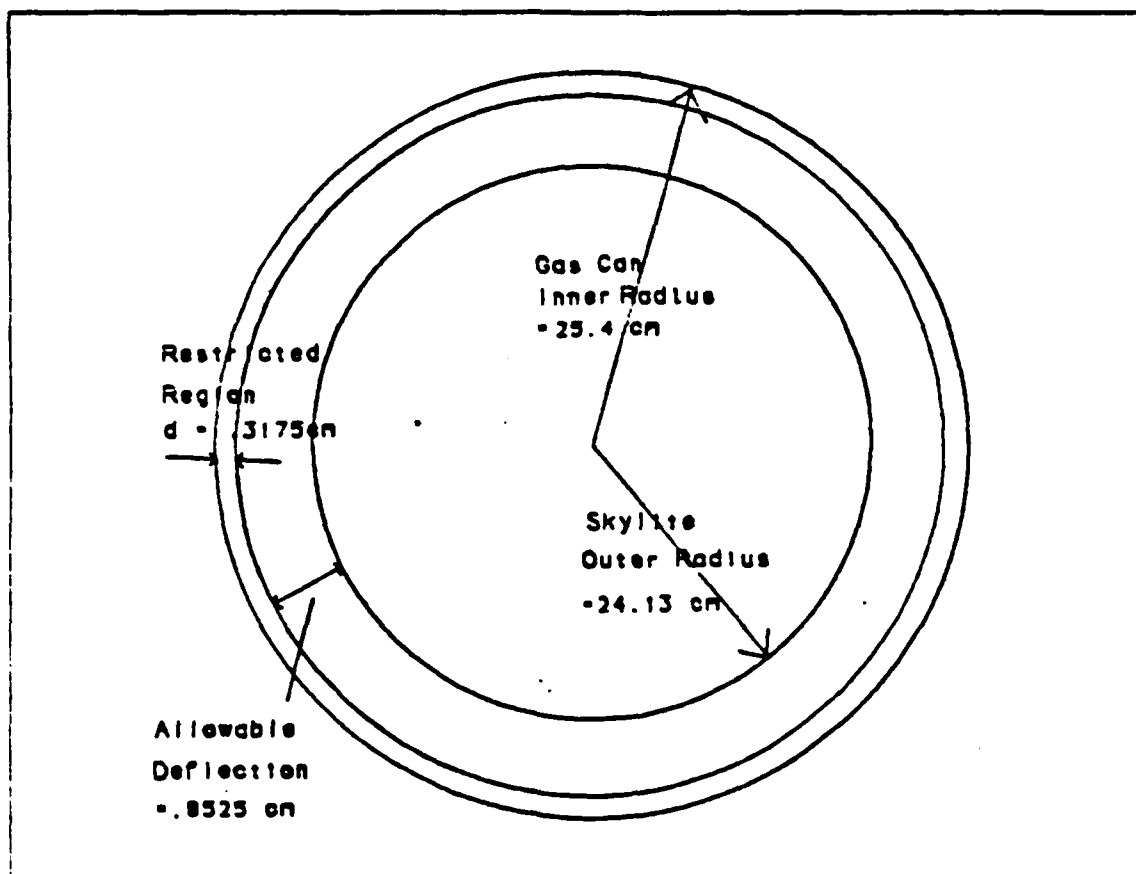


Figure 9.6 Deflection limits for SKYLITE.

Thus, the maximum deflection was calculated as .01078 cm and is well within the deflection driven by NASA guidelines which is .9525 cm. Again the minute amount of deflection is reflective of the stubbiness of the ORION shape and its strength in the cantilevered position. The deflection allowances for SKYLITE in the Extended GAS can are illustrated in Figure 9.6. [Ref. 1: Chap. 2]

G. VIBRATION LIMITATIONS UNDER BASE EXCITATION

The vibration of the STS, and consequently the SKYLITE spacecraft, during launch may substantially multiply the apparent loads experienced. This occurs when the frequency of excitation of the base, in this case, the STS vehicle, is close to the natural structural response frequency of the satellite. The satellite displacement and subsequent acceleration will be magnified should the base excitation frequency approach that of the satellite. For these reasons, the primary vibration frequency of the STS vehicle was acquired from the GAS program office at the NASA Goddard facility.

Although the excitation frequencies of the GAS can in its extended configuration are still under analysis, the NASA engineers said the primary vibration frequency was 27 hz. Based on the quoted 27 hz base excitation frequency, the natural response frequency of SKYLITE must be greater than 27 hz to avoid unforeseen accelerations and loads induced by vibration.

The natural frequency of SKYLITE, as it will be attached to the shuttle, was then determined. Again the approximation of the stowed SKYLITE to a cantilever beam was used. A table, selected from a mechanical engineering handbook, lists the methods to calculate the natural frequencies of certain basic structural arrangements. The table entry for a cantilever beam was selected which is listed below [Ref. 18: p. 498-499].

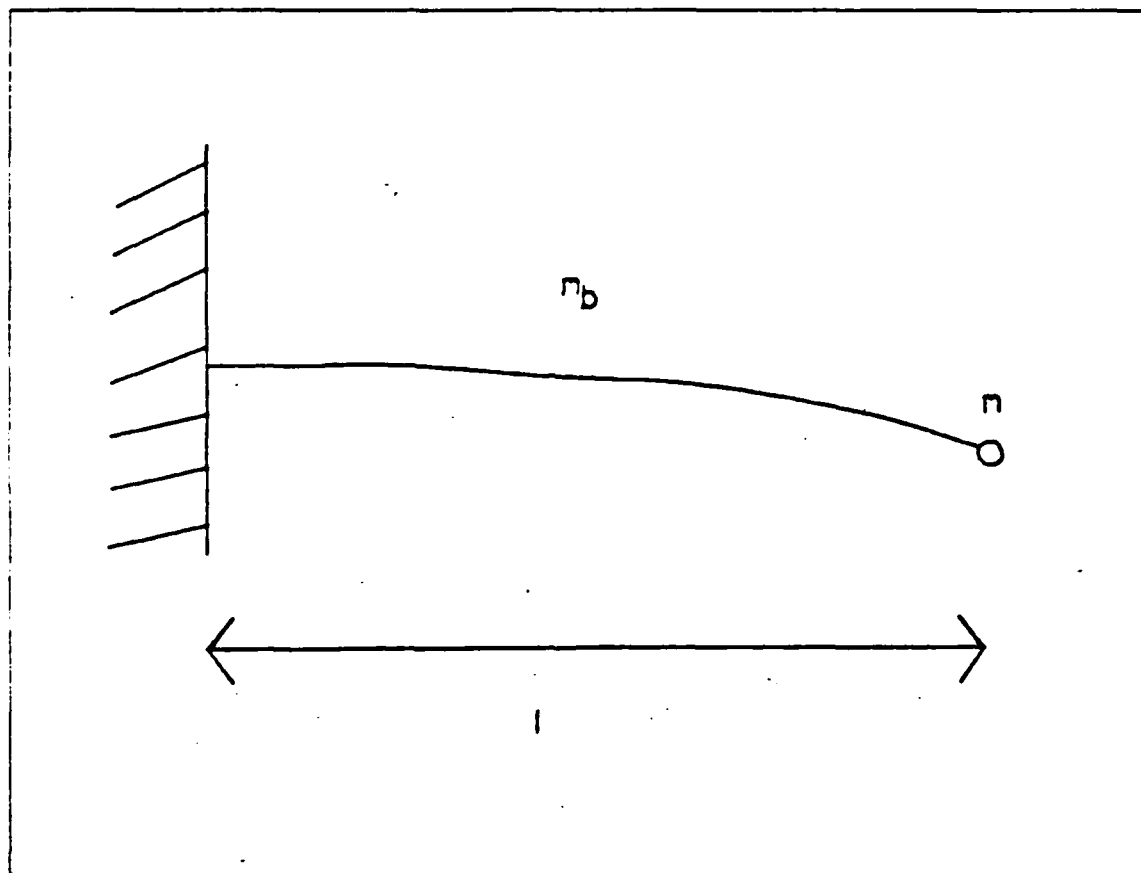


Figure 9.7 Representation used for SKYLITE natural response frequency.

$$\omega_n = \sqrt{3EI / \{l^3(m + m_b)\}}$$

ω_n = Natural response frequency (hz)

I = Moment of inertia(m^4)

E = Modulus of elasticity (N/m^2)

l = Length of the cantilevered beam (m)

m = Mass of the weight at the beam's end (kg)

m_b = Mass of the beam (kg)

This equation derives the natural frequency of the cantilevered beam depicted in Figure 9.7. Although the depicted beam and the cantilever representation of SKYLITE are not identical, the given equation was used to determine the absolutely lowest possible natural frequency attained by SKYLITE. The conservative value was calculated with the listed assumptions.

- The entire mass of SKYLITE resides at the beam's end.
- The beam is massless.
- The moment of inertia selected is that of a cylinder.

The purpose behind the three assumptions was the desire to determine the lowest frequency possible. If some of the mass resided in the beam, or the base plate moment of inertia was selected, the calculated natural frequency would be slightly higher. Using the previous equation, the natural frequency was calculated.

$$m_b = 0.0 \text{ kg}$$

$$m = 125 \text{ kg}$$

$$l = .889 \text{ m}$$

$$I = 5.634 \times 10^{-5} \text{ m}^4$$

$$E = 7.32 \times 10^9 \text{ N/m}^2 \text{ (T6 7075 Aluminum)}$$

$$\omega_n = \sqrt{3(7.32 \times 10^9 \text{ N/m}^2)(5.634 \times 10^{-5} \text{ m}^4)/((.889 \text{ m})^3(125 \text{ kg})}$$

$$\omega_n = 118.7 \text{ hz}$$

The natural vibrational frequency of 118.7 hz was the absolute minimum value possible. This figure was an ideal quantity and the actual SKYLITE vibrational frequency will be higher. However, even at the minimum value possible, the natural frequency is well above the excitation frequency of 27 hz. Thus, SKYLITE will not experience unpredicted vibrational loads and accelerations at launch, which may cause unforeseen failure.

H. MAXIMUM STRESS AND DEFLECTION OF THE DEPLOYED STABILITY BOOMS

Prior to commencing satellite insertion, the spacecraft will be spun up to an angular velocity of 100 rpm to provide spin stability. The moment of inertia about the spin axis exceeds the transverse moment of inertia due to the deployment of four symmetrical stabilizing booms extending through the center of mass of the spacecraft. The length of the boom and mass of the ball at the boom end necessary to achieve stability was calculated in the Propulsion chapter. The boom length is 1.33 m and the mass of each ball is 1.5 kg. An IR sensor and amplifier will be placed in each ball, allowing sampling of the MIRACL laser beam at four separate points. The remainder of the mass required in the balls, if necessary, will be provided by slug weights.

Determining the stress and deflection of the beams is extremely important to the proper operation of an apparently unrelated subsystem. The size of the boom and end mass must not be so great that their shadow from the sun cast across the solar panels exceeds the area of a solar cell. If one solar cell in a string in a solar cell is completely shadowed, the entire string will be shorted. This phenomena may be eliminated by the costly rewiring and shunting of the solar cells, but the procedure is extremely expensive. A more appropriate design was to determine the cross sectional area required by the stabilization booms to withstand the stress of spin up and spin down. The moment inertia was then used to determine the area and cross sectional dimensions of the boom. [Ref. 17]

The acceleration acting on SKYLITE during spin up is illustrated in Figure 9.8. The total acceleration is the vector sum of the radial and tangential forces at any instant.

$$a = \sqrt{a_t^2 + a_r^2}$$

a = Total acceleration (m/s^2)
 a_t = Tangential acceleration (m/s^2)
 a_r = Radial acceleration (m/s^2)

The maximum force on the boom will appear when the total acceleration is also at a maximum. At the instant spin up is begun there is no radial acceleration because the spacecraft is not yet spinning. As the thrusters burn, increasing the angular velocity of the satellite, the radial acceleration increases to a maximum when the angular velocity limit of 100 rpm is achieved. The maximum total acceleration then becomes a vector

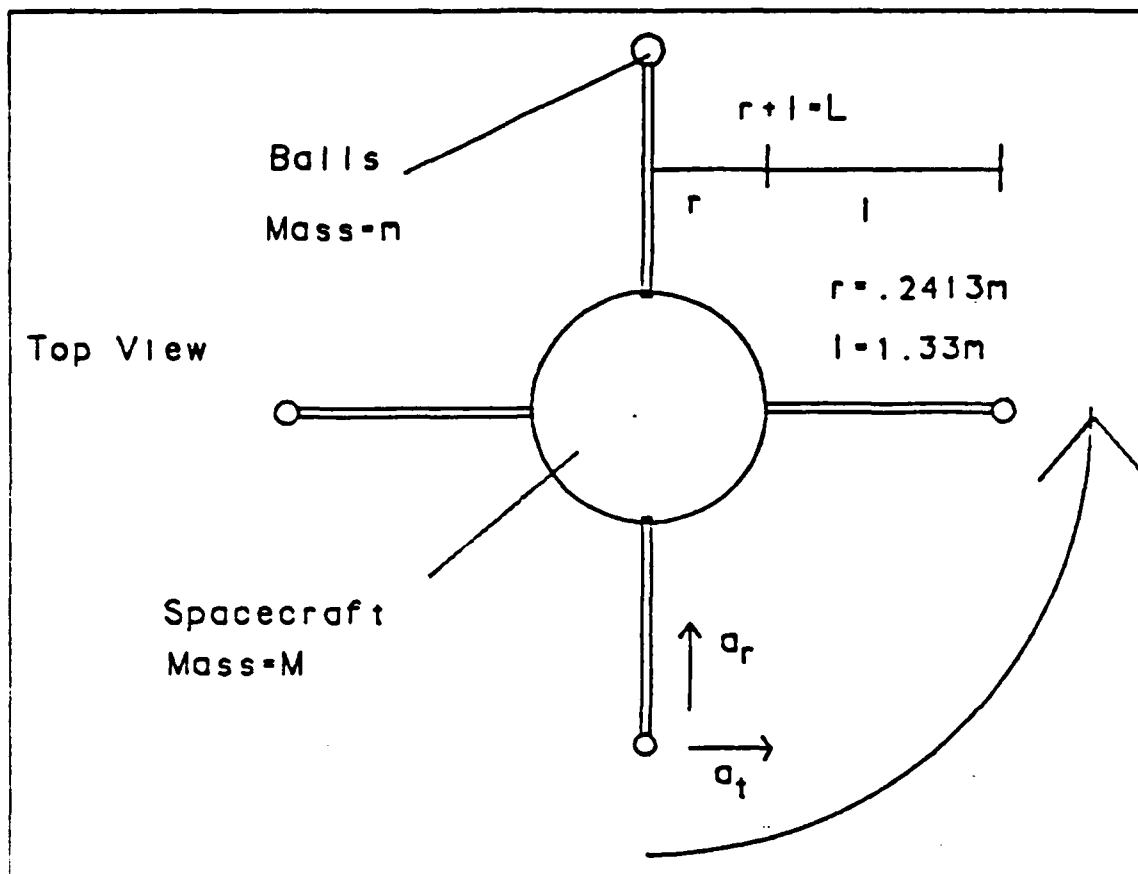


Figure 9.8 Forces Acting on SKYLITE During Spin Up.

sum of the radial acceleration at an angular velocity equal to 100 rpm, and the tangential acceleration provided by the burn of the thruster. The radial acceleration is calculated in the following equations.

$$a_r = \omega^2 r$$

ω = Angular velocity of SKYLITE (rad. sec)

r = Distance from the end of the boom to the axis of spin (m)

$$a_r = (10.472 \text{ rad/sec})^2 (1.5748 \text{ m})$$

$$a_r = 172.7 \text{ rad/sec}^2$$

The tangential acceleration was then calculated, accounting for the force of the spin up thrusters.

$$a_t = d \times \alpha$$

d = Distance from the spin axis to the radius of thrust (m)

α = Angular acceleration (rad/sec²)

$$a_t = (.2413 \text{ m})(5.867 \times 10^{-3} \text{ rad/sec}^2)$$

$$a_t = 1.416 \times 10^{-3} \text{ m/sec}^2$$

The contribution of the tangential acceleration to the total acceleration at the time of maximum angular velocity is unnoticeable. The total angular acceleration is 172.7 m/sec^2 .

The force on the boom, due to the high angular velocity as spin up is completed, is calculated using the analysis below.

$$F_b = m \times a$$

$$F_b = \text{Axial force on the boom (N)}$$

$$a = \text{Total acceleration of the mass at the boom end (m/sec}^2\text{)}$$

$$m = \text{Mass of the ball at the boom end (kg)}$$

$$F_b = (172.7 \text{ m/sec}^2)(1.5 \text{ kg})$$

$$F_b = 259.05 \text{ N}$$

The area of cross sectional area of the boom necessary to counteract the tensile stress imparted by the satellite rotation is based on the Yield Strength of the material comprising the boom. If the Yield Strength is low, the cross sectional area must be larger than that necessary for a higher Yield Strength. Using a safety factor of 5, the cross sectional area is now calculated. The Yield Strength for HT 7075-T6 Aluminum was selected because this value is representative of the materials available for construction. The values for Yield Strength, vice Ultimate Strength were chosen because no plastic deformation, permanently distorting the beams, was desired.

$$A = (F \times N)/Y$$

$$A = \text{Cross sectional area (m}^2\text{)}$$

$$F = \text{Tensile force acting on the boom (N)}$$

$$N = \text{Safety factor}$$

$$Y = \text{Yield strength (N/m}^2\text{)}$$

$$A = (259.05 \text{ N})(5)/(5.143 \times 10^7 \text{ N/m}^2)$$

$$A = 2.518 \times 10^{-5} \text{ m}^2$$

If the boom were cylindrically chaped, this desired cross sectional area could be achieved with a radius of .283 cm. The actual boom must have a hole through its center to allow passage of wires to the IR sensors in the ball mass. Cross sectional area of material lost due to the presence of the hole can be compensated by using a slightly larger diameter boom.

The governing criteria in choosing cross sectional area is the requirement to comply with maximum stress and maximum bending values due to the spin up of the boom. The beam's size is dependent on either the cross sectional area used to calculate stress in tension, or moment of inertia used to calculate the deflection in bending. Since the tangential acceleration and subsequently, the beam deflection, is extremely small due to the small size of the thrusters, the governing criteria became the cross sectional area necessary to oppose the tensile force. The cross sectional area as previously calculated above is attained with a boom radius of .283 cm.

As previously discussed, the boom shadow will short a string of solar cells only if the diameter of the boom is greater than the minimum size a single solar cell. The solar array mounted on the periphery of ORION is composed of many 2 cm by 6 cm solar cells. Since the boom diameter will be approximately .6 cm, under no circumstances will the boom's shadow short the solar cell string.

I. CONCLUSION

The structural analysis of the proposed bus has shown that all structural requirements are adequately satisfied. The ORION bus is constructed of HT 7075-T6 Aluminum, with one gravity gradient boom and four load bearing stabilizing booms. Both the satellite vehicle and stabilizing booms were analyzed for stress and deflection and determined to possess adequate strength and rigidity. The spacecraft is in a cantilever position as mounted in the STS extended GAS Can. This position is more stressful, for a cylinder, than that of an axially loaded position. If SKYLITE is transferred to an expendable launch vehicle, the associated axial loads will be more easily withstood, but additional analysis would be necessary to assess vibrational stresses. The size of the stabilizing booms must be kept small enough so their projected shadow does not completely occlude a 2 cm by 6 cm solar cell. The predicted stresses during spin up can be withstood by sufficiently small booms, avoiding shadowing problems.

X. RETROREFLECTOR DESIGN

The design of SKYLITE involved the analysis and placement of a reflector to enhance the apparent cross sectional area of the spacecraft. This magnified cross sectional area will create sufficient signature to track the satellite through its orbit. Although a small part of the overall design, the retroreflector is extremely important, as no experiments would be possible in its absence. During experimental periods SKYLITE will be lased with an Alexandrite tracking laser whose purpose is to provide pointing information to the higher power MIRACL laser. The elevation restrictions on the tracking laser are slightly less severe than the MIRACL. The tracking laser trains through the identical azimuths of 160 to 080 degrees true, with elevation limits from 45 to 90 degrees. This wider acceptance and lasing cone will provide a period of tracking and preparation prior lasing by the MIRACL. [Ref. 2]

The design focus during the SKYLITE analysis was the satellite itself and space related equipment. The tendency to become mired in laser phenomena such as power, diffraction, signal to noise requirements, etc., was resisted. The Alexandrite laser designers were queried about the necessary enhanced cross sectional area required to adequately track the satellite. The figure given was $3.3 \times 10^6 \text{ m}^2$ [Ref. 19]. A reflector type and size was then selected to provide this appropriate figure.

A retroreflector was necessary to enhance SKYLITE's effective cross sectional area. It has the ideal property of reflecting the incident beam exactly along the axis of arrival. Also the size of the retroreflector would be small enough to allow mounting on the bottom face of the spacecraft. The cross sectional area of the retroreflector is related to its size by the following equation [Ref. 20: p. 23-7 - 23-10].

$$\sigma = (kx^4)/(\lambda^2)$$

$$\sigma = \text{Cross sectional area (m}^2\text{)}$$

$$k = \text{constant}$$

$$x = \text{Aperture size (m)}$$

$$\lambda = \text{Wavelength (m)}$$

The constant k, varied between tables, from a value of 4.04 to 37.1. However, since the aperture is proportional to the fourth root of the remaining terms, the variance in

the k constant did not appreciably vary the retroreflector size. The above equation was evaluated for aperture size, since cross sectional area was provided by the laser engineers.

$$x = (\sigma \lambda^2 / k)^{1/4}$$

$$x = \{ (3.3 \times 10^6 \text{ m}^2) (7.55 \times 10^{-6} \text{ m})^{2.41} \}^{1/4}$$

$$x = 2.59 \text{ cm}$$

The k value was selected that yielded the largest and most conservative value for aperture size. A contractor's catalog was consulted to determine the availability of similar retroreflectors. Three retroreflectors were chosen with an aperture of 3.8 cm. Three retroreflectors will be mounted on the base of the satellite to increase the probability of a blossoming return.

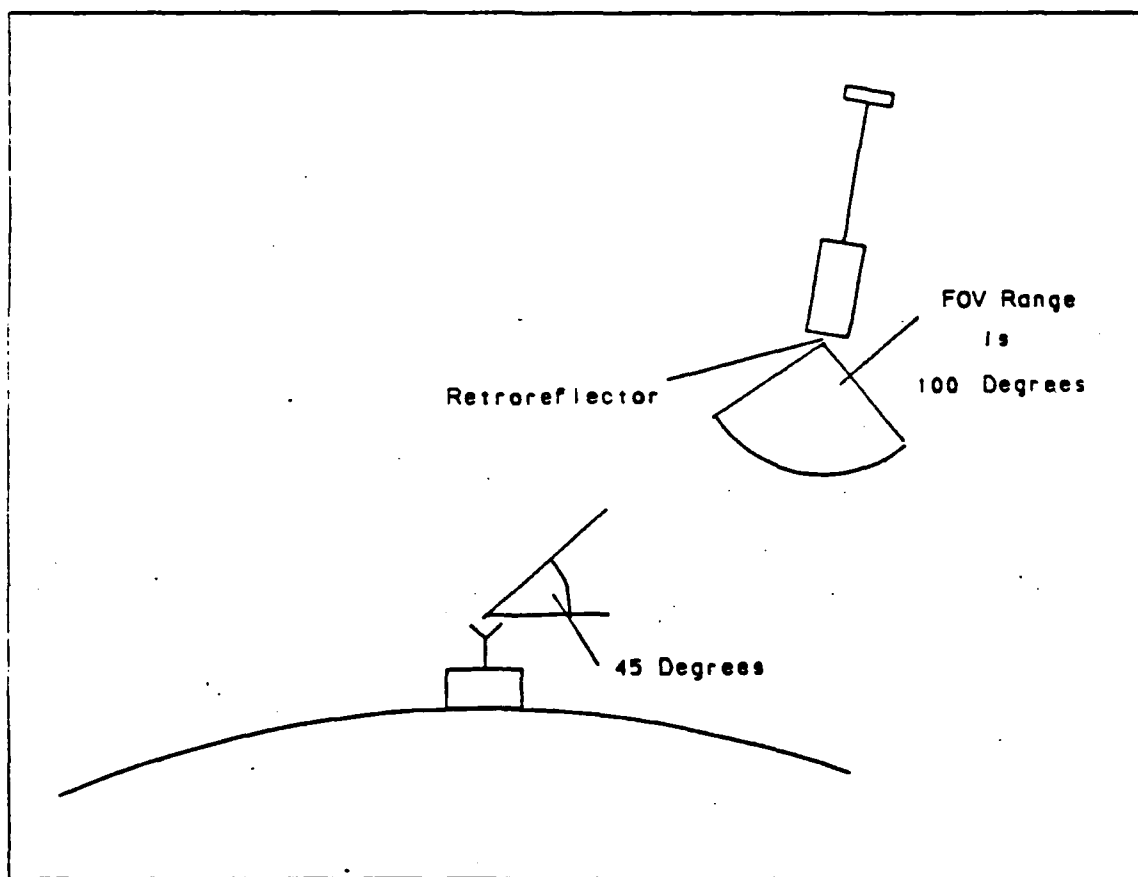


Figure 10.1 Geometry determining Retroreflector Field of View.

The field of view of the aperture was dictated by the geometry in figure 10.1. The satellite will be lased by the tracking laser when the elevation angle is 45 degrees. Combining this requirement with the spacecraft stabilization limits of 5 degrees and an additional 5 degrees provided for unforeseen errors, a field of view of 50 degrees will be required. If the retroreflector alone cannot meet this requirement, its field of view must be expanded using small mirrors. Another detail exists requiring compensation. Modern mirror machining techniques have created mirrors so fine that the returned reflections, when reflected minutely off the incident angle, are not received at the transmitting site at all. The high mirror polish has not created any spoiling and the laser site will be unable to track the satellite. The remedy to this is to intentionally spoil, or roughen the surface of the mirror. The roughness will spread the reflected beam slightly, should the reflected angle deviate slightly from the incident angle.

XI. IR SENSOR SELECTION

A. INTRODUCTION

The sensor selected for SKYLITE must sample the varying levels of the arriving laser irradiance and convert the signal for modulation and transmission. The sensor must be sufficiently sensitive to detect the low signals and appropriately robust to withstand the high power levels. PMW-145 required a sensor sampling rate of 1 khz. [Ref. 2] Each sensor will be sampled at this rate with the subsequent signals multiplexed and modulated onto a carrier frequency.

The sensor design will be done at the systems level. Due to the complexity of sensor selection, and actual sensor selected for SKYLITE must undergo rigorous design and test phases. However, the basic selection and orientation of the sensor will be explained, outlining areas requiring more complex analysis.

The satellite will be illuminated at elevation angles of 60 to 80 degrees from the WSMR facility. The sensor must have a field of view (FOV) allowing signal detection throughout the entire illumination regime. The laser and satellite geometry is presented in Figure 11.1. Strict geometrical considerations require a half angle FOV of 51.3 degrees. However, the FOV enlargement necessary for slight attitude oscillations results in a half angle FOV of 55 degrees. The required sensor FOV is particularly important when the effect of incident solar radiation is considered. If the sensor FOV is greater than the angle to the Earth's limb, the solar irradiance will be collected and mistakenly classified as laser signal. As depicted in Figure 11.2, the total angle between the Earth's limbs at an orbital altitude is 128.6 degrees. This is sufficiently greater than the 110 degree sensor FOV to prevent the arrival of solar radiation at IR wavelengths.

The spectral region of interest for SKYLIGHT is 3.6-4.2 μ . Laser lines for the MIRACL are approximately 3.8 μ , and the experimenters from PMW-145 want the power measurement to include the region between 3.6 and 4.2 μ [Ref. 2]. Thus, a sensor with maximum detectivity in this region must be selected. Specific detectors exhibiting maximum detectivity in this region were PbSe, HgCdTe, and InSb. Selection of a specific detector is based on its ability to detect the laser signal in the background of the Earth's IR noise and the detector noise. For cost considerations and simplicity, a detector which operates without cooling and meets detection requirements is preferable to a detector requiring cooling.

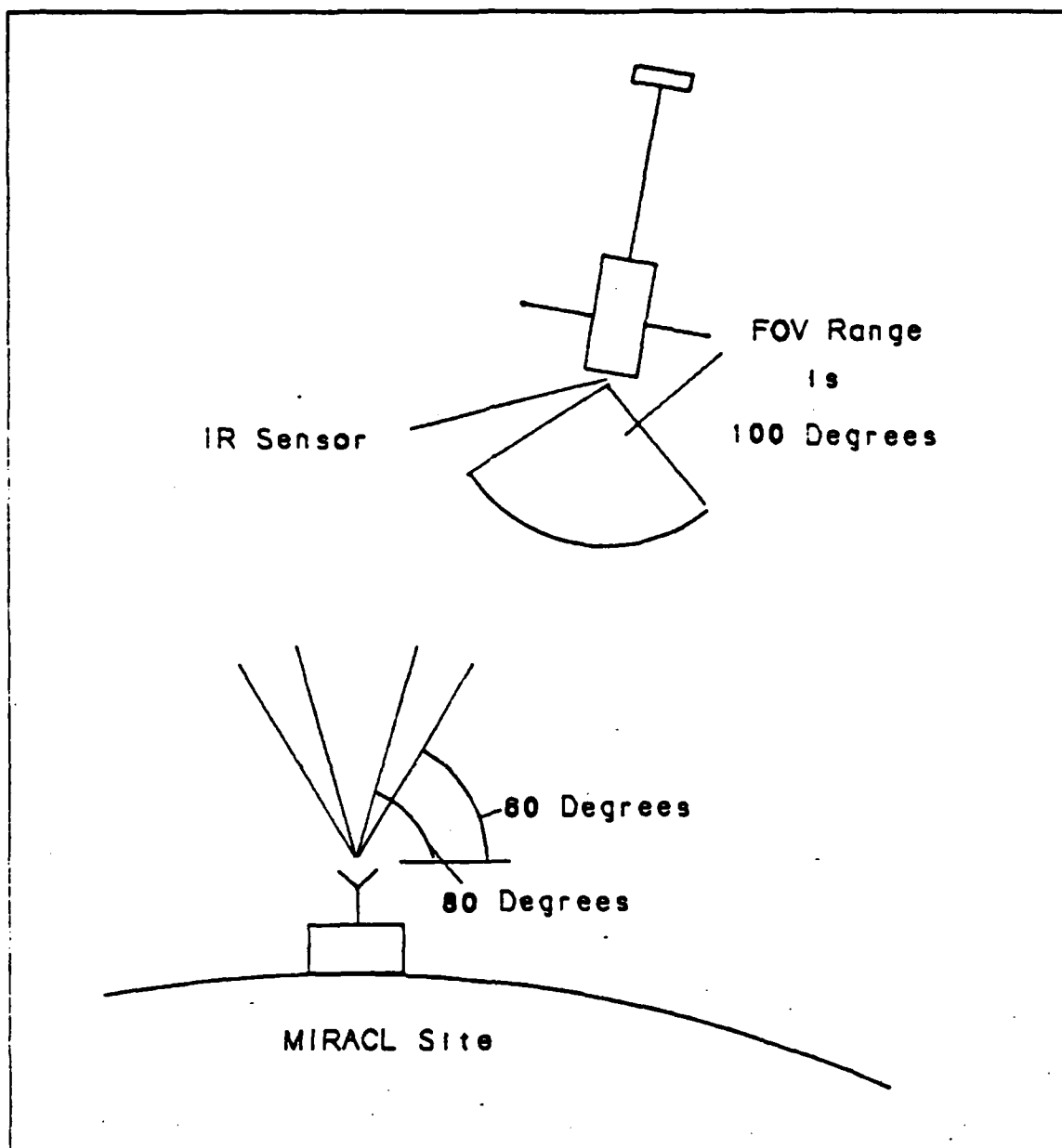


Figure 11.1 Sensor FOV required for Measuring Irradiance.

Preliminary discussions with IR and Optics engineers at Aerospace Corporation, Santa Barbara Research Corporation (SBRC), and Ford Aerospace Corporation indicated that an uncooled detector (295 K) would provide detectivity to detect the lower power laser signal ($.25 \text{ mW/cm}^2$) and may be too sensitive to the high power laser signal (4 W/cm^2). [Refs. 21,22,23] To reduce the response of the detector to the

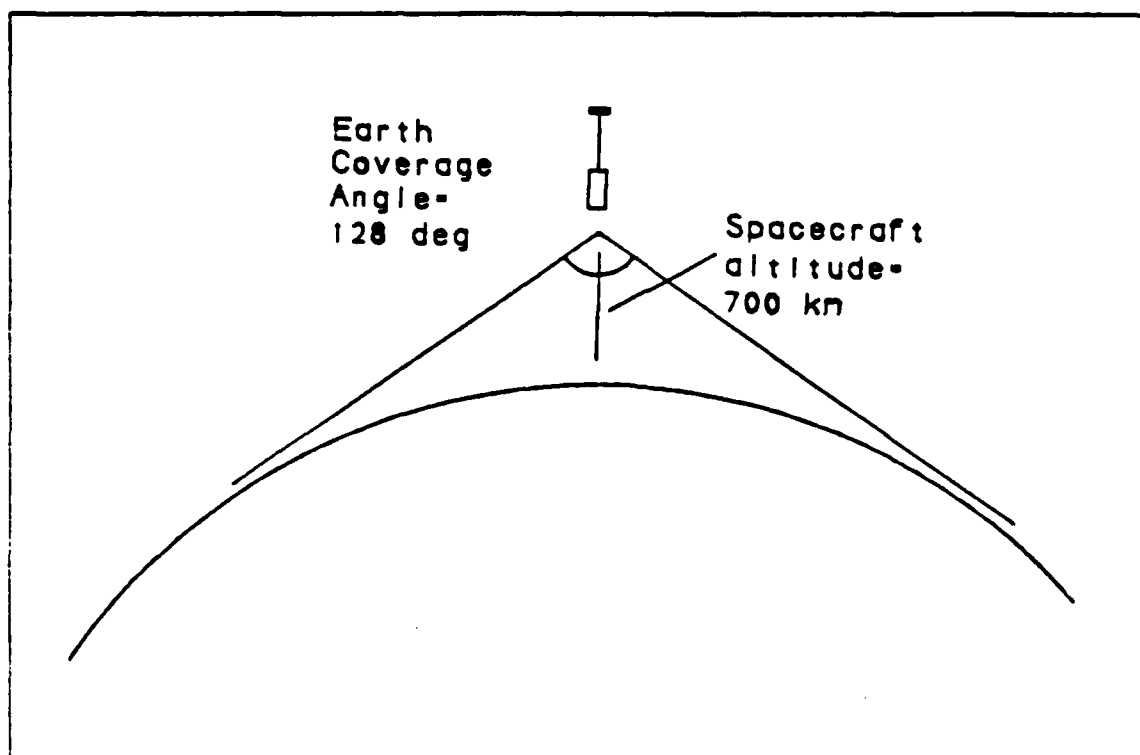


Figure 11.2 Angle Between Earth's Limbs at Orbital Altitude.

high power test while preserving sufficient signal from the low power test, a neutral density filter (NDF) will be placed in front of the detector. The NDF will be designed to bring the irradiance on the detector down to a region that provides a linear response to the detector. This NDF will not attenuate the irradiance so severely that the low power signal cannot be detected. In the unforeseen circumstance that these two goals cannot be obtained with one detector array and one NDF, two detector arrays will be necessary to sense the low and high power levels.

To reduce background noise from the Earth, a bandpass filter will also be placed in front of the detector. The bandpass of the filter will coincide with the 3.6-4.2 μ region of interest to the experimenters [Ref. 13]. Utilizing such a filter will prevent radiation at other wavelengths from impinging on the detector. Two additional components will complete the sensor. A chopper placed before the detector will provide an experimental sampling frequency of 1 kHz. Additionally, a thermoelectric cooler may be necessary to maintain the temperature of the detector at a constant value. Detector response depends on operating temperature, and heating due to high power laser tests may cause the unpredictable detector response. Thus, while a TEC is not required for

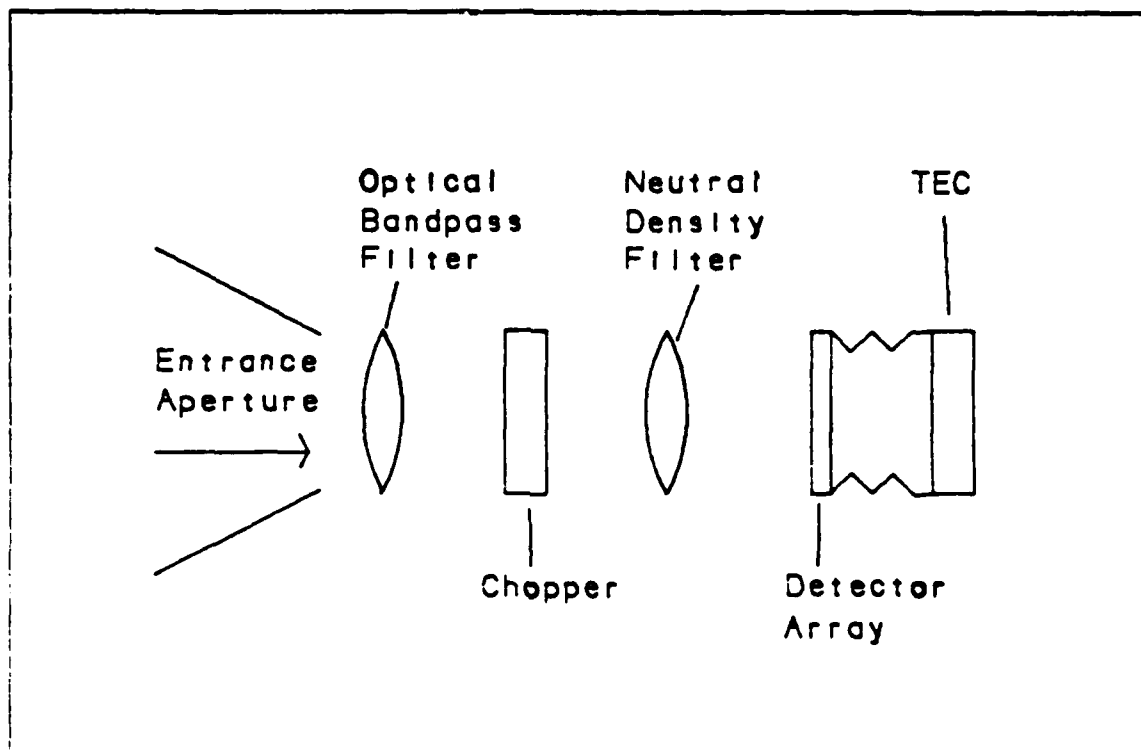


Figure 11.3 Components Required for SKYLITE Sensors.

increasing detectivity, it may prevent poor detector response due to heating. The components comprising SKYLITE's IR sensor are listed in Figure 11.3. The spacecraft will have 6 sensors. Each short stabilization boom will have a detector on its earth facing side, and two detectors will be placed on the bottom of the main spacecraft body. The additional detector on the spacecraft body is for redundancy, as the laser will be aimed at a reflector, also on the satellite body, and these detectors are most essential to the experiment. The four detectors on the stabilization booms were included due to the desires of the experimenters. PMW-145 indicated that placing the peripheral sensors more than 1.5 meters from the central sensor would be of experimental value. [Ref. 2]

XII. COMMUNICATIONS CONSIDERATIONS - DATA & TELEMETRY

A. INTRODUCTION

Many technical problems are encountered when designing a reliable satellite communications system. High cost, low available power, severe weight restrictions, and inaccessibility for maintenance are only a few of the many problems that present a significant challenge to the designer. The problems encountered in designing the communications system for Project SKYLITE were no different. Although these problems are not insurmountable each must be analyzed and trade-offs thoroughly considered to design the optimum system.

There are basically two types of information transfer that must occur between the satellite to the ground site:

- 1) Sensor data passed from the satellite to the ground during the experiment.
- 2) TT&C data passed throughout the lifetime of the satellite from the satellite to the ground and vice versa.

The two subsystems that provide this capability are the Radio Frequency Subsystem and the Telemetry, Tracking and Command (TT&C) Subsystem. Each of these subsystems will be addressed in the chapter.

It should be pointed out, before each subsystem is discussed, that specific components for SKYLITE have not been selected. A general understanding of what is required to optimize the subsystem is known. Further investigation into what equipment and components are currently on the market is necessary. The trade-offs between component size and weight, power requirements and data rate capability are the key concerns.

B. RADIO FREQUENCY SUBSYSTEM

The Radio Frequency Subsystem will provide SGLS compatible communications capability in the S-band for the receipt and transmission of RF signals from and to the dedicated SGLS ground site. This subsystem will provide omnidirectional command receiving capability, and omnidirectional transmitting capability. The Radio Frequency Subsystem will contain at least the following hardware elements:

- Receiver/Demodulator
- Receiving Signal Routing Devices

- Receiving/Transmitting Antenna
- Receiver/Demodulator Power Convertors
- Transmitter
- Transmitter Signal Routing Devices
- Transmitter Power Convertors
- Stable Clocks
- Stable Clock Power Convertor

Because of weight volume and cost constraints the Radio Frequency Subsystem will have no built in redundancy features. There will be only one of each hardware element.

C. TELEMETRY, TRACKING AND CONTROL (TT&C) SUBSYSTEM

SKYLITE's telemetry system will consist principally of various sensors and transducers, and the telemetry encoder. Information from the five sun sensors and the magnetometer used for attitude control along with other temperature, power supply voltage, bus voltage, battery voltage, battery temperature, solar array voltage, and stored fuel pressure information must be properly formatted at the required signal levels, in digital form and encoded for transmission. The telemetry encoder will multiplex the various digital channels carrying the information from these various sensors and transducers. The encoder will modulate a subcarrier on the transmitter for transmission through the antenna. The transmitter will phase modulate the signal at a SHF frequency compatible with SGLS.

The Telemetry, Tracking and Control subsystem provides the following:

- 1) Operational control of the SKYLITE satellite in accordance with uplink commands.
- 2) On board software stored commands.
- 3) Real time equipment performance data.
- 4) Subsystem status parameters from necessary spacecraft subsystems.

The TT&C subsystem will decode, store, and execute commands transmitted from ground sites and will provide a means of controlling SKYLITE functions in accordance with the commands and data received from the ground sites. The TT&C will contain at least the following hardware elements:

- Memory and Control Unit
- Remote Telemetry Unit
- Remote Command Unit
- Timing Distribution Unit

- **Wideband Downlink Formatter**

A specific hardware component for each of the telemetry elements listed above has not yet been determined. Investigation into the optimum requires significant analysis and coordination with Naval Research Laboratory. The design of a data and telemetry system is required for completion of the SKYLITE satellite initial design review.

D. PRELIMINARY COMMUNICATIONS ANALYSIS

1. Satellite Downlink

The satellite downlink is constrained by the fact that the transmitter, amplifier, antenna, etc. must be spaceborne. This requires small, efficient, light weight devices.

The type of antenna proposed for the communications subsystem is an omnidirectional, crossed dipole. This antenna has a 0 db gain. The satellite can send and receive data while in line of sight (LOS) of a ground command station. Sites in California, Colorado and New Mexico are being considered. One important communications parameter pertaining to the transmitter is the power required to successfully transmit data to these sites. This can be calculated by finding the slant range and atmospheric propagation losses and determining the necessary bit error rate.

A slant range of 3100 km is approximately the maximum range between any of the proposed sites and the satellite, when the spacecraft is just above the horizon. The pathloss at this range is approximately 168 db at a S-band frequency of 2 Ghz. The assumed bit error rate required for the successful transmission of data is 1×10^{-4} . The proposed data rate is 1 Mbps. Using these parameters, the required output power of the satellite is approximately 0.75 watts. This assumes the receiving antenna has a gain of 36db and the satellite antenna has a T_{sys} of 500 degrees.

2. Data Storage

The data transmitted to the ground site will be real time which negates a requirement for data storage onboard the satellite.

3. Transmitter Power On/Off Capability

A command on/off switch or a clock command to power on and off the transmitter may be necessary in order that the satellite does not randomly transmit information while not in field of view of a mission ground site.

E. CONCLUSION

The communications subsystem for SKYLITE is simple, due to the few sensors aboard and no requirement for on board processing. Each of the six IR sensors are sampled at 1 kilohertz. These signals are converted to a digital signal and multiplexed onto the appropriate carrier frequency. The data subcarrier frequency will not be utilized unless an experiment is pending or occurring. The satellite health and welfare will be monitored on a priority basis, using the Satellite-Groundlink System (SGLS). A significant payload margin, in volume, weight and power, allows latitude in the selection of power supplies and transmitter for the communications system. The requirements for telemetry are within the bounds of commercially available systems.

XIII. PROJECT SKYLITE COST ESTIMATION UTILIZING THE SPACE DIVISION UNMANNED SPACECRAFT COST MODEL

A. INTRODUCTION

The cost of the SKYLITE satellite must be estimated, balancing expenses against available funds. If the spacecraft price is too expensive, less capable hardware elements, or less redundant systems must be accepted. A means is necessary for projecting satellite cost based on engineering design factors. As set forth in the Office of Management and Budget Circular Number A-109, emphasis should be placed on the exploration of alternative system design concepts in response to mission needs. This exploration is not only for technical and operational feasibility but also for economic feasibility. Cost and not state of the art technology, may be the driving factor and could reduce the choice of possibilities.

B. THE FOUR METHODS OF COSTING

There are basically four methods of costing currently accepted in the estimating community: Engineering Estimates; Learning Curve Analysis; Analogous Estimates; and Parametric Estimates. [Ref. 24: p. I-1]

Engineering estimates deal with the accumulation of costs from the lowest level of detail. Costs at component level are summarized and combined with estimated labor costs at all levels of the program work breakdown structure. This type of estimate can be tailored to a specific program and contractor, in addition to providing an audit trail for particular details. However, this estimation requires voluminous documentation and the detailing of design specifications. It must also be updated continually with each change in design specification and program configuration. These estimates may also fail to realize management and economic efficiencies, thus resulting in excessive cost projections. [Ref. 24: p. I-1]

Estimates of the learning curve analysis are derived by extrapolating actual costs from one of several units along a learning curve. This method is advantageous in that actual costs of the subject program are being used. However, this type of costing is only good for programs for which many units are to be produced. Space programs typically have extremely small production quantities - seldom are more than ten spacecraft built. [Ref. 24: p. I-2]

Analogous estimates are performed by comparing one or more past program cost figures which are technically representative of the program to be estimated. This method is subjective in nature in that it rests upon the analyst's judgment in drawing parallels between past programs and the subject program. The cost data are then subjectively adjusted upward or downward, dependent on the analyst's intuition of whether the subject program is more or less complex than the analogous program. [Ref. 24: p. I-1]

Parametric estimates, like the Space Division's Unmanned Spacecraft Cost Model, are performed by statistically correlating historical cost data of several systems to their respective physical or performance characteristics. The mathematical relationships that are observed between cost and technical variables are called Cost Estimating Relationships (CER). The CERs are treated as time constant expressions of reality. The CERs are updated and revised as additional and more current data are retrieved from newer systems. This type of model relies on the premise that through the use of CERs, the cost of future spacecraft systems may be estimated. This type of cost estimation relies on the assumption that the same forces that affected cost in the past will continue to affect cost in the future. [Ref. 24: p. I-2,I-3]

The purpose of performing a cost estimation in the conceptual phase of a program is to provide a planner with a crude estimate of anticipated future costs. The accuracy of the model is worse in the conceptual phase of a system than in the developmental phase. Less correlation should be expected between the cost data for detailed elements and quoted costs for existing equipment. This primarily is due to the lack of standardization of costing methods throughout the space industry.

The Space Division Unmanned Spacecraft Cost Model will be used to estimate the cost of the Project SKYLITE satellite. This parametric cost model has been recognized by the space industry estimating community as having the widest application and broadest data base of any of the currently available cost models. [Ref. 24: p. iii]. A statement cited in a RAND corporation study of cost models gives credence to this claim. "For the user who lacks detailed knowledge of a program and is interested in obtaining an estimate based on basic spacecraft characteristics such as weight and maximum array output, the various SAMSO - Space Division was then known as the Space and Missile Systems Organization (SAMSO) - models appear to be most reliable." [Ref. 24: p. iii]

The model used for this estimate is the fifth edition of the unmanned spacecraft cost model. It is the most recent research of the spacecraft acquisition environment, which can provide decision makers with pertinent and useful resource allocation information.

C. UNMANNED SPACECRAFT COST MODEL DESCRIPTION

1. Unmanned Spacecraft Data Base

Tables 7 and 8 summarize the technical and programmatic characteristics of spacecraft used in the unmanned spacecraft cost model. As depicted in these tables, the unmanned spacecraft programs fall into distinct categories defined by mission type. The five basic mission categories are military, communications, weather, experimental, and lunar probe. The data points are stratified according to their mission - communication, sensor, or probe. The satellites can also be stratified according to their application - military, NASA, or commercial. Depending on the application, different characteristics, such as radiation hardening, reliability, channelization, encryption, etc. may be required. Table 9 shows how the data base has been developed since the first edition was published in November 1969. [Ref. 24: p. II-5]

2. Nonrecurring vs Recurring Cost

The cost model takes into account the type of work in a program. The work is subdivided into two categories: nonrecurring and recurring. Work costs associated with designing, developing, manufacturing and testing a spacecraft qualification model is termed nonrecurring. Costs attributed to peculiar ground support equipment such as mechanical and electrical ground equipment are also considered nonrecurring. [Ref. 24: p. III-6]

Recurring costs deal with all the effort and activity of fabrication, manufacturing, integrating, assembling, and testing of the spacecraft flight hardware. Any costs attributed to the launch and the initial orbital operations are also considered recurring costs. [Ref. 24: p. III-7]

3. Areas of Activity

The cost drivers of a satellite are typically found in the physical and performance characteristics of the satellite's subsystems. The estimated cost for each major area of spacecraft design such as structure, TT&C, etc., is dependent on a characteristic of the particular area of design. For example, the subsystem cost for the structure of a spacecraft is predictable, given the weight of the structure. The weight of the structure in this case is the cost driver. The cost driver is not always measured in

TABLE 7
TECHNICAL AND PROGRAMMATIC SUMMARY (FROM AFSD)

System	Contract Start Date	No. of Satellites	Dry Weight ² (lbs)	Stabilization Type	Orbital (Alt) (in miles)	Solar Array Type (area ft ²)	Design Life (months)	Max Array Output (watts)
Military (USAF)								
Vela	1961	6	247	One-axis	Synchronous	Body (28.5)	6	104
VASP	1965	5	506	Three-axis	Synchronous	Body (32.6)	18	120
OSP 1	1967	4	1074	One-axis	Synchronous	Mix (438.0)	36	670
OSP II	1971	8	1142	One-axis	Synchronous	Mix (424.0)	36	865
CPS-1	1974	7	903	Three-axis	10,898	Paddle (54)	60	515
Weather USAF								
DMSP-50	1972	4	811	Three-axis	450	Paddle (96.0)	30	910
NASA								
NIMBUS E/F	1969	2	1343	Three-axis	500-600	Paddle (56.0)	12	510
TIMOS-M	1967	4	590	Three-axis	790	Paddle (49.0)	12	508
SMS	1970	3	408	One-axis	Synchronous	Body (72.0)	60	173
NIMBUS A,B,C Experimental	1961	2	1350	Three-axis	600	Paddle	12	450
USAF								
P72-2	1972	1	1003	Three-axis	4100	Body (22.5)	6	260
SJ	1972	3	343	One-axis	273/280 S3-1 650/135 S3-2 4685/135 S3-3	Body (24.2)	6	110
P78-1	1976	1	957	Three-axis	320	Paddle (25)	12	330
P78-2	1976	1	500	One-axis	Synchronous	Body (10)	12	310

pounds, but may be other quantities such as total impulse, as in the propulsion subsystem estimate. The total cost for a spacecraft depends on the sum of the costs for each subsystem. The subsystems accounted for in the Unmanned Spacecraft Cost Model, with their associated cost drivers in parenthesis, are listed below.

- Structure (Weight)
- TT&C (Weight)
- Communications (Weight)
- Attitude Control System (Weight)
- Electrical Power Supply System (Weight, Beginning of Life Power Supply)
- Apogee Kick Motor (Weight, Total Impulse)
- Aerospace Ground Support Equipment (Platform Cost)
- Launch and On Orbit Support (Weight)

4. The Model Methodology

The Unmanned Spacecraft Cost Model methodology is structured around several ground rules and assumptions. The basic assumption of any cost model derived from historical cost data is that historical cost will accurately reflect current and future costs. Ground rules for this model are taken verbatim from the Unmanned Spacecraft Cost Model and are listed below [Ref. 24: p. III-17,III-18]:

- "The model addresses unmanned earth-orbiting spacecraft (Lunar Orbiter is the only exception)."
- "The model addresses platform hardware costs only, and except for Communications payloads, it does not include mission hardware (e.g., observational sensors). Launch vehicles, stage vehicles, and their ground equipment are not included within the scope of this model."
- "By observing several spacecraft programs, mathematical relationships (CERs) are obtained by relating costs at the subsystem level (e.g., structure, electrical power supply) to subsystem physical and performance characteristics. The technical characteristics of the programs are then used as independent variables, or "cost drivers" of the CERs."
- "Spacecraft costs (both development and production) are segregated between nonrecurring (NR) and recurring efforts. CERs are derived for each subsystem's NR and recurring costs. (CERs for recurring costs represent first unit costs and require appropriate consideration for production learning)."
- "All costs included in this model are end-of-program actual costs or estimates of mature programs (with at least one launch)."
- "CERs are based upon burdened costs (direct plus indirect) with General and Administrative (G&A) costs included. In other words this model consists of total cost through G&A application CERs."

TABLE 8
TECHNICAL AND PROGRAMMATIC SUMMARY (CONTINUED)

System	Contract Start Date	No. of Satellites	Dry Weight ² (lbs)	Stabilization Type	Orbital Altitude (in miles)	Solar Array Type (area ft ²)	Design Life (months)	Max Array Output (watts)
NASA								
ERTS	1969	2	1548	Three-axis	500	Paddle(56.0)	12	546
OSO-1	1970	1	1097	One-axis	300	Paddle(50.0)	12	460
AE	1971	3	806	Three-axis	120x4000	Body (42.6)	12	170
DAO	1960	3	3004	Three-axis	400	Paddle (274)	36	1320
OGO	1961	3	872	Three-axis	150x80,000	Paddle(93.0)	18	500
HEAO	1974	3	2777	Three-axis	250	Paddle (117)	6	500
Lunar Probe								
Lunar Orbiter Communications	1964	3	438	Three-axis	Moon Orbit	Paddle(52.0)	1	400
USAF								
DMSP (DSCS I)	1964	23	103	One-axis	Synchronous	Body (20.0)	18	40
DMSP/A	1966	2	204	One-axis ³	Synchronous	Body (35.3)	60	110
TACSAT (Prog 191)	1967	1	1499	One-axis ³	Synchronous	Body (311)	36	980
DSCS II (777)	1969	6	1013	One-axis ³	Synchronous	Body (145.4)	60	535
WATO III	1973	3	771	One-axis ³	Synchronous	Body (160.0)	84	540
FLTSATCOM	1972	5	1856	Three-axis	Synchronous	Paddle (148)	60	1640
NASA								
SYNCOM	1961	3	69	One-axis	Synchronous	Body (9.4)	18	25
ATS-B,C (S/S)	1964	2	520	One-axis	Synchronous	Body (54.0)	36	180
ATS-A (H/G)	1964	1	502	Three-axis	6X10	Body (50.0)	36	125
ATS-D,E (S/G)	1964	2	801	Three-axis	Synchronous	Body (50.0)	36	150
ATS-F	1971	1	2402	Three-axis	Synchronous	Paddle (116)	24	645
Commercial								
Intelsat III	1966	6	276	One-axis	Synchronous	Body (54.1)	60	178
Intelsat IV	1968	6	1340	One-axis	Synchronous	Body (220.9)	84	569
INRISAT	1973	3	858	One-axis ³	Synchronous	Body (116)	60	402

2. Dry weights for communication satellites include the communication subsystem. Other dry weights exclude payload.

3. Despun platform.

4. Philco-Ford and Aeronutronics Ford are the same company which currently is named Ford Aerospace and Communications Corporation.

- "Cost estimates from spacecraft subsystem and program level CERs are summarized to obtain a spacecraft program cost subtotal. This cost estimate is expressed in terms of U.S. government Fiscal Year 1979 dollars, and the appropriate inflation costs must be added to express costs as a function of future expenditures. Fee and incentive costs must then be added to the subtotal. Finally, costs exogenous to the model, such as sensor payload costs, must be obtained separately/analogously."
- "The model is considered to yield a "starting point estimated which represents the "average" cost for a program with "average" problems, "average" technology, "average" schedule, "average" engineering changes, etc."
- "95% cumulative average learning curve is used to derive first unit costs."

D. SKYLITE COST ESTIMATES

Both nonrecurring (RDT&E) and recurring costs (Production) were estimated using the Unmanned Spacecraft Cost Model. The light weight of the satellite provides problems when estimating the cost of several subsystems. Based on the database of the model, the cost drivers are valid only for a certain range. For example, the cost driver of the propulsion system is weight. Given the weight of spacecraft propulsion components, the cost can be projected, provided it is within the specified range. For the Apogee Kick Motor the weight was not within the range specified. The assumption, in this case, was to use the minimum value of the weight range. The same problem occurred when estimating the Launch and On Orbit Support Costs. Two available solutions compensate for these deficiencies. First, the CER's in the model can be extrapolated to the lower weight. Second, the minimum weight given can be used to calculate the cost and reduce the expense based on the percentage of actual weight to allowed weight. The second method was used to evaluate the cost of SKYLITE. To frequently use the model for spacecraft smaller than SKYLITE new sets of CER's and cost drivers would be required, orienting the acquired database toward lighter weights.

As explained above, the model divides the cost analysis into recurring and nonrecurring costs. The computation for projected costs are similar, however the CER's vary between the two types of cost.

1. SKYLITE Cost Estimates

The following cost drivers were used to estimate SKYLITE's cost. As the cost drivers were taken from the engineering analysis presented in the preceding chapters, the importance of their accuracy in cost estimation cannot be overstated. The cost drivers were:

- Structure (Weight = 40.26 lbs)
- TT&C (Weight = 16.2 lbs)

TABLE 9

UNMANNED SPACECRAFT COST MODEL DATABASE HISTORY (FROM AFSD)

Customer	First Edition	Phase I Update	Second Edition	Third Edition	Interim Report	Fourth Edition	Fifth Edition
Air Force	Vela VASP IDCSP IDCSP/A TACSAT	Vela VASP IDCSP IDCSP/A TACSAT DSP 1	Vela VASP IDCSP IDCSP/A TACSAT DSP 1 DSCS II	Vela VASP IDCSP IDCSP/A TACSAT DSP 1 DSCS II DSP 11 DMSP (SD) P72-2 S3	Vela VASP IDCSP IDCSP/A TACSAT DSP 1 DSCS II DSP 11 DMSP (SD) P72-2 S3 NATO III	Vela VASP IDCSP IDCSP/A TACSAT DSP 1 DSCS II DSP 11 P72-2 S3 NATO III	Vela VASP IDCSP IDCSP/A TACSAT DSP 1 DSCS II DSP 11 P72-2 S3 NATO III
NASA	OGC SYNCOM Lunar Orbiter ATS A (M/G) ATS B,C (S/S) ATS D,E (S/G)	OGC SYNCOM Lunar Orbiter ATS A (M/G) ATS B,C (S/S) ATS D,E (S/G) OAO TIROS M	OGC SYNCOM Lunar Orbiter ATS A (M/G) ATS B,C (S/S) ATS D,E (S/G) OAO TIROS M NIMBUS A,B,C NIMBUS E,F ERIS A,B	SYNCOM Lunar Orbiter ATS A (M/G) ATS B,C (S/S) ATS D,E (S/G) TIROS M NIMBUS E,F ERIS A,B SMS OSO I ATS F AE	SYNCOM Lunar Orbiter ATS A (M/G) ATS B,C (S/S) ATS D,E (S/G) TIROS M NIMBUS E,F ERIS A,B SMS OSO I ATS F AE	SYNCOM Lunar Orbiter ATS A (M/G) ATS B,C (S/S) ATS D,E (S/G) TIROS M NIMBUS E,F ERIS A,B SMS OSO I ATS F AE HEAD	SYNCOM Lunar Orbiter ATS A (M/G) ATS B,C (S/S) ATS D,E (S/G) TIROS M NIMBUS E,F ERIS A,B SMS OSO I ATS F AE HEAD
Commercial	Intel III	Intel III	Intel III	Intel III Intel IV	Intel III Intel IV	Intel III Intel IV MARISAT	Intel III Intel IV MARISAT

TABLE 10
SKYLITE NONRECURRING COSTS, FY 87S (COST IN THOUSANDS \$)

Structure	2498.24
TT&C	1559.20
Communications	00.00
Electrical Power System	402.86
Attitude Control System	2157.63
Apogee Kick Motor	407.56
Platform	7025.49
Program	3259.83
Aerospace Ground Eqpt	1163.27
FY 79S	11448.59
FY 87S	19336.66
Fee	2513.77
TOTAL	21850.43

- Communications (Weight = 0 lbs, for cost purposes)
- Electrical Power System (Weight \times BOL Power = 2539)
- Apogee Kick Motor (Total Impulse = 17133.6 lb-sec, Weight = 17.9 lb)
- Attitude Control System (Weight = 16.5 lb)

The values given in Table 10 and 11 are the cost estimates for the SKYLITE satellite, independent of launch and payload costs. Several points must be made concerning the listed costs. The Platform category is the sum of the hardware costs for the six preceding categories. The Program costs include all those not attributable to a specific subsystem, such as engineering and management costs. The SKYLITE design did not accrue charges directly related to Communications because of its very simple TT&C system. Other than the housekeeping and rare experimental periods, SKYLITE does not communicate. This approach differs substantially from satellites designed with the explicit and demanding mission of communication. The Fee listed for each cost category was 13 percent and the inflation factor from 1979-1987 was 1.635 (Nonrecurring) and 1.845 (Recurring). The last item of note is the Adj FY 79S category. Since the SKYLITE was projected to be the fourth spacecraft constructed, a learning curve is associated with the construction of many similar spacecraft. The cost

TABLE 11
SKYLITE RECURRING COSTS, FY87S (COST IN THOUSANDS)

Structure	261.11
TT&C	521.40
Communications	00.00
Electrical Power System	491.92
Attitude Control System	417.07
Apogee Kick Motor	118.84
Platform	1810.33
Program	826.96
FY 79S	2637.29
Adj FY 79S	2380.15
LOOS	108.22
FY 87S	4215.31
Fee	547.99
TOTAL	4763.30

for a fourth satellite should be less than the first, and is reflected in the difference between the FY79 and Adj FY79 categories.

2. Cost Variations

The cost figures presented are an estimate and a means of assessing the variability of the estimate is available in the model. The cost model provides a figure for how much each category may vary under the constraints of the model. This figure is called the CER standard error category to provide a range of costs. For example, the CER error for the Nonrecurring Structure cost is 2043.95 (Thousand \$). This value is added and subtracted from the actual structural cost to achieve a cost range of 454.79-4531.69 (Thousand \$). Although this is a wide range, the confidence that the actual cost will be in this range is high. The CER errors for each category are summed and an overall error is added and subtracted to the total cost estimate. A problem arose here in applying the cost model to SKYLITE. The CER errors, in some cases, exceeded the category cost. For example, the CER error for Nonrecurring Attitude Control System cost is 2737.93, which is greater than the estimated cost of 2157.63. In these instances the lower bound of the cost range becomes meaningless. The problem

arose several times and led to a lack of confidence in the higher boundaries, as well. For the purposes of the SKYLITE estimate, the costs given must stand alone, with no indication of cost variability.

3. Normalized Cost Estimates

The cost model also has the means to assess the cost differences arising from the selection of different technologies and designs. This allows cost benefit tradeoffs in assessing different design approaches. The cost advantage between constructing a satellite using wholly proven hardware as opposed to state of the art hardware may be ascertained. This additional feature of the cost model is ideal for evaluating the cost benefits of the Orion concept. The Orion emphasizes simplicity and nonredundancy with proven, space rated subsystems. The model provides factors of complexity which adjust the cost according to the estimated difficulty in construction and operation. These factors were gathered from an extensive industry survey which asked engineers and scientists to rank the complexity of technology in each subsystem. The adjusted cost calculations are called point estimates because they focus on a specific design, rather than a broad, generic design. The compensated costs are called normalized costs and are provided below for the SKYLITE design.

TABLE 12
SKYLITE NORMALIZED NONRECURRING COSTS, FY 87S (COST IN
THOUSANDS \$)

Structure	1916.45
TT&C	922.56
Communications	00.00
Electrical Power System	264.47
Attitude Control System	1398.85
Apogee Kick Motor	407.56
Platform	4909.89
Program	2278.19
Aerospace Ground Eqpt	812.97
FY 79S	8001.05
FY 87S	13081.72
Fee	1700.62
TOTAL	14782.34

TABLE 13
SKYLITE NORMALIZED RECURRING COSTS, FY87S (COST IN THOUSANDS \$)

Structure	177.91
TT&C	352.74
Communications	00.00
Electrical Power System	425.37
Attitude Control System	265.54
Apogee Kick Motor	118.84
Platform	1340.40
Program	612.29
FY 79S	1952.69
Adj FY 79S	1762.31
LOOS	108.22
FY 87S	3451.10
Fee	448.60
TOTAL	3899.77

The cost differential between two similar satellites using slightly different technology can be seen by comparing the normalized and nonnormalized tables. The SKYLITE design, stressing simplicity, is a point design and makes significant cost savings available through the utilization of this simplicity. However, the nonnormalized table would be very useful in comparing the costs of different classes of satellites. For example, the expense of a low earth orbiting satellite can be evaluated against a geosynchronous satellite, used for the same mission.

4. Launch and Payload Costs

As indicated above, the Unmanned Spacecraft Cost Model does not address the cost of launching the particular satellite, nor its associated payload. The launch costs are not considered because of their disparity when varying launch configurations are used. For example, a Delta rocket, dedicated to a single satellite, would be much more expensive than a small, STS launch. The costs for launching a specific satellite are provided by the launching sponsor. The two primary launch sponsors for the U.S. are NASA and The U.S. Air Force. There are a few U.S. satellites launched by other countries, but given the DOD sponsorship of SKYLITE, the Air Force is the most

likely sponsor. Also, if the SKYLITE spacecraft were dispensed from the STS, NASA would be the responsible party. The thesis design of SKYLITE required an STS launch, using the Extended GAS can dispenser. As the Extended GAS can is currently under design the launch costs must be derived from those of the smaller GAS can.

The primary costs associated with using the GAS can were the integration expenses. The interface between spacecraft and dispenser are standard and specified, so the costs are predictable. First time integration charges for Orion will be less than \$500K, with a significant decrease for subsequent launches. If the SKYLITE is the first Orion spacecraft, all integration costs will most likely be borne by PMW-145. However, if another Orion were to precede the SKYLITE, the costs would be divided. For SKYLITE estimates, total launch costs of 500K are used.

TABLE 14
APPROXIMATE PAYLOAD COSTS FOR SKYLITE

Retroreflector	10,000.00
Treated Solar Cell Covers	100,000.00
Sensors and Optical Filters (6)	400,000.00
TOTAL	510,000.00

The remaining costs are those of the payload. The SKYLITE's simple purpose substantially minimizes payload costs. These costs are the sum of retroreflector, sensor, and coverglass costs. Since the technology to manufacture each of the payload components currently exists, the cost risk is minimal. Several companies surveyed, Optical Coating Laboratory Lab, Santa Barbara Research Laboratory, and Ford Aerospace Corporation, provided very rough cost estimates. The lack of preciseness was based on retaining a lucrative bargaining position for a future contract. However, all payload components could be purchased for approximately the costs listed in Table 14.

E. CONCLUSION

Costs for the SKYLITE satellite were estimated using the Air Force Unmanned Spacecraft Cost Model. The total of recurring and nonrecurring costs varied when the normalized values were selected. A valuable feature of the cost model is the ability to

adjust costs based on varying complexity and technology. Price estimates for SKYLITE were 3.9MS for recurring costs and 14.8MS for nonrecurring costs. Payload estimates of .5MS and launch costs of .5MS must be added for each satellite deployed. The nonrecurring costs can be divided among different agencies purchasing the Orion spacecraft. If five Orion satellites were produced, the nonrecurring costs for each purchase would be approximately 2.95MS. Additional buyers would further reduce the cost per spacecraft. However, using the estimate of five production Orions, the total cost for the SKYLITE bus, payload, and deployment is 7.85MS.

XIV. CONCLUSIONS

This thesis has presented a conceptual design for the project SKYLITE satellite. The proposed design and spacecraft subsystems are the result of an iterative process, accounting for many conflicting objectives. The engineering risk for subsystem components included in the spacecraft design is low. Only hardware which is reliable and flight tested will be used in the final spacecraft assembly. Therefore, although the SKYLITE design does not emphasize redundancy, the reliability of the vehicle is high.

The selected orbit of 33 degrees inclination and 700 kilometers altitude successfully meets the specifications regarding thermal damage mitigation, satellite lifetime, and laser slew rate. The periodicity of one minute firing intervals was not met. However, at least one firing period will be available every other day. Given the few tests per year, the reduction in available firing periods was not judged an impairment to satisfying mission objectives. Selection of the Orion bus proved to be an effective choice. Pairing the Orion bus with gravity gradient stabilization results in a significant fuel savings which extends the STS operating regime allowing successful satellite insertion. Also, an optimization routine reduced the fuel required for the plane change from the parking orbit to the operational orbit by 10 percent. Using a gravity gradient boom for spacecraft stabilization maintains the ground site within the field of view of the retroreflectors and sensors during experimental periods. The attitude knowledge requirement specified by experimenters is exceeded with the use of magnetometers, supplemented by sun sensors. All attitude calculations will be done at the ground site, as the satellite will not have autonomous attitude determination. The thermal analysis demonstrated that temperatures can be maintained within limits allowing component operation. However, these values are sustained only when a reflective cover glass is placed on the body mounted solar cell array. Power for all spacecraft evolutions is adequately met with body mounted solar cells and Nickel Cadmium batteries. Solar cells are also placed on the tip mass to raise the average solar power available.

There will be six detectors mounted on the spacecraft earth facing side which will be sampled at 1 kilohertz. Since IR detector and sensor technology is currently available to meet SKYLITE requirements, payload costs and cost risk are low. Due to the high laser power, a thermoelectric cooler is necessary to ensure linear detector

response. Another means of reducing laser damage effects on the sensor is placing a neutral density filter prior to the detector array. Since all sensor readings are immediately relayed to the ground site, an on board memory is not necessary. The cost of SKYLITE will strongly depend on how many Orion vehicles are constructed and the associated learning curve. If experimenters are faced with the prospect of constructing the only Orion bus, locating other users will be effective in reducing their total experimental cost.

The spacecraft design presented is tailored for the requirements of an STS launch and deployment. However, the engineering considerations are also valid for launch by an expendable launch vehicle (ELV). The satellite payload interfaces must be changed accordingly, but should not cost more than interfaces associated with the Extended GAS Can. Stress calculations for the SKYLITE satellite assumed an acceleration limit of 5 g's. If the acceleration limits for the ELV are higher, an additional analysis is required. Also, an ELV, if employed, must eject the SKYLITE satellite into the parking orbit illustrated in Figure 5.3.

The design of a satellite is evolutionary and involves three distinct phases. These phases are the Conceptual Design, the Intermediate Design, and the Critical Design. This thesis, as a conceptual design, highlights areas needing further analysis. Details of the spacecraft requiring subsequent analysis for the interim design are:

- Assess the most reliable and economical method of damping satellite librations resulting from gravity gradient stabilization.
- Determine the reflectance of the solar cell cover glass as a function of lasing angle.
- Evaluate the thermal characteristics of discrete points within the satellite, determining the maximum temperature of the solar cells and the gravity gradient boom.
- Due to the long satellite lifetime and large payload margin, sufficient room may be available for another long duration, low power experiment. Sharing the satellite with another payload will divide recurring costs.

The contribution of satellite design techniques by corporations and government agencies cannot be overemphasized. Due to familiarization with the design process and the unique operating environment, these techniques optimize and accelerate the design process. Two aspects of the SKYLITE satellite design substantially enhanced by corporate assistance were the orbital and spacecraft decay analysis. Both areas are important to satellite engineering, and manuals addressing the important aspects of each design area have been developed. Educational approaches necessary in most

design textbooks, are neither essential nor helpful once a design process begins. The proper starting point for a novice satellite designer, once a solid engineering background is developed, is with a firm or agency experienced in satellite engineering.

LIST OF REFERENCES

1. Boyd, Austin, *A Design for Small, General Purpose, Low Earth Satellites*, Thesis Draft, Naval Postgraduate School, Monterey, California, 1987.
2. Interview with LT. Steve Painter, John Albertine, PMW-145, Crystal City, Virginia, 27 April 1987.
3. Koelle, Heinz H. *Handbook of Astronautical Engineering*, New York: McGraw-Hill Co., 1961.
4. Justus, C.G., et al., *The NASA/MSFC Global Reference Atmospheric Model Mod 3 (With Spherical Harmonic Wind Model)*, NASA CR-3256, 1980.
5. Agrawal, Brij N., *Design of Geosynchronous Spacecraft*, New Jersey Englewood Cliffs, Prentice-Hall, 1986.
6. Interview with Fred Mobley, Eric Hoffman, John Dassoulas, John Hopkins University Applied Physics Laboratory, Maryland, 30 April 1987.
7. Hazard, Hap, *U.S. Space Launch Systems, 2nd Ed.*, Navy Space Systems Activity, NSSA-R-20-72-2, 1977.
8. Interview with Hans Karrenberg, Aerospace Corporation, El Segundo, California, 26 May 1987.
9. Ginsberg, L. J., Luders, R.D., *Orbit Planner's Handbook*, El Segundo, California: The Aerospace Corporation.
10. Minzer, R.A., Champion, K.S.W., and Pond, H.L., *The ARDC Model Atmosphere, 1959*, Air Force Research and Development Center, Bedford, Massachusetts, 1959.
11. Gordon, Gary D., *Spacecraft Thermal Design*, Spacecraft Technology Report, Communications Satellite Corp. Clarksburg, Md, 1980.
12. Radecki, J.T., *Power, Hughes Aircraft Geosynchronous Spacecraft Case Histories Vol. I*, Hughes Aircraft Company, Los Angeles, California, 1981.
13. Interview with W.T. Beauchamp, and Isadore M. Sachs, Optical Coating Laboratory Inc., Santa Rosa, California, 27 July 1987.

14. Roberson, Robert E., *Gravity Gradient Stabilization*, Third Winter Institute on Advanced Control, Space Vehicle Guidance and Control, University of Florida College of Engineering, 1965.
15. Riley, Francis E., and Sailor, J. Douglas, *Space Systems Engineering*, New York: McGraw-Hill Book Co., 1962.
16. Naval Research Laboratory, *Low Power Compensation Experiment (LACE) Satellite Description Document*, Washington D.C.: NRL SSD-D-IL002 Rev. 2, 15 March 1987.
17. Interview with Howard Pollard, Ford Aerospace Corporation, Palo Alto, California, 23 April 1987.
18. Eshbach, Ovid W., and Souders, Matt, eds., *Handbook of Engineering Fundamentals*, New York: John Wiley and Sons, 1975.
19. Interview with Don Cutter, Allied Corporation, Thousand Oaks, California, 27 May 1987.
20. Wolfe, William L., and George J. Zissis, eds., *The Infrared Handbook*, Washington D.C., Office of Naval Research, 1978.
21. Interview with Nelson Wallace, Aerospace Corporation, El Segundo, California, 28 May 1987.
22. Interview with Jerry Zwirn, and Tim Abbot, Ford Aerospace Corporation, Palo Alto, California, 6 May 1987.
23. Interview with Paul Norton, Santa Barbara Research Corporation, Goleta, California, 22 July 1987.
24. Air Force Space Division, *Unmanned Spacecraft Cost Model*, (5th ed.), Air Force Space Division, Los Angeles, California, 1981.

BIBLIOGRAPHY

- Air Force Space Division, *Unmanned Spacecraft Cost Model*, (5th ed.), Los Angeles, California: Air Force Space Division, 1981.
- Agrawal, Brij N., *Design of Geosynchronous Spacecraft*, Englewood Cliffs N.J.: Prentice-Hall, 1986.
- Bate, Roger R., Mueller, Donald D., and White, Jerry E., *Fundamentals of Astrodynamics*, New York: Dover Publications Inc., 1971.
- Boyd, Austin, *A Design for Small, General Purpose, Low Earth Orbit Satellites*, Thesis Draft, Naval Postgraduate School, 1987.
- Chappel, Alan, ed., *Optoelectronics Theory and Practice*, New York: McGraw-Hill Book Co., 1978.
- Coppolino, R.N., and Fleming, E.R., *Vehicle Engineering State of the Art, Vol. IV, State of the Art*, El Segundo California: Prepared by Aerospace Corporation for USAF Space Division, 1983.
- Corliss, William R., *Propulsion Systems for Space Flight*, New York: McGraw-Hill Book Co., 1960.
- Corning, Gerald, *Aerospace Vehicle Design*, Ann Arbor Michigan: Braun-Brumfield, 1968.
- Denner, J.S.A., *Orbit Planner's Handbook*, Report by Aerospace Corporation. El Segundo, Ca: 1980.
- Eisele, John A., *Astrodynamics, Rockets, Satellites and Space Travel, An Introduction to Space Science*, Washington D.C.: The National Book Company of America, 1967.
- Eisele, John A., and Nichols, Stephen A., *Orbital Mechanics of General-Coverage Satellites*, Washington D.C.: Naval Research Laboratory, 1976.
- Elion, Glenn R., and Herbert A. Elion, eds., *The Electro-optics Handbook*, New York: Marcel Dekker, Inc., 1979.
- Eshbach, Ovid W., and Matt Souders, eds., *Handbook of Engineering Fundamentals*, New York: John Wiley and Sons, 1975.
- Fuhs, Allan, *1987 Spacecraft Design Class Notes*, Naval Postgraduate School, Monterey, Ca., 1987. (Unpublished Papers)
- Gagliardi, Robert M., *Satellite Communications*, New York: Van Nostrand Reinhold Co., 1984.
- Gorden, Gary D., *Spacecraft Thermal Design*, Report by Communications Satellite Corp., Clarksburg, Md.: 1980.
- Greensite, Arthur L., *Analysis and Design of Space Vehicle Flight Control Systems*, vol. 2, New York: Spartan Books, 1970.

- Justus, C. G., et al., *The NASA/MSFC Global Reference Atmospheric Model Mod 3 (With Spherical Harmonic Wind Model)*, NASA CR 3256, 1980.
- Hudson, Richard P., *Infrared Systems Engineering*, New York: John Wiley and Sons, 1969.
- Koelle, Heinz, *Handbook of Astronautical Engineering* New York: McGraw-Hill Book Co., 1961.
- Leondes, Cornelius T., ed., *Guidance and Control of Aerospace Vehicles*, New York: McGraw-Hill Book Co., 1963.
- Lucas, John W., ed., *Progress in Astronautics and Aeronautics, Heat Transfer and Spacecraft Thermal Control*, vol. 24, Boston, Mass.: Alpine Press, 1971.
- Mayer, Raymond I., and Paul Norton, *PbSe Detector Test Data and Device Model*, Galeta, California: Santa Barbara Research Company, 1984.
- Melles Griot, *Optics Guide 3, Melles Griot Optical Buyers Catalog*, Irvine, California.
- Naval Research Laboratory, *Low Power Compensation Experiment (LACE) Satellite Description Document*, Washington D.C.: NRL SSD-D-IL002 Rev. 2, 15 March 1987.
- Radecki, J.T., *Power, Hughes Aircraft Geosynchronous Case Histories, Vol. I*, Hughes Aircraft Company, Los Angeles, California, 1981.
- Reeves, Robert G., ed., *Manual of Remote Sensing*, Falls Church, Virginia: American Society of Photogrammetry, 1975.
- Riley, Francis E. and Sailor, J. Douglas, *Space Systems Engineering*, New York: McGraw-Hill Book Co., 1962.
- Roberson, Robert E., *Gravity Gradient Stabilization, Third Winter Institute on Advanced Control, Space Vehicle Guidance and Control*, University of Florida, College of Engineering, 1965.
- Santa Barbara Research Center, *Infrared Components Brochure, Ed. 17*, Galeta, California: Santa Barbara Research Company.
- Singer, S. Fred, ed., *Torques and Attitude Sensing in Earth Satellites*, New York: Academic Press, 1964.
- Tada, H.Y., Carter, J.R., Anspaugh, B.E., and Downing, R.G., *Solar Cell Radiation Handbook*, Pasadena Ca.: NASA, Jet Propulsion Laboratory, 1982.
- University of California at Santa Barbara, *Landsat Sensor Design and Operation*, Course Notes, University of California, Santa Barbara, 1983.
- Wolfe, William L., and George J. Zissis, eds., *The Infrared Handbook*, Washington D.C.: Office of Naval Research, 1978.

INITIAL DISTRIBUTION LIST

	No. Copies
1. Defense Technical Information Center Cameron Station Alexandria, VA 22304-6145	2
2. Library, Code 0142 Naval Postgraduate School Monterey, CA 93943-5002	2
3. LT William J. Welch 4738 Greenlaw Dr. Va Beach, VA 23464	1
4. LT Mark Landers 1092 Skyway Dr. Annapolis, MD 21401	1
5. Professor Philip Durkee Code 63De Naval Postgraduate School Monterey, CA 93943	1
6. Professor Richard Christopher Olsen Code 61 Naval Postgraduate School Monterey, CA 93943	1
7. CDR Robert Meurer Office of Naval Research Code-1221 800 N. Quincy St. Arlington, VA 22217-5000	1
8. The Aerospace Corporation Attn: Mr. Hans Karenberg 2350 East El Segundo Blvd. El Segundo, CA 90245-4691	1
9. LT COL William J. Welch 1811 Marlene Drive Eules, TX 76040	1
10. Professor Rudolf Panholzer Code 62PC Naval Postgraduate School Monterey, CA 93943	1

- | | | |
|-----|---|---|
| 11. | LT Steve Painter
PMS-405
Crystal Mall 2 Rm 113
Washington, D.C. 20362 | 1 |
| 12. | Mr. Martin Mosier
Code 67
Naval Postgraduate School
Monterey, CA 93943 | 1 |
| 13. | Ford Aerospace and Communications Corp.
ATTN: Gerald Zwirn
3939 Fabian Way
Palo Alto, CA 94303 | 1 |
| 14. | Professor Carl Jones
Code 74
Naval Postgraduate School
Monterey, CA 93943 | 1 |

END

FEB.

1988

DTic